



# **Role and visualization of the single-stranded and double-stranded DNA in the biofilm of *Neisseria gonorrhoeae***

Dissertation

zur Erlangung des Doktorgrades

der Naturwissenschaften

(Dr.rer.nat.)

dem

Fachbereich Biologie

der Philipps-Universität Marburg

vorgelegt von

**Dipl.-Biologin Maria Zweig, geb. Valevich**

aus Moskau, Russland

Marburg an der Lahn, April 2013

Die Untersuchungen zur vorliegenden Arbeit wurden von Oktober 2008 bis Mai 2012 am Max-Planck-Institut für terrestrische Mikrobiologie unter der Leitung von Prof. MD, PhD Lotte Sørensen und Dr. Chris van der Does durchgeführt.

Vom Fachbereich Biologie (Fb. 17) der Philipps-Universität Marburg (HKZ: 1180) als Dissertation angenommen am: 05.06.2013

Erstgutachterin: Prof. MD, PhD Lotte Sørensen-Andersen

Zweitgutachter: Prof. Dr. Martin Thanbichler

Weitere Mitglieder der Prüfungskommission:

Prof. Dr. Uwe Maier

Prof. Dr. Renate Renkawitz-Pohl

Tag der mündlichen Prüfung: 19.06.2013

Die während der Promotion erzielten Ergebnisse sind zum Teil in folgenden Originalpublikationen veröffentlicht:

**Characterization of the Single Stranded DNA Binding Protein SsbB Encoded in the Gonococcal Genetic Island, PLOS One, 7(4):e35285, (2012)**

Samta Jain<sup>+</sup> **Maria Zweig**<sup>+</sup>, Eveline Peeters, Katja Siewering, Kathleen T. Hackett, Joseph P. Dillard, Chris van der Does

<sup>+</sup> Contributed equally

**Role and Visualization of Extracellular Single-stranded DNA involved in Biofilm Formation by *Neisseria gonorrhoeae*.**

**Maria A. Zweig**, Sabine Schork, Andrea Koerdt, Katja Siewering, Claus Sternberg, Kai Thormann, Sonja-Verena Albers, Soren Molin, and Chris van der Does, (2012), Submitted to Environmental Microbiology Journal.

*Dedicated to my*

*Mum*

**Table of contents**

Zusammenfassung ..... 8

Abstract..... 10

Abbreviations ..... 12

Introduction ..... 13

1.1 *Neisseria gonorrhoeae* ..... 13

1.2 The Gonoccal Genetic Island..... 16

1.3 Type IV secretion systems..... 17

1.4 The Type IV secretion system encoded with the GGI ..... 19

1.5 Role of the GGI in host–pathogen interactions ..... 21

1.5.1 GGI in *N. meningitidis* ..... 21

1.5.2 Regulation of GGI ..... 22

1.5.3 Secretion of single stranded DNA ..... 22

1.6 Single-stranded DNA binding Proteins (SSBs) ..... 22

1.6.1 Oligosaccharide/Oligonucleotide binding domain ..... 23

1.6.2 Classification of SSBs..... 24

1.6.3 Binding of SSBs to ssDNA ..... 25

1.6.4 Additional functions of SSBs ..... 26

1.7 Biofilms..... 27

1.7.1 Extracellular DNA as important matrix component in biofilms..... 28

1.7.2 Biofilm formation by *Neisseria gonorrhoeae*..... 29

1.7.3 Visualization of eDNA in biofilms..... 30

1.8 Scope of the thesis..... 30

Chapter 2..... 32

Characterization of the Single Stranded DNA binding protein SsbB encoded in the Gonoccal Genetic Island ..... 32

2.1 Aim of the study..... 33

2.2 Results..... 33

2.2.1 Sequence Analysis..... 33

2.2.2 Overexpression, purification and determination of the oligomeric state of SsbB ..... 38

2.2.3 SsbB binds to fluorescently and radioactively labeled ssDNA with high but different affinities... 40

2.2.4 Quenching of intrinsic tryptophan fluorescence ..... 43

2.2.5 Determination of the minimal binding frame for one or two SsbB tetramers.....	44
2.2.6 SsbB binding to ssDNA visualized by atomic force microscopy .....	45
2.2.7 The physiological characterization of the SsbB .....	48
2.2.8 SsbB stimulates topoisomerase activity .....	48
2.3 Discussion.....	49
Chapter 3.....	52
Biosensor development for the visualization of single-stranded DNA and double-stranded DNA in the biofilms and planktonic cultures.....	52
3.1 Aim of the study.....	53
3.2 Results .....	53
3.2.1 Expression and purification of the SsbB from <i>Neisseria gonorrhoeae</i> .....	53
3.2.2 Detection of ssDNA with labeled SsbB.....	54
3.2.3 Expression and purification of the SulSSB from <i>Sulfolobus solfataricus</i> .....	55
3.2.4 Expression and purification of the TteSSB2 from <i>Thermoanaerobacter tengcongensis</i> .....	56
3.2.5 ssDNA and dsDNA can be visualized in biofilms of the thermoacidophilic archaea <i>Sulfolobus acidocaldaris</i> using fluorescently labelled TteSSB2 and Sac7d.....	62
3.3 Discussion.....	64
Chapter 4.....	65
Role and Visualization of Extracellular Single-stranded DNA involved in Biofilm Formation by <i>Neisseria gonorrhoeae</i> .....	65
4.1 Aim of the study.....	66
4.2 Results .....	66
4.2.1 Exonuclease I inhibits the initial stages of biofilm formation.....	66
4.2.2 DNA secretion facilitates biofilm formation .....	69
4.2.3 Treatment of biofilms with Exonuclease I only affects strains that secrete ssDNA .....	71
4.2.4 Visualization of single-stranded DNA.....	72
4.2.5 The majority of eDNA in biofilms of <i>N. gonorrhoeae</i> MS11 is double-stranded .....	73
4.3 Discussion.....	76
Chapter 5.....	79
Materials and Methods.....	79
5.1 Reagents and equipment .....	79
5.1.1 Reagents.....	79
5.1.2 Enzymes and Kits.....	79

## Table of contents

---

5.2 Microbiological methods .....	81
5.2.1 Cultivation of bacteria.....	81
5.2.1.1 Cultivation of <i>E.coli</i> .....	81
5.2.1.2 Cultivation of <i>N. gonorrhoeae</i> .....	81
5.2.1.3 Cultivation of <i>Sulfolobus ssp.</i> .....	81
5.2.2 Strains used in this study .....	82
5.3 Molecular biological methods .....	84
5.3.1 Polymerase Chain Reaction (PCR).....	84
5.3.2 Primers and plasmids used in this study.....	84
5.3.3 Colony lysis for colony PCR .....	92
5.3.4 Agarose gel electrophoresis.....	92
5.3.5 DNA restriction.....	93
5.3.6 Ligation.....	93
5.3.7 Transformation of competent <i>E.coli</i> cells .....	93
5.3.8 Transformation of <i>N. gonorrhoeae</i> .....	94
5.3.9 DNA Sequencing.....	94
5.3.10 Co-culture assay for DNA uptake and transformation .....	94
5.3.11 Complementation of <i>E. coli</i> SSB.....	95
5.3.12 Transcriptional Mapping.....	95
5.3.13 Quantitative PCR.....	96
5.3.14 DNA secretion assays .....	96
5.3.15 Isolation of secreted fraction .....	96
5.4 Biochemical methods.....	97
5.4.1 Induction and overexpression of recombinant proteins in <i>E.coli</i> .....	97
5.4.2 Cell disruption and purification of recombinant proteins .....	97
5.4.3 TCA precipitation .....	98
5.4.4 SDS-PAGE .....	98
5.4.5 Expression and purification of TteSSB2, Sac7d, ExoI and ExoIII .....	99
5.4.6 Expression and purification of SsbB.....	100
5.4.7 Polyacrylamide Gel Electrophoresis Mobility Shift Assays .....	101
5.4.8 Fluorescence titrations .....	102
5.4.8 Protein isolation from Neisseria cells for Western Blotting .....	102

## Table of contents

---

5.4.9 Western Blotting .....	102
5.4.10 Site-specific labeling of proteins via cysteines.....	102
5.4.11 Activity assays for specificity of ExoI and ExoIII .....	103
5.4.12 Topoisomerase DNA relaxation assay.....	103
5.4.13 Visualisation of ssDNA/dsDNA in the biofilms.....	103
5.5 Bioinformatics .....	103
5.6 Microscopy.....	104
5.6.1 Fluorescent light microscopy .....	104
5.6.2 Confocal Laser Microscopy .....	104
6 Appendix .....	105
Physiological characterization of SsbB.....	105
6.1 SsbB is expressed in <i>N. gonorrhoeae</i> .....	105
6.2 SsbB has no effect on DNA secretion or uptake .....	106
7 References .....	110
Acknowledgments.....	120
Lebenslauf.....	121
Erklärung.....	122
Einverständniserklärung .....	123



### Zusammenfassung

*Neisseria gonorrhoeae*, der Erreger der sexualübertragenden Erkrankung Gonorrhoe, ist ein gram-negatives menschen-adaptiertes Diplococcus. 80% der klinischen Isolate enthalten durch den horizontalen Gentransfer erworbene Gonococcale Genetische Insel (GGI), welche ein ungewöhnliches Type-Vier-Secretionssystem (T4SS) kodiert. In manchen Stämmen von *N. gonorrhoeae* ist Einzelstrang-DNA-Bindendes Protein (SSB) nicht nur auf dem Chromosom kodiert, es gibt ein zweites SSB, SsbB, welches innerhalb der GGI kodiert ist. SSB sind hoch konservierte, essentielle Proteine, die in allen Domänen des Lebens vertreten sind. Diese Proteinklasse bindet mit sehr niedriger Sequenzspezifität und gleichzeitig mit sehr hoher Affinität an die Einzelstrang-DNA (ssDNA), außerdem sind sie bei der DNA-Rekombination, Replikation und Reparatur unerlässlich. Die zweite Kopie von SSB kann entweder auf einem Chromosom oder einem Plasmid kodiert sein. Diese SSBs sind bei diversen Mechanismen wie natürliche Kompetenz, Plasmidtrennung und DNA Transport, tätig. Wir haben die physiologische Rolle von SsbB Protein analysiert, sowie seine Funktionen biochemisch charakterisiert. Wir stellten fest, dass die nächsten Homologe von SsbB innerhalb konservierter genetischer Kluster auf den genetischen Inseln verschiedener Proteobacteria lokalisiert sind. Diese Kluster kodieren DNA Prozessierungs Enzyme wie ParA und ParB, Partitionierungsproteine, TopB, Topoisomerase und vier konservierte hypothetische Proteine. Die in diesen Klustern gefundene SsbB Homologe bilden eine separate/gesonderte von den anderen Familie der einzelstrang DNA Binde Proteine. Wir konnten demonstrieren, dass im Gegensatz zu den meisten anderen SSBs, SsbB kann nicht *Escherichia coli* *ssb* Deletionsmutante komplementieren. Aufgereinigtes SsbB bildete ein stabiles Tetramer. Elektrophoretische Mobilitäts Gel-Shift Assay, Fluoreszenztitrationsassay und die Raster-Kraft Mikroskopie demonstrieren, dass SsbB mit hoher Affinität an die ssDNA bindet. Ein SsbB-Tetramer braucht minimum 15 nucleotide, Zwei SsbB-Tetramere brauchen 70 Nucleotide, um an die ssDNA zu binden. Der Bindungsmotif war von  $Mg^{2+}$  oder NaCl Konzentration unabhängig. Wir konnten keine Rolle von SsbB weder für die DNA Sekretion noch für die DNA Aufnahme zeigen, jedoch wir konnten demonstrieren, dass SsbB die Aktivität der Topoisomerase I stimuliert. Wir vermuten, dass SsbB eine noch unbekannte Rolle für die Erhaltung der genetischen Inseln spielt.

Bemerkenswerterweise wurde für die T4SS von *N. gonorrhoeae* Secretion von ssDNA gebunden an die Relaxase direkt ins Medium gezeigt. Derzeit ist fast nichts über die exakte Funktion der sekretierten DNA bekannt. Studien haben gezeigt, dass nicht nur die Exopolysaccharide aber auch die extrazelluläre DNA (eDNA) eine wichtige Rolle für die anfängliche Etablierung von Biofilmen spielen kann. Die Zusammensetzung und der Ursprung der eDNA sind nicht komplett erforscht. Die Biofilme von *N.*

*gonorrhoeae* enthalten große Mengen der eDNA, welche eine wichtige Rolle für die Biofilmbildung spielt. Um die Rolle der ssDNA für die Biofilmbildung zu untersuchen, wurde der Verlauf der Biofilmbildung von *N. gonorrhoeae* Stamm MS11 mit dem MS11 $\Delta$ *TraB* Stamm, welcher in Secretion von ssDNA beeinträchtigt ist, und dem komplementierten Stamm MS11  $\Delta$ *traB::traB*, wo die Secretion wieder hergestellt ist, verglichen. Des Weiteren wurde die Rolle der ssDNA für die Biofilmbildung durch die Behandlung der Biofilme mit der Exonuklease I, welche spezifisch nur ssDNA degradiert, untersucht. Diese Experimente demonstrierten, dass die secretierte ssDNA stark die Biofilmbildung stimuliert, vor allem aber in der Phase der anfänglichen Anhaftung.

Darüber hinaus haben wir eine einzigartige Methode entwickelt, um die ssDNA and dsDNA separat zu detektieren. Für die Visualisierung der ssDNA, wurden SSB Proteine, welche mit sehr niedriger Sequenzspezifität und gleichzeitig mit sehr hoher Affinität an die ssDNA binden, eingesetzt. Das hochstabile SSB Protein aus *Thermoanaerobacter tengcongensis* sowie verschiedene Cysteine-Mutanten in diesem Protein wurden isoliert. Die verschiedenen Cystein-enthaltene Proteine wurden mit umweltempfindlichen Fluoreszenzproben markiert. Die spezifischen Kombinationen von Cystein-Mutanten und Fluoreszenzproben wurden getestet, um solche Kombinationen zu erhalten, bei denen eine Zunahme der Fluoreszenz nach der Bindung des Proteins stattfindet. Für die Detektion der dsDNA wurde das thermostabile doppel-strang DNA bindendes Protein Sac7d aus *Sulfolobus acidocaldarius* verwendet. Beide Proteine wurden für die Visualisierung von ssDNA und dsDNA in den Biofilmen sowie planktonischen Kulturen verwendet. Bemerkenswerterweise, konnte mit dieser Methode nur dsDNA in den Biofilmen von *N. gonorrhoeae* detektiert werden. Wir schlussfolgern, dass ssDNA eine wichtige Rolle für die Biofilmbildung spielt, jedoch sind die Mengen der ssDNA in den Biofilmen viel geringer als der dsDNA.

## Abstract

*Neisseria gonorrhoeae*, the causative agent of the sexually transmitted disease gonorrhoea, is a Gram-negative human-adapted diplococcus. 80% of the clinical *N. gonorrhoeae* isolates encode an unusual Type IV secretion system (T4SS) within the horizontally acquired region - the Gonococcal Genetic Island (GGI). Next to the Single Stranded DNA binding protein (SSB) encoded on the chromosome, a second SSB, SsbB, is encoded within the GGI. SSBs are highly conserved, essential proteins found in all kingdoms of life. They bind single stranded DNA (ssDNA) with high affinity, have low sequence specificity and are involved in DNA recombination, DNA replication and DNA repair. A second copy of SSBs can be encoded on the chromosome or on a plasmid. These SSBs can be involved in diverse mechanisms like natural competence, plasmid segregation and DNA transport. We analyzed the physiological role of SsbB and characterized its function biochemically. We found that close homologs of SsbB are located within a conserved genetic cluster found in genetic islands of different proteobacteria. This cluster encodes DNA processing enzymes such as the ParA and ParB partitioning proteins, the TopB topoisomerase and four conserved hypothetical proteins. The SsbB homologs found in these clusters form a family separated from other ssDNA binding proteins. Remarkably, in contrast to most other SSBs, SsbB did not complement the *Escherichia coli* *ssb* deletion mutant. Purified SsbB formed a stable tetramer. Electrophoretic mobility shift assays, fluorescence titration assays, as well as atomic force microscopy demonstrated that SsbB binds ssDNA specifically with high affinity. SsbB binds single stranded DNA with minimal binding frames of 15 and 70 nucleotides for one or two SsbB tetramers respectively. The binding mode was independent of increasing  $Mg^{2+}$  or NaCl concentrations. No role of SsbB in ssDNA secretion or DNA uptake could be identified, but SsbB strongly stimulated Topoisomerase I activity. We propose that these novel SsbBs play an unknown role in the maintenance of genetic islands.

Remarkably the T4SS of *N.gonorrhoeae* was shown to secrete ssDNA directly into the medium. Currently nothing is known about the exact function of the secreted DNA. Studies have shown that not only exopolysaccharides but also extracellular DNA (eDNA) can play an important role in the initial establishment of biofilms. The composition and the origin of the eDNA are not completely understood. *N. gonorrhoeae* biofilms contain large amounts of extracellular DNA which play an important role in biofilm formation. To study the role of ssDNA in biofilm formation, the development of biofilms of *N. gonorrhoeae* strain MS11 was compared with a MS11  $\Delta traB$  strain, which is impaired in ssDNA secretion and the MS11  $\Delta traB::traB$  complementation strain in which ssDNA secretion is restored. Furthermore, the role of ssDNA in biofilm formation was studied by treating biofilms with Exonuclease I which

specifically degrades ssDNA. These experiments demonstrated that the secreted ssDNA strongly stimulated biofilm formation especially during initial attachment.

Furthermore, we developed a unique technique to separately detect ssDNA and dsDNA. To visualize ssDNA, SSB proteins, which specifically bind ssDNA with high affinity in a sequence-independent manner, were employed. The highly stable SSB protein from *Thermoanaerobacter tengcongensis*, and different cysteine mutants within this protein were purified to homogeneity. The different cysteines containing proteins were labelled with environmentally sensitive fluorescent probes. Specific combinations of cysteine mutants and fluorescent probes were selected to obtain proteins that showed a strongly increased fluorescence upon binding of ssDNA. To visualize dsDNA the thermostable double stranded DNA binding protein Sac7d of *Sulfolobus acidocaldarius* was used. Both proteins were applied to visualize single- and double-stranded DNA in biofilms and planktonic cultures. Remarkably, only dsDNA could be detected in *N. gonorrhoeae* biofilms using this approach. We conclude that ssDNA plays an important role in biofilm formation, but that the amount of ssDNA necessary is much lower than the amount of dsDNA found in mature biofilms.

**Abbreviations**

AFM	Atomic Force Microscopy
Bp	Base pairs
Cm	Chloramphenicol
CLSM	Confocal Laser Scanning Microscopy
DAPI	6-diamidino-2-phenylindole
DDAO	7-hydroxy-9H-(1,3-dichloro-9,9-dimethylacridin-2-one)
DGI	Disseminated Gonococcal Infection
dsDNA	Double-stranded DNA
DUS	DNA Uptake Sequence
EMSA	Electrophoretic Mobility Shift Assay
EPS	Exopolymeric Substances
Hrs	Hours
GGI	Gonococcal Genetic Island
IB	Inclusion Bodies
IM	Inner Membrane
IPTG	Isopropyl $\beta$ -D-1-thiogalaktopyranoside
IANBD	<i>N</i> -((2-(iodoacetoxy)ethyl)- <i>N</i> -Methyl)amino-7-Nitrobenz-2-Oxa-1,3-Diazole
LB	Luria-Bertani medium
Mpf	mating pair formation (complex)
Min	Minutes
Ni-NTA	Nickel-nitriloacetic acid
OD	Optical Density
OM	Outer Membrane
PID	Pelvic Inflammatory Disease
RT	Room Temperature
SSB	Single-stranded DNA Binding protein
ssDNA	single-stranded DNA
SDS-PAGE	Sodium Dodecyl Sulfate PolyAcrylamide Gel Electrophoresis
T4SS	Type IV Secretion System
T4P	Type IV Pili
WT	Wild Type

## Introduction (Chapter 1)

### 1.1 *Neisseria gonorrhoeae*

Of the genus *Neisseria*, which currently consists of eleven species that can colonize humans, only two, *Neisseria meningitidis* and *Neisseria gonorrhoeae*, are human pathogens. *N. meningitidis* (also referred to as the *meningococcus*) causes bacterial meningitis and is the causative agent of meningococcal septicaemia. *N. gonorrhoeae* (also referred to as the gonococcus) causes the sexually transmitted disease gonorrhoea. Many individuals carry *N. meningitidis* in the upper respiratory tract and remain perfectly healthy, but *N. gonorrhoeae* is never part of the healthy flora and is only found after contact with an infected person. Gonorrhoea was reported as a human disease as early as 5 B.C. making it one of the earliest described human diseases. Nowadays, despite intensive studies on the mechanisms of its pathogenicity, no vaccines are available and gonococcal infections remain a major global health threat with more than sixty million cases worldwide every year [1]. Due to the rapid development of high resistance to many different antibiotics many drugs are no longer effective in killing many of the *N. gonorrhoeae* strains. The emergence and spread of resistance in *N. gonorrhoeae* has occurred mainly by the acquisition of new DNA via conjugation and transformation.

*N. gonorrhoeae* is an obligate human pathogen that primarily infects superficial mucosal surfaces lined with columnar epithelium such as urethra, cervix, rectum, pharynx and conjunctiva. As a sexually transmitted disease agent, the gonococcus normally colonizes the genital tract [2]. Most of the gonococcal infections in males are inflammatory and pyogenic infections of the urogenital tract, whereas about 50% of infections in woman are asymptomatic. When untreated, the bacterium can leave the genital tract and the infection can become systemic. Women with a persistent infection may develop pelvic inflammatory disease (PID), ectopic pregnancy, infertility and/or a disseminated gonococcal infection (DGI) [3].

Although a mouse model has been used in several studies and this model is currently further optimized to more resemble an infection in humans, no animal model exists that represents the full spectrum of disease during gonococcal infection. The insights of the pathogenicity mechanism have therefore mainly been studied in human volunteers, tissue and organ cultures, and immortalized or malignant tissue culture cell lines [4-7]. These studies have shown that gonococci adhere mainly to the nonciliated epithelial cells and that attachment to ciliated cells does not occur [8]. Attachment is mediated by type IV pili and outer membrane Opa proteins [9-11]. Type IV pili not only are important for attachment, but pilus retraction allows gonococci to form organized microbial communities on the cell surface via both specific and nonspecific interactions [12]. These microcolonies stimulate the formation of cortical plaques—structures in the cell cortex which

contain high concentrations of transmembrane receptors, nonreceptor tyrosine kinases and their anchors, and components of the cortical cytoskeleton [13]. The different Opa proteins bind to different carcinoembryonic antigen-related cellular adhesion molecules (CEACAMs) which are receptors on the human cells [14]. Binding of the Opa proteins to the CEACAMs inactivates the lymphocyte cells and the proliferation of these cells is switched off, thereby hindering the memory of the immune system and increasing the susceptibility to opportunistic pathogens [15]. After adherence, the gonococci enter the epithelial cell by receptor-mediated endocytosis [16]. The major porin protein Por was proposed to be the invasin that mediates the penetration into the host cell [17]. The gonococci then transverse the cell and multiply on the basal-lateral membrane [15]. For a persistent infection, the *N. gonorrhoeae* cells have to evade the immune system. Many surface structures among which the Type IV pili and the Opa proteins can undergo both phase and antigenic variation. The ability to modulate the surface antigenic structure rapidly is one of the most important requirements for a successful gonococcal infection. Furthermore, *N. gonorrhoeae* can modulate its lipooligosaccharides (LOS) and is able to utilize host-derived N-acetylneuraminic acid (sialic acid) to sialylate the oligosaccharide component of its LOS [18]. Also this sialylation undergoes phase variation [19]. Gonococci with nonsialylated LOS are more invasive than those with sialylated LOS but on the other hand sialylation of LOS makes them more resistant to bactericidal effects of serum [20].

Many other processes contribute to the evasion of the immune system by *N. gonorrhoeae*. For example, the secreted IgA protease can cleave the human IgA immunoglobulin, thus preventing the recognition of *N. gonorrhoeae* by the immune system [21]. Finally the ability of the gonococcus to bind only human transferrin- or lactoferrin could be a reason, why *N. gonorrhoeae* is a exclusively human pathogen [15].

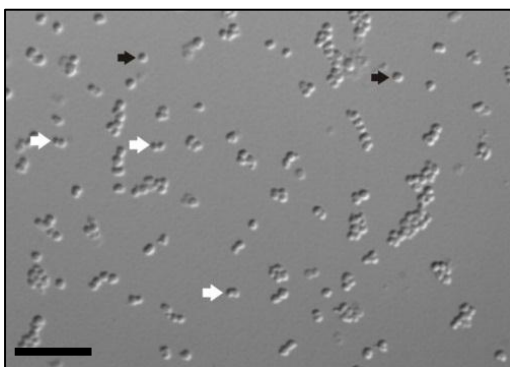


**Figure 1-1:** Differential interference contrast microscopy (DIC) of a mixture of diplococcal and monococcal planctonic *Neisseria gonorrhoeae* MS11 cells. Black arrows indicate monococcal bacteria, white arrows show diplococcal bacteria. The bar is 10  $\mu\text{m}$  in length.

Gonococci are gram-negative aerobic or facultative anaerobic bacteria which exist as a mixture of monococcal and diplococcal cells (Fig. 1-1) [22]. Although *N. gonorrhoeae* is very efficient in colonizing humans and shows an effective transmission from human to human during sexual contact, *N. gonorrhoeae* is a fragile organism outside its human host. *N. gonorrhoeae* is susceptible to many parameters such as temperature, drying, UV light, pH and others. The cultivation of gonococcal cultures requires very stringent conditions like a temperature between 35 and 37 °C in an atmosphere of 3-10 % CO<sub>2</sub> [23].

*N. gonorrhoeae* is not well-suited for growth in liquid. The gonococcus is a pathogen of mucosal surfaces and expresses potent autolysins whose activity increases following glucose depletion during stationary phase, leading to rapid cell lysis especially during growth in medium [23]. Liquid cultures require a relatively high initial inoculum relative to most organisms. Traditional undefined broths (e.g. nutrient broth, brain heart infusion, Thayer-Martin agar etc.) allow limited multiplication of bacteria, but a large inocula in excess of 10<sup>5</sup> CFU ml<sup>-1</sup> is needed to achieve growth in the liquid culture [24]. Chemically defined liquid media for *N. gonorrhoeae* are usually minimal media which do not support the growth of low inocula. The M199 cell culture medium is often used as a component of a defined liquid medium and has a stabilizing effect for *N. gonorrhoeae* [25]. The most commonly used medium for cultivation of gonococci is chemically defined, clear and protein-free Graver-Wade liquid medium [26]. The gonococcus is also capable of anaerobic growth when provided with a suitable electron acceptor [27].

Although the gonococcus is a very fastidious organism outside the host, careful handling of the bacterium is still required, since strains rapidly develop a high resistance against many different antibiotics. This is based on its high rate of obtaining mutations, and the fact that it is highly naturally competent during all phases of growth [28]. *N. gonorrhoeae* preferentially takes up DNA that contains a 10-12 base (5'-ATGCCGTCTGAA-3') genus-specific DNA uptake sequence (DUS) [29]. The DUS is found frequently in the neisserial genome, with on average one DUS per 1100 bp [30]. Neisseria use Type IV pili (T4P) to take up DNA. A direct correlation is observed between the piliation status of the gonococci and competence. The piliated gonococci are much better transformable than the non-piliated bacteria [31]. DNA transfer occurs at such a high rate that *N. gonorrhoeae* is considered a panmictic or non clonal organism [32]. The DNA for transformation is obtained from neighboring gonococci by either autolysis of a subpopulation or via secretion via a Type IV secretion system encoded within a Gonococcal Genetic Island (GGI) [33].

*N. gonorrhoeae* is very sensitive to its surroundings and readily undergoes autolysis. The exact mechanism of autolysis is not known, but the N-acetylmuramyl-alanine amidase, AmiC was identified as the major autolysin *in vitro* [34]. Further endopeptidase activities capable of cleaving



the peptide-cross links in peptidoglycan and N-acetylglycoseaminidase activities that cleave the glucan backbone were described [35,36]. Recently the peptidoglycan transglycosylase AtIA was identified as an autolysin which acts in the stationary phase [37].

The exact role of autolysis is not known, but possible advantages are the release of nutrients to a starving population, modulation of the host immune response and DNA donation for natural transformation. DNA released by autolysis was suggested to be the primary source of DNA for natural transformation, but recent findings show that *N. gonorrhoeae* can also donate DNA for transformation via a type IV secretion encoded on the Gonococcal Genetic Island (GGI) [38]. This secreted DNA is the focus of this thesis.

### 1.2 The Gonoccal Genetic Island

Approximately 80 % of gonococcal and some meningococcal strains contain a 57-kb horizontally acquired genomic island called the Gonococcal Genetic Island, GGI [38-40]. Sequencing of the GGI revealed that the G+C content of the GGI was 44 % [38]. This is significantly lower than the 51 % G+C contents which was found for the currently sequenced genomes of *N. gonorrhoeae* strains [33], suggesting that the GGI was horizontally acquired. The origin of the GGI is unknown, but since *N. gonorrhoeae* is an obligate human pathogen, it is assumed that the GGI was acquired from another human pathogen [40]. The GGI was found inserted into the chromosome at the *dif* site, resulting in duplication of the site [33]. One site, the *difA* site contains the original *dif* consensus sequence (5'-AATTCGCATAATGTATATTATGTTAAAT-3') while the *difB* site has four mismatches compared to the consensus sequence. *dif* sites are recognized by the site-specific recombinase XerCD [33,41] which separates the chromosomal dimers during replication [42]. It was demonstrated that XerCD can excise from the GGI when the *difB* site is mutagenized to the consensus *dif* site [41]. The excised GGI is unstable and can only be rescued by either integration of an essential gene in the GGI or by re-integration in the chromosome [41].

The GGI contains 62 open reading frames (ORFs) (Fig. 1-2). The first three operons contain genes that encode proteins related to Type IV secretion systems ([33], Pachulec *et al*, manuscript in preparation). The other half of the GGI encodes mainly proteins for which the function is still unknown and putative DNA processing proteins like e.g. the partitioning proteins ParA and ParB, the single stranded DNA binding protein SsbB, the DNA topoisomerase TopB, the DNA helicase Yea and the DNA methylases Ydg and YdhA [33] (Fig.1-2).

### 1.3 Type IV secretion systems

Secretion systems of Gram-negative bacteria are classified into six major evolutionarily and functionally related groups, termed type I to type VI secretion systems [43]. The Type IV Secretion Systems (T4SS) form one of the most diverse secretion systems. They can transport diverse substrates, like DNA and proteins, to many different recipient cells [44-48]. Based on the substrates that the T4SS systems transport they are divided into 2 large groups of the conjugative and effector translocation T4SSs, and a small group containing the DNA release/uptake T4SSs [43]. Conjugation systems deliver DNA substrates to the target cell. These systems require the establishment of direct contact between the donor and the recipient cell (mating pair formation, Mpf). Conjugation systems play an important role in disseminating DNA among bacterial populations [49,50]. T4SSs are also involved in the delivery of virulence factors and toxins to other hosts. The subfamily of the effector translocation systems comprises for example the phytopathogen *Agrobacterium tumefaciens* and several pathogens of mammals, such as *Heliobacter pylori*, *Legionella pneumophila*, and *Brucella* and *Bartonella* species. Also effector translocator systems deliver their cargo to mostly eukaryotic target cells through direct cell-to-cell contact, with the exception of the *B. pertussis* Ptl system, which exports the A/B pertussis toxin (PT) to the extracellular milieu [40]. DNA uptake and release systems form the smallest subfamily. The secretion process does not require the contact to the target cell: DNA uptake and release are mediated from or into the extracellular milieu. It consists of the ComB DNA uptake system, *H. pylori* [51] and the Tra-like DNA-release system that is encoded in the GG1 of *N. gonorrhoeae* [52].

All substrates are transported through a cell envelope-spanning structure that forms a channel across the inner and the outer membrane. Almost all T4SSs consist of multiple components, which can be divided in components that form the mating pair formation complex that spans the inner and outer membranes, components that form the pilus and the type IV coupling protein (T4CP) that acts as substrate receptor and that transfers the substrate to the mating pair formation complex. In addition, conjugative T4SS also contain components involved in the processing of the DNA. The currently best studied T4SS is the T4SS encoded on the Ti plasmid of *A. tumefaciens*. Most of the proteins of this T4SS are either named VirB (involved in the formation of the Mpf complex, the transport process or pilus formation) or VirD (the relaxase and coupling protein) [43].

In the T4SS encoded on the Ti plasmid of *A. tumefaciens* 11 proteins, VirB1 to VirB11, are involved in the formation of the Mpf complex and the pilus. The core of the T4SS is formed by VirB7, VirB9 and VirB10. The structure of the core complex of the pKM101 plasmid, which consists of the TraN (homolog of VirB7), TraO (homolog of VirB9) and TraF (homolog of VirB10) proteins was recently

solved. Fourteen copies of TraN, TraO and TraF together form a large complex of approximately 20 nm in diameter and more than 1 MDa in size [53]. The pilus is built of major and minor T-pilus components VirB2 and VirB5 [54]. The T4SS of *A. tumefaciens* encodes the VirB4, VirB11 and VirD4 ATPases. Recent biochemical and structural data shows that these proteins are most likely active in their hexameric form [55,56]. VirD4 is the coupling protein that is involved in transfer of the substrates to the Mpf complex. Remarkable, both the F-plasmid and the T4SS encoded within the GGI do not contain a homolog of VirB11 [57].

The key protein in conjugation is the relaxase. It recognizes the origin of transfer (*oriT*), catalyzes the initial cleavage of the *oriT* in the donor and mediates the ligation of the transported DNA. Currently eight MOB (Mobility) classes have been identified: MOB<sub>B</sub>, MOB<sub>T</sub>, MOB<sub>F</sub>, MOB<sub>H</sub>, MOB<sub>O</sub>, MOB<sub>C</sub>, MOB<sub>P</sub>, and MOB<sub>V</sub> [58-61]. The main characteristics of the MOB<sub>F</sub> and MOB<sub>H</sub> families, which are most relevant for this thesis will be shortly introduced here.

Many different members of the MOB<sub>F</sub> family have been identified and studied, among which the Tral relaxase of the F plasmid and the TrwC relaxase of R388 plasmid [59]. The relaxases of the MOB<sub>F</sub> family are large proteins which consist of two domains: an N-terminal relaxase domain (containing two catalytically active tyrosines) and a characteristic C-terminal helicase domain. The relaxase domain contains three well conserved motifs. Motif I harbors two catalytic tyrosine residues, motif II contains a conserved aspartate, and motif III represents a conserved histidine triad motif [62]. The prototype of the new MOB<sub>H</sub> family is the Tral relaxase from the IncHI1 group plasmid R27. Some clades of the MOB<sub>H</sub> family are composed entirely of integrative and conjugative elements (ICEs) and genomic islands (GIs) [59]. The Tral relaxase encoded within the GGI of *N. gonorrhoeae* is the best analyzed member of the MOB<sub>H</sub> systems. It exhibits some features of relaxases, but also has some hallmarks like a metal-dependent HD phosphohydrolase domain, an N-terminal hydrophobic region and a C-terminal DUF1528 domain, which have not been identified in previously characterized relaxases [59].

It was demonstrated that MOB families occur not randomly, but have adapted to plasmids of different sizes [63]. MOB<sub>V</sub> is found almost exclusively among mobilizable plasmids, while MOB<sub>F</sub> and MOB<sub>H</sub> were present almost exclusively in conjugative plasmids. Next to the different MOB classes, T4SS can also be annotated according to their MPF complexes. Currently 8 different classes are identified, but the known proteobacterial T4SSs were classified into four classes: the vir system in MPF<sub>T</sub>, the F-plasmid like systems in MPF<sub>F</sub>, the R64 plasmid like systems in MPF<sub>I</sub>, and the systems resembling ICEHIN1056 of the *Haemophilus influenzae* genomic island in MPF<sub>G</sub>. MPF<sub>T</sub> is by far the most abundant T4SS, and MPF<sub>G</sub> and MPF<sub>F</sub> might derive from an ancestral MPF<sub>T</sub>. However, MPF<sub>I</sub> and

T4SSs from other clades have not derived from MPF<sub>T</sub>, and seem to be a proteobacterial invention [63]. Although certain combinations of families of mobility factors and families of MPF complexes appear much more frequently, mobility factors of different families can be found associated with different families of MPF complexes [60].

The process of conjugative DNA transfer proceeds in three steps: 1) DNA substrate processing, 2) substrate recruitment, and 3) translocation. The first step of the DNA processing for transfer (Dtr) is well conserved among the conjugative systems [64]. The relaxosome, which contains the relaxase and accessory proteins, is involved in DNA processing and delivery to the mating pair formation complex (Mpf). First the origin of transfer (*oriT*) is recognized by binding auxiliary proteins, like e.g., TraY and TraM of the F-plasmid [65]. These proteins stimulate the relaxase binding by facilitating the access to the *oriT* [66-68]. After the relaxase is bound to the *oriT* sequence, the relaxase cleaves one strand of the DNA [69]. After cleavage the relaxase often remains bound to the 5' end of the DNA via a covalent bond [70]. In a next step, the relaxosome is targeted to the coupling protein, which transfers the relaxosome complex to the Mpf. The exact mechanism of translocation is not clear. Different models for the substrate translocation have been proposed. The channel model suggests that the substrate is recruited by the coupling protein and transported across the membrane via the Mpf complex [71]. The shoot-and-pump model proposes that the unfolded relaxase and the DNA are transported independently from each other. DNA is pumped by the coupling protein (pump) and the relaxase is first unfolded and then translocated across the membrane via the Mpf complex (shoot) [72]. The ping-pong model postulates that the coupling protein is the only translocase, which recruits the T-DNA and transfers the relaxase to the chaperone for unfolding (ping) [71]. In the next step the chaperone protein transfers the unfolded substrate back to the coupling protein (pong) [54].

### **1.4 The Type IV secretion system encoded with the GGI**

Approximately half of the genes encoded within the GGI show homology to proteins involved in Type IV secretion. These genes are located in the first half of the GGI. The genes encoding the relaxase TraI and the coupling protein TraD are encoded in one operon with the *yaf* and *yaa* genes. *yaf* and *yaa* encode proteins of unknown function. The relaxase TraI and the coupling protein TraD belong to the Mob<sub>H</sub> mobilization family. The genes that encode for proteins involved in formation of the MPF complex are encoded in opposite direction of the genes involved in targeting. These proteins show homology to the proteins of the F-plasmid, and sequence analysis shows that the MPF complex belongs to the MPF<sub>F</sub> family. Between the genes that encode for known components of the MPF complex of the F-plasmid, also several genes which encode for proteins of unknown function are

identified (e.g. *yag*, *ybe*, *ybi* and *yhc*). The function of these genes/proteins is currently unknown. The GGI also encodes the TraA pilin protein. The N- and C- termini of TraA are circularized by TrbI after removal of the signal peptide by the leader peptidase LepB [73]. Such a circularization reaction was previously only seen for pili subunits with MPF complexes of the MPF<sub>T</sub> family [60].

A function of the T4SS encoded within the GGI was discovered by the group of Joseph Dillard. It was demonstrated that strains containing the T4SS secrete large amounts of DNA into the medium. Mutations of different genes of the Type IV secretion system (the *traI*, *traD*, *atla*, *traH*, *traN*, *traF*, *traL*, *traE*, *traK*, *traB*, *dscbC*, *traV*, *traC*, *traW*, *traU* and *traG*) genes led to a strong reduction of DNA secretion (Emilia Pachulec, thesis). Remarkably, the *traA* gene of our *N. gonorrhoeae* laboratory strain MS11 encodes a truncated variant of the TraA pilin, and neither TraA nor TrbI are essential for DNA secretion. Remarkably, deletion of *parA* and *parB* leads to the abolishment of secretion, while the rest of this region, from *exp1* – *yfeB*, encoding 35 hypothetical proteins, can be deleted without any effect on DNA secretion (Fig.1-2).

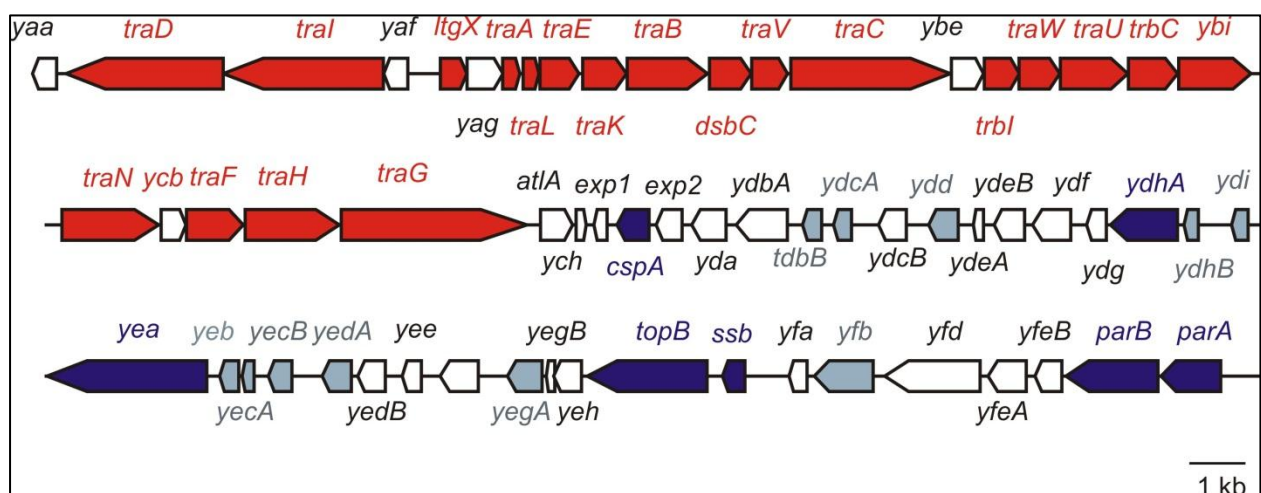


**Figure 1-2:** Map of the gonococcal genetic island (GGI) from *N. gonorrhoeae* strain MS11. Arrows represent ORFs, red colored arrows indicate ORFs with homology to T4SS, white arrows display ORFs of unknown function, dark blue arrows represent ORFs with homology to DNA processing proteins, blue arrows represent proteins with putative DNA processing activities (adapted from [40]).

Further experiments demonstrated that the secreted DNA was single stranded, and that the DNA was protected from its 5' end, most likely by the TraI relaxase bound to the DNA [74]. The secreted DNA can be taken up by neighboring cells. Comparison of the MS11 strain which contains the GGI, with the ND100 strain which was derived from MS11 but does not contain the GGI demonstrated that the transfer of chromosomal markers increased 500-1000 fold in the presence of the GGI (Emilia Pachulec, thesis).

## 1.5 Role of the GGI in host–pathogen interactions

Genetic islands often are important for pathogenicity [75] and provide selective advantages, such as enhanced pathogenicity, additional metabolism routes, or ecological fitness [75]. The most prominent example of a pathogenicity island encoding a T4SS is the *cytotoxin-associated gene (cag)*-pathogenicity island of *Helicobacter pylori*. This T4SS forms a syringe-like pilus structure for the injection of virulence factors such as the CagA effector protein into host target cells [76].

There is currently no direct evidence for the role of the GGI in pathogenesis, since the presence of the GGI does not correlate with any particular disease form. However, certain versions of GGI have been correlated with DGI [38]. The GGI is present with a similar frequency in gonococcal strains isolated from women with either symptomatic or asymptomatic infection and in clinical isolates causing both pelvic inflammatory disease and local infection [77].

However, it was recently found that gonococcal strains which contain the GGI can survive intracellularly in epithelial cells even if they lack a functional Ton complex [78]. The Ton-complex is involved in the uptake of iron. Strains that lack a functional Ton complex cannot survive in the absence of the GGI. The structural components of the T4SS were required for Ton-independent survival, whereas DNA secretion was not important. A functional Ton complex is required for iron import [79], which led to the suggestion that either iron can pass the cell membrane through the T4SS apparatus, or that an unknown factor is secreted via the T4SS, which chelates iron for the uptake by gonococci [78].

### 1.5.1 GGI in *N. meningitidis*

The GGI has also been identified in *N. meningitidis*. In contrast to 80 % of *N. gonorrhoeae* strains which possess the GGI, only 17.5 % of the *N. meningitidis* strains were found to carry the GGI. Five distinct meningococcal GGI types which have insertions or deletions relative to the gonococcal GGI were identified. In the majority of meningococcal strains insertions or deletions disrupted the genes for T4SS, and only two strains were found that carry GGIs with a nearly complete T4SS-encoding region. The GGI of *N. meningitidis* was also integrated into the *dif* sites of the meningococcal chromosome by the site-specific recombinase XerCD. This GGI can be excised and lost from the genome. In contrast to the gonococcal T4SS, the meningococcal T4SS does not secrete DNA, nor does it confer Ton-independent intracellular survival [80].

### 1.5.2 Regulation of GGI

Currently only very little is known about the regulation of DNA secretion in *N. gonorrhoeae*. It was shown that DNA secretion is increased in strains producing T4P, so called piliated strains. Microarray analysis demonstrated that a piliated strain showed increased expression of the gene for the putative type IV secretion coupling protein TraD and the relaxase TraI, whereas a nonpiliated variant showed increased expression of genes for transcriptional and translational machinery. It is proposed that the T4SS apparatus is made constitutively, while its activity is controlled through regulation of *traD* and *traI* [74].

### 1.5.3 Secretion of single stranded DNA

The DNA transported via conjugative Type IV secretion systems to other cells and the DNA transported via the T4SS of *N. gonorrhoeae* were both shown to be single stranded. When DNA forms the double helix structure, it is stabilized by hydrogen bonds and base-stacking interactions between the nucleotides [81]. Single stranded DNA deaminates significantly faster (> 100 times) than double stranded DNA and is much less stable than double stranded DNA [82]. ssDNA is also more sensitive to enzymatic digestion. In conjugative Type IV secretion systems, the single stranded DNA is replicated after it is transported to the acceptor. The single stranded Ti-DNA which is transported into the plant cell by the Type IV secretion system encoded on the *Agrobacterium tumefaciens* The pTi plasmid is bound and protected by VirE2 as soon as it arrives in the recipient cell. VirE2 is a single stranded DNA binding protein encoded on the Ti plasmid that is transported into the recipient plant cell. VirE2 is transported separately from the transported DNA and is kept in an unfolded state in the donor cell by its chaperone VirE1. Except for its role in the protection of the transported ssDNA, VirE2 was also proposed to aid in the transport of the ssDNA by pulling the single stranded DNA into the recipient cell after the VirE2 has bound [83].

### 1.6 Single-stranded DNA binding Proteins (SSBs)

In many other processes which involve DNA, like DNA recombination or DNA repair, the double helix is unwound and separated into the two complementary strands. At this state the DNA is sensitive to degradation by nucleases. All living organisms express a single-stranded DNA binding protein which binds and protects the single stranded DNA at these stages. Single-stranded DNA-binding proteins (SSBs) are essential proteins which are found in all kingdoms of life as well as in bacteriophages and adenoviruses [84-87]. SSBs bind with a high affinity to single-stranded DNA and with much lower affinity to other DNA forms [88]. Binding to ssDNA is essential sequence independent. All SSBs structures contain a very similar fold. This structural motif is called the Oligosaccharide/Oligonucleotide binding domain OB-domain or the OB-fold [89].

### 1.6.1 Oligosaccharide/Oligonucleotide binding domain

The family of nucleotide-binding OB-domains is characterized by a high extent of structural homology [90] and the absence of pronounced similarity of amino acid sequences. Individual OB-domains range from 70 to 150 amino acid residues [89]. The OB fold is found in all domains of life and also viruses suggesting that ssb proteins arose through gene duplication events from a common ancestral SSB protein [91,92]. The OB-fold consists of two three-stranded antiparallel  $\beta$ -sheets, where strand 1 is shared by both sheets [89]. As shown in Figure 1-3, the  $\beta$ -sheets pack orthogonally, forming a five-stranded  $\beta$ -barrel arranged in a 1-2-3-5-4-1 topology. OB-folds share several structural determinants [93].

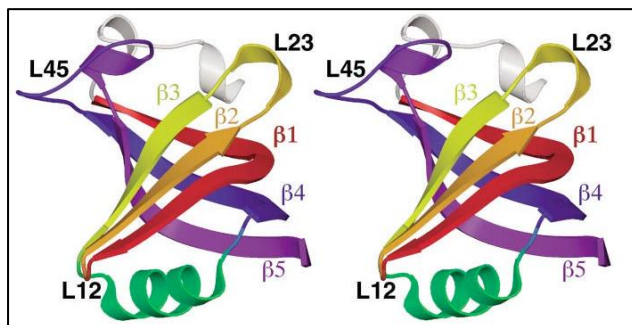


**Figure 1-3:** The canonical OB-fold domain. The OB-fold from AspRS is shown in stereo as representative of the OB-fold domain (reproduced from [90]).

A glycine (or other small residue) in the first half of the  $\beta 1$  and a  $\beta$ -bulge in the second half of  $\beta 1$  allow this strand to contribute to both  $\beta$ -sheets by curving completely around the  $\beta$ -barrel. A second glycine residue often occurs at the beginning of strand 4, breaking the  $\alpha$ -helix between strands 3 and 4. As shown in Figure 1-4, the canonical interface is augmented by the loops between  $\beta 1$  and  $\beta 2$  (referred to as L12),  $\beta 3$  and  $\alpha$  (L3 $\alpha$ ),  $\alpha$  and  $\beta 4$  (L $\alpha 4$ ), and  $\beta 4$  and  $\beta 5$  (L45). These loops define a cleft that runs across the surface of the OB-fold perpendicular to the axis of the  $\beta$ -barrel. The majority of nucleic acid—binding partners bind within this cleft, typically perpendicular to the anti-parallel  $\beta$ -strands, with a polarity running 5' to 3' from strands  $\beta 4$  and  $\beta 5$  to strand  $\beta 2$ . Loops presented by a  $\beta$ -sheet appear to provide an ideal recognition surface for single-stranded nucleic acids, allowing binding through aromatic stacking, hydrogen bonding, hydrophobic packing, and polar interactions [90].



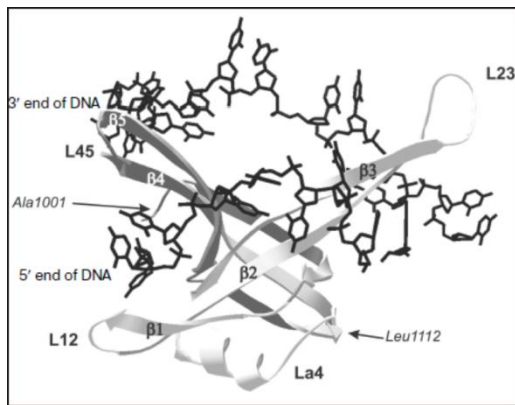


**Figure 1-4:** Tertiary structure of OB-domain of SSB from *E.coli* bound to 23-base oligonucleotide (reproduced from [88]).

Most of the interactions between the DNA and the protein occur via interaction of the protein with the nucleic acid nitrogen bases, whereas no interaction with the phosphate groups is found [94]. *Escherichia coli* SSB is the best studied member of this protein family. The 3D-structure of *Escherichia coli* SSB bound to two 35-mer ssDNAs was determined. This revealed several residues involved in ssDNA binding. Trp40, Trp54 and Phe60 make extensive interactions with the ssDNA in the SSB-ssDNA complex [95].

Binding of the DNA to the protein is promoted via stacking interactions between nucleotide residues and aromatic amino acid residues of the protein, as well as through non-polar interactions of ribose or nitrogen base rings with hydrophobic chains of amino acid residues [90,94].

Contrary to the OB-domain, the C-terminal part is less structured. It contains many negatively charged amino acid residues (in the eubacterial SSBs). The C-terminal region is important for cell survival *in vivo*. It is not involved in either DNA binding nor in oligomerization, but it is crucial for SSB interaction with different proteins [96]. The three-dimensional structure of the C-terminal domain was not resolved up to date [97].

### 1.6.2 Classification of SSBs

Many SSBs form higher oligomeric structures, where the OB-folds play an important role in the oligomerisation of the subunits. The large family of SSBs has been divided in three major subgroups in accordance with their oligomeric state [88]. The first major subgroup consists of the eubacterial SSBs. Most eubacterial SSBs contain a single OB-fold, but the functional form of these proteins requires oligomerization of the single monomers to form homotetramers. In addition to the DNA-binding activity, the OB-domain is involved in formation of the homotetrameric structure [88]. The second major subgroup is formed by SSBs that form homodimers. Currently only a few eubacterial

(the SSBs from the extreme thermophiles *Thermus thermophilus*, *Thermus aquaticus* and *Deinococcus radiodurans*), some euryarcheal SSBs (replication protein A from *Methanosarcina acetivorans* and *Methanopyrus kandleri*) and some SSB proteins from bacteriophages (gp32 of phage T4, gp2.5 of phage T7) belong to this subgroup [98-100]. The third major subgroup of SSB proteins includes heterotrimeric complexes. Such structural organization is characteristic for most eukaryotic SSBs, often also known as replication protein A (RPA). (Most mitochondrial SSBs are an exception to this rule and form functional dimers, similar to the eubacterial SSBs.) Eukaryotes studied to date possess the RPA trimeric complex, with subunits of 70 kDa (RPA1), 29 kDa (RPA2), and 14 kDa (RPA3) [101,102]. The RPA1 subunit contains four structurally related domains and is responsible for high affinity ssDNA binding. In addition to ssDNA-binding, RPA1 has been shown to interact with a number of cellular proteins that regulate the cell cycle, DNA repair and recombination. RPA3 does not bind to ssDNA but is required to form the stable heterotrimer [84]. In contrast to the RPA1 proteins which are conserved among various species, the RPA2 subunit appears to be poorly conserved. RPA2 is thought to have a regulatory function, thought to be controlled by phosphorylation [103]. Remarkably, the SSBs found in Archaea differ in the two major subdivisions of the euryarchaea and the crenarchaea. The euryarchaea have a eukaryotic-type RPA [104] while the crenarchaea resemble the bacterial SSB proteins [105].

Some recently characterized SSBs do not fit in to the standard classification. For example proteins from *Methanococcus jannaschii* and *Methanobacterium thermoautotrophicus* contain four and five OB-domains and a zinc finger domain [104,106].

Another interesting exception is the SSB from *Sulfolobus solfataricus*. This is the only known monomeric SSB. The OB fold is distinct from that from *Escherichia coli* SSB and shares closer structural similarity with the DNA-binding domain of RPA [107]. Despite the monomeric structure the SSB of *Sulfolobus solfataricus* seems to form tetramers upon DNA binding, which is not highly co-operative [108].

### 1.6.3 Binding of SSBs to ssDNA

The binding behavior of SSBs is often dependent on the conditions and many SSBs can bind ssDNA in different modes. For the well-studied SSB from *E.coli*, two types of complexes with ssDNA have been identified. These DNA binding modes are denoted as the (SSB)<sub>65</sub> and (SSB)<sub>35</sub> modes. In the (SSB)<sub>65</sub> mode, ~65 –nucleotides of ssDNA wrap around and interact with all four subunits of the tetramer. The (SSB)<sub>65</sub> binding mode is a limited co-operativity mode in which SSB shows only some tendency to form protein clusters along ssDNA. This binding mode is observed at salt concentrations (>0,2 M NaCl or > 3mM MgCl<sub>2</sub>) and low protein binding density [109-111]. In the (SSB)<sub>35</sub> mode, ~35-

nucleotides interact with only two of the four subunits. The  $(SSB)_{35}$  binding mode is a high unlimited cooperativity mode in which the SSB forms long protein clusters along DNA. This binding mode is preferred at low monovalent salt concentrations (<10 mM NaCl) and high protein to DNA ratios (Fig. 1-5) [109-111].

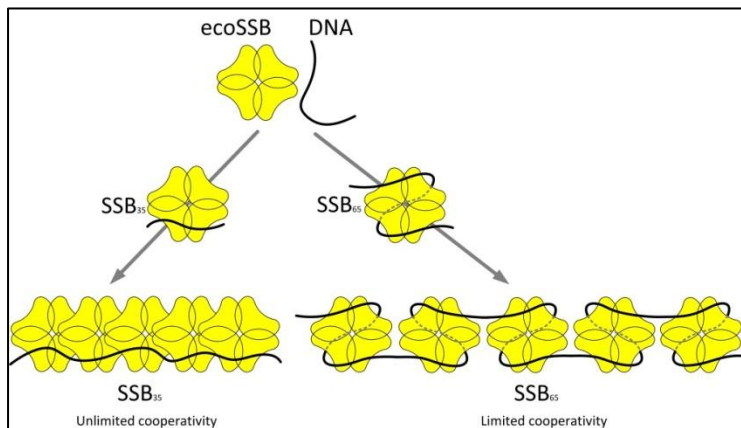


**Figure 1-5:** A hypothetical model of the  $SSB_{35}$  and  $SSB_{65}$  type complex formation upon SSB interaction with the ssDNA (adapted from [112])

The binding modes are flexible and the transitions among these different binding modes can be modulated by the monovalent salt concentration, divalent and multivalent cations, as well as the SSB to ssDNA concentrations [113-115].

#### 1.6.4 Additional functions of SSBs

Next to their essential role in DNA replication, recombination and repair, SSBs fulfill additional functions. Some naturally competent bacteria like *Bacillus subtilis* and *Streptococcus pneumoniae* contain next to the main SSB a second SSB. For example, in the genome of *Bacillus subtilis* two paralogous SSB genes are encoded, *ssb* and *ywpH*. Whereas SSB is essential for cell survival, YwpH is required for natural transformation [116]. These paralogous proteins have distinctive expression patterns. Also in *Haemophilus influenzae*, HI0250, the second SSB protein encoded within the genome is induced 3.4 fold when the cells become naturally competent [117]. Another example is *Streptococcus pneumoniae*, whose genome encodes two paralogues, designated SsbA and SsbB. The SsbA protein is expressed constitutively whereas SsbB is induced during competence [118,119]. Benam *et. al.* have suggested that the SSB from *Neisseria meningitidis* might also have a functional role in transformation [120]. A second additional role for SSBs is found in conjugative plasmids. Nearly all conjugative plasmids encode a SSB homolog [121]. These plasmid *ssb* genes appear to be coordinately regulated with the *tra* regulon (conjugal transfer) genes, but their presence does not appear to be necessary for conjugal transfer of the plasmids involved [122,123]. They seem not to be

necessary for conjugal transfer of the plasmids, but might be involved in plasmid stability [124]. Thus the exact function of these SSBs is still unclear.

### **1.7 Biofilms**

Biofilms are defined as surface-attached microbial communities embedded in a self-produced extracellular matrix of polymeric substances and are considered the favored lifestyle of bacteria in natural and clinical settings [125]. About 80% of the world's microbial biomass resides in biofilms and more than 75% of human microbial infections are assisted by the stable formation of biofilms [126]. Biofilms confer a number of survival advantages to bacteria, including increased resistance to antimicrobial agents [127].

The formation of biofilms protects the cells from the environment. The EPS matrix provides protection from a variety of environmentally stresses, such as UV radiation, pH shift and osmotic shock. The water channels in the biofilm enable the exchange of nutrients and metabolites with the bulk aqueous phase. Bacteria involved in biofilm formation undergo a transition from a planktonic and motile form to an aggregated mode that is essentially sessile and embodied in an exopolymer matrix. Planktonic bacteria first localize on a suitable surface for attachment. This attachment is initially reversible and becomes irreversible once the bacteria start to produce exopolymeric substances (EPS). This EPS enables the maturation of the biofilm. The maturing biofilm begins to take on a 3-dimensional shape. The last stage in the cycle is the detachment of bacteria from the biofilm [128].

EPS produced by different biofilm communities are very diverse in their composition. Many different exopolymers like exopolysaccharides, secreted proteins, membrane vesicles and extracellular DNA are major components of the EPS. But also outer membrane proteins and a variety of cell appendages like fimbriae, pili, flagella may function as a part of the biofilm matrix [129]. Recent studies indicate that not only exopolysaccharides but also extracellular DNA can play a key role in the initial establishment of biofilms [130].

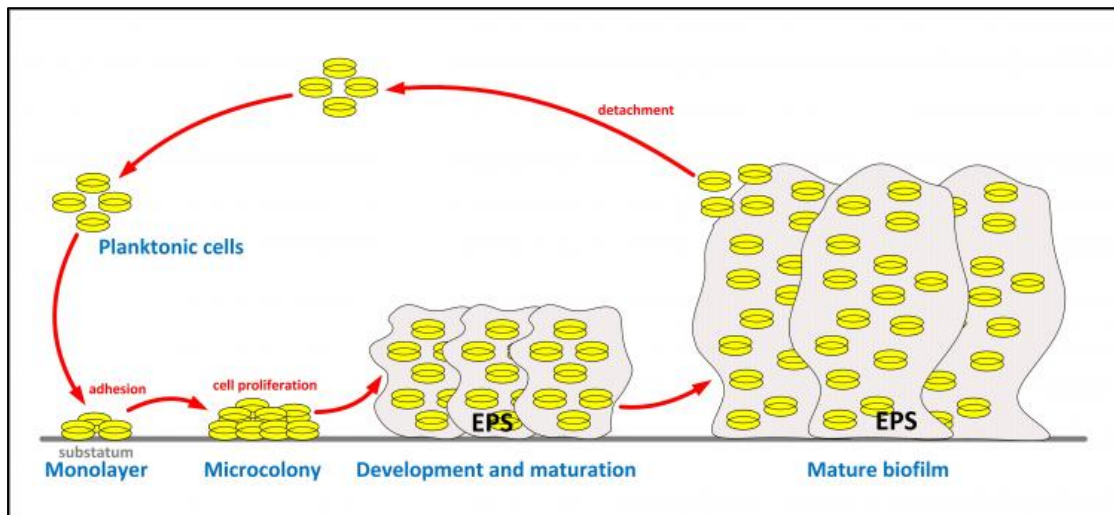


**Figure1-6:** Scheme of biofilm formation.

### 1.7.1 Extracellular DNA as important matrix component in biofilms

During the last decade, extracellular DNA was discovered as a key component for initial biofilm formation for *Streptococcus pneumoniae*, *Enterococcus faecalis*, *Staphylococcus aureus*, *Staphylococcus epidermidis*, *Haemophilus influenzae*, *Neisseria meningitidis*, *N. gonorrhoeae* and many others [131-137]. Evidence that extracellular DNA may function as a cell-to-surface adhesin and/or cell-to-cell adhesin during the initial phase of biofilm formation was first presented by Whitchurch *et.al.* [130]. They showed that biofilm formation of *P. aeruginosa* was inhibited by the presence of DNase I. A structural role of eDNA has been demonstrated in the biofilm of many bacterial species both Gram-negative such as *Pseudomonas aeruginosa* [130,138] and Gram-positive such as *Staphylococcus aureus*, *Streptococcus pneumoniae*, *Bacillus cereus* and *Listeria monocytogenes* [137,139-141]. For example extracellular DNA was shown to be a crucial structural matrix component of *Bordetella* biofilms when the biofilm was isolated from patient and when the biofilms were grown under laboratory conditions. But in contrast to other gram negative bacteria DNase I treatment disrupted also mature *Bordetella* biofilm grown under both static and hydrodynamic conditions. These findings suggest that *Bordetella* utilizes external DNA as a key component to confer structural stability to biofilms [142]. Next to important roles for external DNA in initial attachment and as a structural component, other roles for DNA in the biofilm have also been suggested. Several studies have shown that extracellular DNA can provide nutrition and energy for sessile cells [143,144]. Furthermore, it is very likely that extracellular DNA not only stabilizes biofilms, but also plays a role in exchange of genetic material within the biofilm [145-147].

DNA can be released into the biofilm via several different mechanisms. The most common mechanism by which extracellular DNA is released into the biofilm is autolysis. For *S. epidermidis* it

was demonstrated that the major autolysin, AtlE which is important for eDNA release, is indispensable for primary attachment and biofilm development [148]. Different mechanisms that induce autolysis have been identified. For example, in *P. aeruginosa* a part of the population lyses under the control of a quorum sensing system, while in *E. faecalis* autolysis occurs via a fratricidal mechanism. In *S. aureus* autolysis originates from an altruistic suicide, i.e., a programmed cell death similar to apoptosis of eukaryotic cells. DNA can however also be released via active secretion, as has been observed in *P. aeruginosa* and in *N. gonorrhoeae*. The release of vesicles containing DNA and prophage-mediated lysis of a sub-population of cells are further possible sources of extracellular DNA. The amount of extracellular DNA is further regulated by nucleases.

### 1.7.2 Biofilm formation by *Neisseria gonorrhoeae*

Microscopic examination of biopsied human cervical tissue showed that gonococci are capable to form biofilms during natural cervical infection [149]. Further studies revealed the ability of *N. gonorrhoeae* to form biofilms both on glass, on primary urethral epithelial cells and on cervical epithelial cells and in continuous flow-chamber systems [150]. Those data strongly suggest that *N. gonorrhoeae* biofilms do not only contribute to persistent infection but are also directly associated with the absence of symptoms in women [151]. *N. gonorrhoeae* lacks the genes for production of exopolysaccharides, thus the biofilm matrix must be stabilized by a number of other components [112]. Microscopic examinations on *N. gonorrhoeae* biofilms showed bacteria embedded in a continuous matrix containing water channels and membranous structures, which are derived from the outer membrane [150]. Another study demonstrated that outer membrane blebbing is an important factor in gonococcal biofilm formation and that hypo- or hyperblebbing directly affects biofilm thickness and density [149].

Comparison of transcriptional profiles of planktonic *N. gonorrhoeae* cells with *N. gonorrhoeae* cells grown in biofilms demonstrated that 3,8 % of the genome was differently regulated. Genes required for anaerobic respiration (*aniA*, reductase, *ccp*, cytochrome c peroxidase and *norB*, nitric oxide reductase) were more highly expressed during biofilm growth, while other genes involved in respiration with NADH as an electron donor (the *nuo* operon) were more highly expressed during planktonic growth. The expression of these genes was shown to be required for the mature biofilm formation over glass and human cervical cells [151]. It was demonstrated that anaerobic respiration occurs predominantly in the substratum of gonococcal biofilms and nitric oxide (NO) can be used in the biofilm as a substrate for anaerobic growth. On the other hand NO can also stimulate biofilm dispersal when it is present at a sublethal concentrations [152]. Many genes involved in oxidative stress tolerance were shown to be important for efficient biofilm formation [151],[153-156].

Similar to other well studied bacterial biofilms, also the *N. gonorrhoeae* biofilm was shown to contain large amounts of DNA. The possible sources of the extracellular DNA in gonococcal biofilms are diverse. Gonococci are well known to be highly autolytic. For *N. meningitidis*, it was demonstrated that the release of DNA in biofilms was mediated by lytic transglycosylases, cytoplasmic N-acetylmuramyl-L-alanine amidases and at later stages of biofilm formation, by outer membrane phospholipase A. Furthermore, the release of membrane blebs, which are associated with large amounts of DNA is also important for gonococcal biofilm formation. The gonococcus expresses a thermonuclease Nuc, which is homologous to the staphylococcal thermonuclease. Deletion of *nuc* results in the formation of a significantly thicker biofilm containing more biomass and more extracellular in comparison to the wild-type *N. gonorrhoeae* biofilms [137]. Another source of DNA within the biofilm might be the DNA secreted by the unusual Type IV secretion system (T4SS) within a horizontally acquired region, the gonococcal genetic island (GGI). This secretion system and its function in biofilm formation is one of the topics of this thesis.

### 1.7.3 Visualization of eDNA in biofilms

The most advanced technique to study microbial biofilms is the use of a confocal laser scanning microscope (CLSM). Using this technique, different molecules are detected by fluorescence. Currently many different fluorescent markers are available to detect the DNA. Most of the DNA within a biofilm is located inside the cells. To specifically visualize DNA outside of the cell, fluorescent probes which cannot penetrate the intact membrane of living bacteria can be used. For this purpose, currently for example propidium iodide, ethidium bromide and 7-hydroxy-9H-(1,3-dichloro-9,9-dimethylacridin-2-one) (DDAO) can be used.

### 1.8 Scope of the thesis

This study describes first the characterization of the single-stranded DNA binding protein SsbB encoded on the GGI, secondly the development of the novel method on the basis of the SSB for the visualization of the single-stranded DNA in the biofilms of different *N. gonorrhoeae* strains, and finally the effect of secreted ssDNA on biofilm formation by *N. gonorrhoeae*.

The first part of the study provides a detailed biochemical characterization of the single-stranded DNA binding protein SsbB, encoded on the GGI. The role of the SsbB encoded within this region has not been previously characterized. It is shown that SsbB is part of conserved homologous cluster, found in several other proteobacteria. The physiological role of this protein belonging to a novel class of SSBs is characterized and its function is studied biochemically.

In the second part we present the development of a novel method where SSB is used as a biosensor for the visualization and detection of the single-stranded DNA. DNA is the structural component of biofilms of many species. Whether this DNA is present in a single stranded or double stranded form and whether other components are bound to this DNA is currently still unknown. Single-stranded DNA binding proteins (SSBs) bind to ssDNA with high specificity but without clear sequence specificity and bind to dsDNA only with much lower affinity. Fluorescently labeled SSB were used to specifically detect ssDNA. This technique could be used for the planktonic cultures and for the biofilms of different species as well.

The third part deals with the role of the extracellular single- and double-stranded DNA in the biofilm formation of *N. gonorrhoeae*. Biofilms formed by *N. gonorrhoeae* contain large amounts of DNA. It has been proposed that this DNA is either released via autolysis or via membrane blebs and that an endogenous nuclease controls its incorporation into the biofilm. Many clinical isolates of *N. gonorrhoeae* contain a GGI which encodes a Type IV Secretion System (T4SS). This T4SS was shown to secrete single stranded DNA. By specific degradation of either ssDNA or dsDNA during and after the biofilm formation we revealed the important role of the ssDNA for the initial biofilm formation.



## Chapter 2

### Characterization of the Single Stranded DNA binding protein SsbB encoded in the Gonococcal Genetic Island

Samta Jain <sup>1,4</sup> \*,  **Maria Zweig**  <sup>4</sup> \*, Eveline Peeters <sup>2</sup>, Katja Siewering <sup>4</sup>, Kathleen T. Hackett<sup>3</sup>, Joseph P. Dillard <sup>3</sup> and Chris van der Does<sup>1,4</sup>#

\* Both authors contributed equally

<sup>1</sup> Department of Microbiology, Groningen Biomolecular Sciences and Biotechnology Institute, University of Groningen, Groningen, The Netherlands.

<sup>2</sup> Research Group of Microbiology, Department of Sciences and Bio-engineering Sciences, Vrije Universiteit Brussel, Brussel, Belgium.

<sup>3</sup> Medical Microbiology and Immunology, University of Wisconsin, Madison, USA.

<sup>4</sup> Department of Ecophysiology, Max-Planck-Institute for terrestrial Microbiology, Marburg, Germany.

Published in PLoS One. 2012;7(4):e35285. Epub 2012 Apr 19.

## 2.1 Aim of the study

*N. gonorrhoeae* is a highly naturally competent organism [52,157]. It encodes a chromosomal SSB that showed DNA binding properties comparable to *E. coli* SSB [158] and a SSB (SsbB) that is encoded within a 57 kb horizontally acquired genetic island called the Gonococcal Genetic Island (GGI). This GGI is found in 85 % of the clinical isolates [38]. Approximately half of the GGI encodes a T4SS which is involved in the secretion of ssDNA directly into the medium [33]. The secreted DNA is rapidly taken up by the highly active competence system of *Neisseria* species and incorporated in the genome. The presence of the T4SS in the GGI increases the transfer rate of chromosomal markers approximately 500 fold [38]. The function of the other half of the GGI is currently unknown. It contains mostly hypothetical proteins, but also putative DNA processing proteins like partitioning proteins *parA* and *parB*, single stranded DNA binding protein *ssbB*, DNA topoisomerase *topB*, DNA helicase *yea* and DNA methylases *ydg* and *ydHA* [33].

The role of the SsbB encoded within this region has not been characterized. We show that SsbB is part of conserved homologous cluster, found in several other proteobacteria.

This chapter presents the biochemical characterization of the GGI-encoded ssDNA binding protein, SsbB.

The physiological characterization of the SsbB was performed by Samta Jain and the results of the physiological characterization are presented in the appendix.

## 2.2 Results

### 2.2.1 Sequence Analysis

The SSB encoded within the GGI was previously annotated as SsbB on the basis of 28 % identity to *Xylella fastidiosa* XF1778 SsbB [33]. Based on the nucleotide sequence, the predicted SsbB monomer has a length of 143 amino acid residues and a calculated molecular mass of 16,36 kDa. SsbB contains an N-terminal conserved OB fold in the region between residues 5 and 108 [89] and a relatively short disordered acidic C-terminus. SsbB shares only relatively low sequence similarity with the essential chromosomal SSBs from e.g. *E. coli* and *N. gonorrhoeae*. Figure 2-1 shows a sequence comparison of different ssDNA binding proteins with SsbB encoded on the GGI.

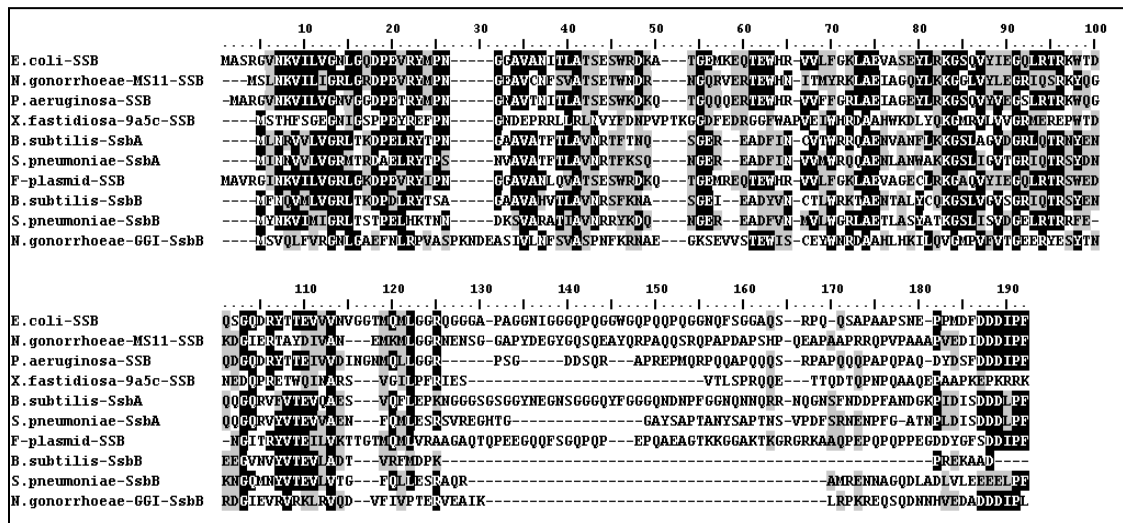


**Figure 2-1: Sequence comparison of different ssDNA binding proteins.** (*Escherichia coli* SSB (GenBank: AAA24649.1), the chromosomal SSB of *Neisseria gonorrhoeae* MS11 (GenBank: ZP\_06132898.1), *Pseudomonas aeruginosa* SSB (GenBank: AAG07620.1), *Xylella fastidiosa* 9a5c SSB (NP\_299066.1), *Bacillus subtilis* SsbA (ADM40106.1), *Streptococcus pneumoniae* SsbA (GenBank: ABJ55175.1), F-plasmid SSB (GenBank:NP\_061439.1), *B. subtilis* SsbB (ADM39609.1), *S. pneumoniae* SsbB (GenBank: ABJ54110.1) and SsbB of *N. gonorrhoeae* MS11. Identical residues are highlighted in black, similar residues are highlighted in grey.

Four essential aromatic residues Trp40, Trp 54, Phe 60 and Trp 88 participate in binding of ssDNA via stacking interactions in the EcoSSB-DNA complex [95]. These residues are conserved in most SSB families as Phe/Tyr/Trp residues. The corresponding residues in SsbB are Lys42, Trp56, Trp62 and Tyr90. The glycine residues in the glycine-rich hinge of EcoSSB (Gly125, Gly 128 and Gly 129) are not conserved in SsbB. Remarkably, the C-termini of the paralogous SSBs from *B. subtilis*, *S. pneumoniae* and SsbB from *N. gonorrhoeae* lack a large glycine rich domain.

Analysis of the genetic surroundings of the closest homologs of SsbB revealed that SsbB is located in a cluster of homologous genes that is found in several proteobacteria (Figure 2-2).

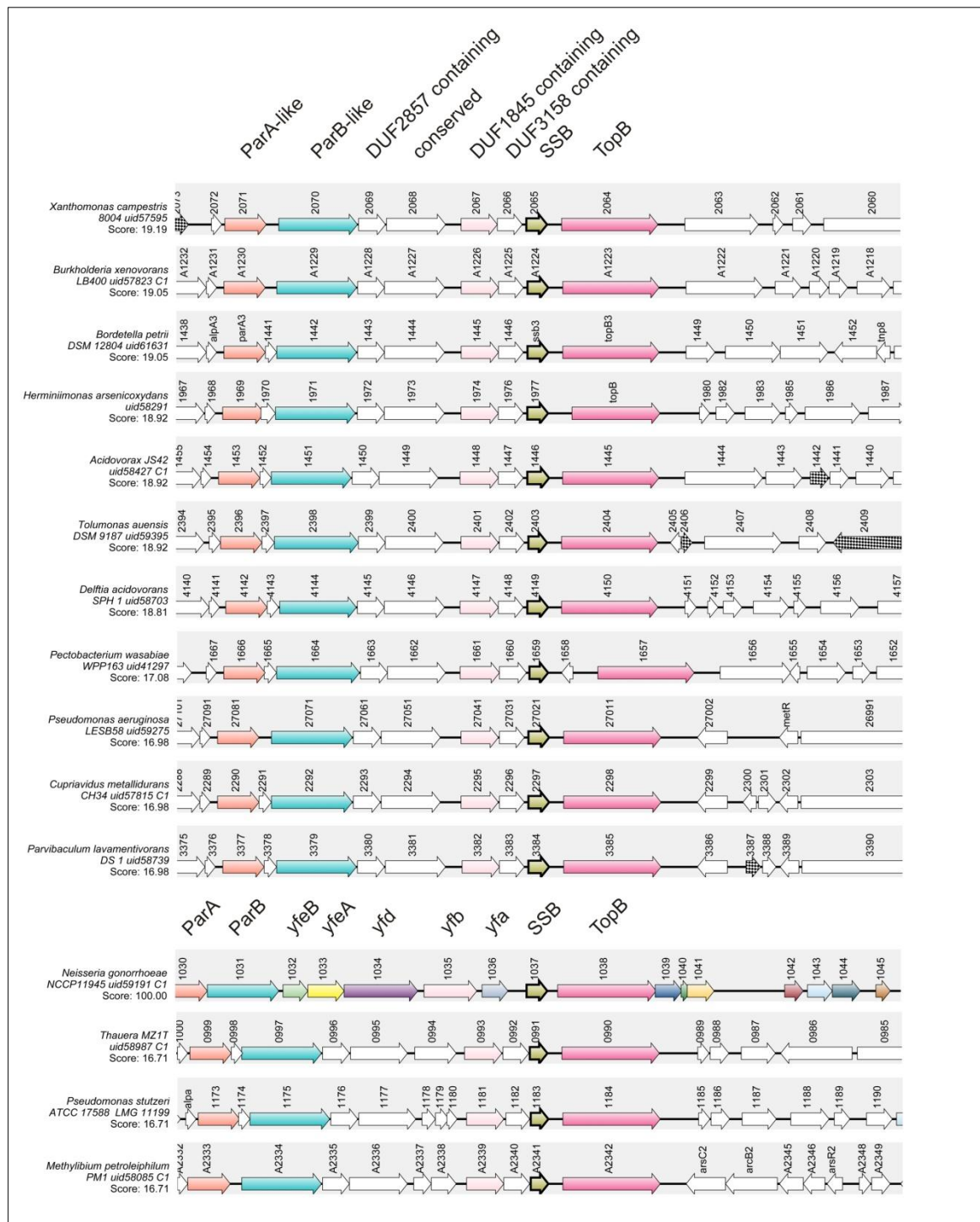


**Figure 2-2:** Comparison of the genetic environment of homologs of SsbB of *N. gonorrhoeae* reveals that the *ssbB* gene is located within a cluster conserved in several proteobacteria. Shared synteny was determined and the figure was composed using the Absynte website (<http://archaea.u-psud.fr/absynte>). Homologous proteins are indicated using similar colors.

Remarkably, this cluster contains the DNA partitioning proteins ParA and ParB, four conserved hypothetical proteins containing different domains of unknown functions and a Topoisomerase. Three of the four conserved proteins contain conserved domains of unknown function (DUF2857, DUF1845 and DUF 3158). These clusters are often found at the borders of large genetic islands, like the PEGI-3(SG), PEGI-2(C) and the *clc*-like genetic islands found in *Pseudomonas aeruginosa* and other organisms [159,160]. The cluster found within the GGI contains next to SsbB, the ParA and ParB proteins, the Topoisomerase, the proteins with the DUF 2857 (YfeB) and the DUF1845 (Yfb) domain. YfeA, Yfd and Yfa show only very little to no homology to the other two conserved hypothetical proteins. Other clusters in which some of the proteins are missing are also identified in other species. The sequence conservation of these SSBs and their genetic surroundings suggests that they form a novel class of SSBs with a possible role in partitioning, stability or transport of the DNA of the genetic islands in which they are encoded.

To determine the relation of these SSBs encoded within genetic islands with other SSBs, a phylogenetic tree was constructed. The sequences used to generate this tree were based on 78 ssDNA-binding protein sequences, which were recently used to identify different subfamilies of eukaryotic, crenarchaeal, euryarchaeal, mitochondrial, gram-negative and gram-positive bacteria SSBs and a subfamily proposed to consist exclusively of the proteins from lactococcal bacteriophages [161]. The sequences of proteins with strong homology to *N. gonorrhoea* SsbB, encoded within genetic islands and their chromosomal homologs were included in this set, and a phylogenetic tree was created (Figure 2-3).



a possible role in partitioning, stability or transport of the DNA of the genetic islands in which they are encoded.

To further characterize a member of this protein family, the operon structure and the expression levels of *ssbB* have been determined by Katja Siewering (see appendix). It was demonstrated that the *ssbB*, *topB*, *yeh*, *yegB* and *yegA* genes form an operon (Data not shown). It was further shown that the *parA*, *parB*, *yfeB* and *yfb* genes, although they are often found genetically linked to *ssb*, are not encoded in the same operon. Furthermore expression of the operon containing *ssb* seems constitutive and no differences in the expression levels of the *ssbB* and *topB* genes were observed between piliated and non-piliated cells.

Since it was determined that the *ssbB* gene is expressed in *N. gonorrhoeae*, we set-out to further characterize SsbB. Many SSBs, independently of whether they were encoded on plasmids or on the chromosome [121,122,162,163] have been shown to be able to complement the essential chromosomal *E. coli* *ssb* gene for cellular viability. In collaboration with the group of prof. Joseph Dillard, it was tested whether SsbB could complement the *E. coli* SSB. Shortly, *ssbB* was cloned downstream of a lac promoter in an *E. coli* expression vector, and tested using a complementation assay described previously [162]. Remarkably, SsbB was not able to complement the *E. coli* *ssb* mutation. Since this strongly differs from other characterized SSBs, and none of the members of this cluster of SSB proteins have been studied, we further set out to characterize the function of *N. gonorrhoeae* SsbB.

### **2.2.2 Overexpression, purification and determination of the oligomeric state of SsbB**

SsbB was expressed in *E. coli* as the native protein and with N-terminal OneSTrEP- and His-tags. The three proteins were purified to homogeneity (> 99% purity as assayed by Silver staining, data not shown) with yields of 1.7, 3.5 and 10 mg/g wet cells for native, His-tagged and OneSTrep-tagged SsbB respectively. Analysis by gel filtration chromatography revealed single peaks for the WT and N- His- and OneSTrEP tagged proteins respectively, indicating that all three proteins form stable tetramers (Figure 2-4).

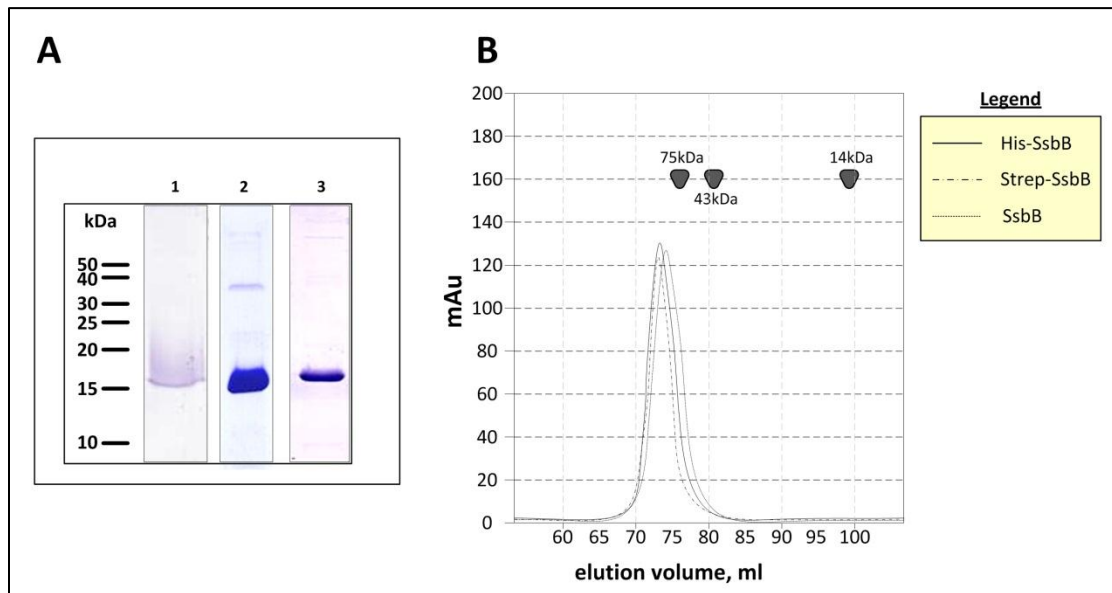


**Figure 2-4:** Purification and gel filtration of different SsbBs proteins. A) SDS-PAGE Analysis of 1 = SsbB, 2 = His-SsbB, 3 = Strep-SsbB. B) All three proteins eluted as tetramers from the SD200 gel filtration column. The positions of the various markers for both the gel filtration and the SDS-PAGE are indicated.

Attempts to destabilize the tetramer by incubations at increasingly higher temperatures or with increasing concentrations of chaotropic agents like guanidinium and urea led to aggregation of the protein before any monomeric proteins could be detected (data not shown), demonstrating that SsbB forms a stable tetramer that is difficult to dissociate.

In a next step it was attempted to fluorescently label SsbB using cysteine specific fluorescent probes incorporated at different positions. Therefore, the single native cysteine at position 56 was changed to a serine, and several other residues were mutated to cysteines. Remarkably, SsbB was shown to be very sensitive to mutations: attempts to exchange the native cysteine to a serine led to formation of inclusion bodies, and complete loss of soluble protein. The same result was observed after deletion of the last 32 amino acids of the C-terminus. Remarkably, these last 32 amino-acids are not part of the OB fold, and show no conservation with other SsbBs (Figure 2-5). We therefore conclude that SsbB is remarkably sensitive to mutations and that the native Cysteine is indispensable for the correct folding and stability.



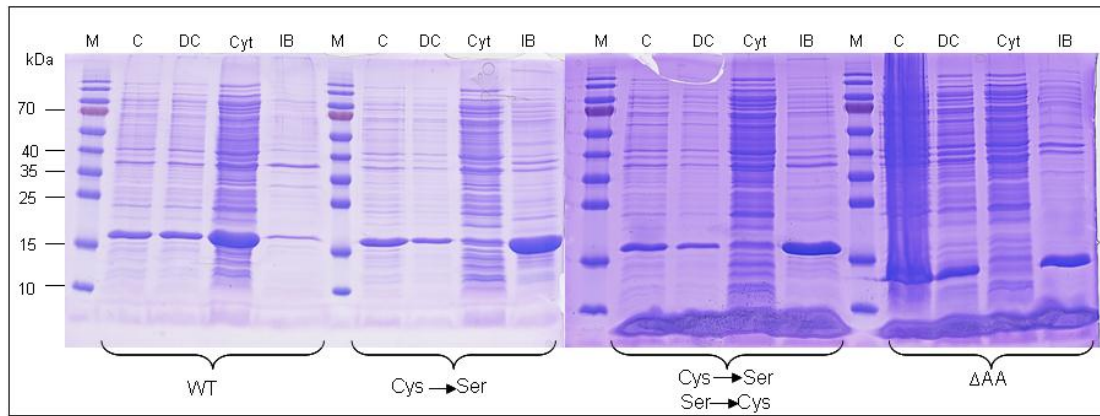


**Figure 2-5:** SDS-PAGE analysis of the purified SsbB mutants. Abbreviations: M = Page Ruler prestained protein Ladder; C = cells, D = disrupted cells; Cyt = cytosolic fraction; I = inclusion bodies, WT = native SsbB, Cys-Ser = SsbBC56S, Cys-Ser Ser-Cys = SsbBC56S/S128C,  $\Delta$ AA = SsbB with truncated last 32 amino acids.

### 2.2.3 SsbB binds to fluorescently and radioactively labeled ssDNA with high but different affinities

To determine whether SsbB binds ssDNA, fluorescently Cy3-labeled dT<sub>35</sub> and dT<sub>75</sub> oligonucleotides were incubated with increasing amounts of purified SsbB and used in electrophoretic mobility shift assays (EMSA). The 35-mer Cy3-labeled oligonucleotide showed a single mobility shift upon binding to SsbB (Figure 2-6 A). Binding occurred with a stoichiometry of one dT<sub>35</sub> oligonucleotide per tetramer. A similar experiment performed with the Cy3-labeled 75-mer showed two complexes with different mobilities (Figure 2-6 B).

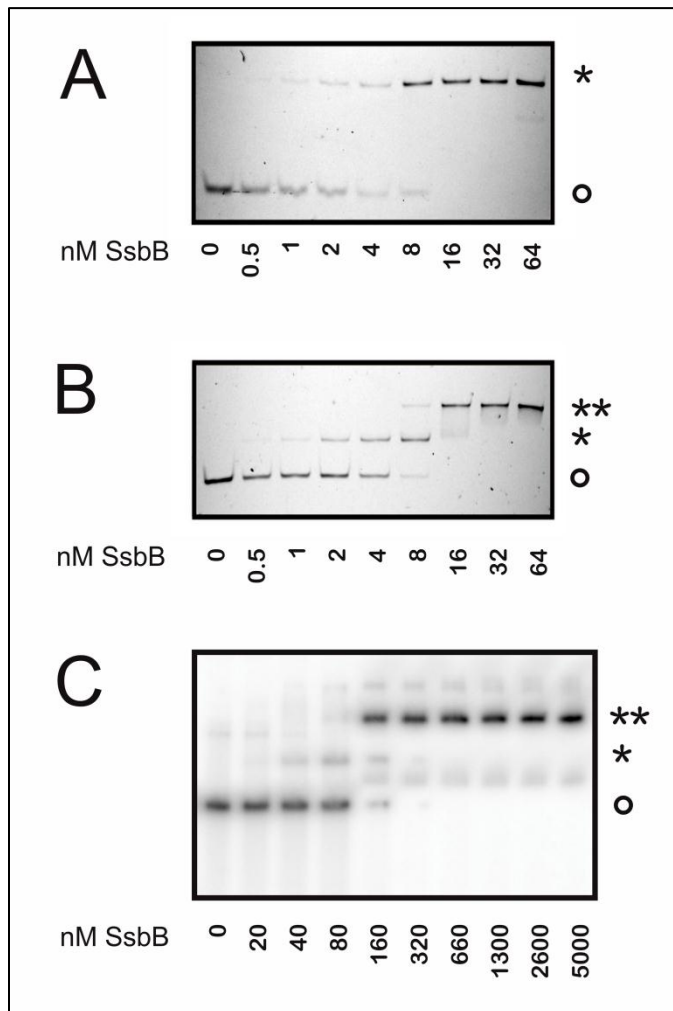


**Figure 2-6: Analysis of the binding mode of SsbB by electrophoretic mobility shift assays.**

A) 8 nM of fluorescently labeled dT<sub>35</sub> and B) dT<sub>75</sub> oligonucleotides were incubated in SBA buffer (10 mM NaOH, 2 mM EDTA, pH 7.5) with increasing concentrations (0-64 nM) tetrameric SsbB. The reactions were separated by polyacrylamide gel electrophoresis and were visualized using a LAS-4000 imager (Fujifilm). C) 2 nM of a <sup>32</sup>P- labeled dT<sub>75</sub> oligonucleotide was incubated with increasing concentrations (0-5000 nM) tetrameric SsbB in SBA buffer. The reactions were separated by polyacrylamide gel electrophoresis and were visualized by autoradiography. The circle (o) indicates the free oligonucleotide, while one (\*) or two (\*\*) asterixes represent oligonucleotides bound with one or two SsbB tetramers.

The first complex was formed at a (SsbB)<sub>4</sub>/dT<sub>75</sub> ratio of 1 and the second complex was formed at a (SsbB)<sub>4</sub>/dT<sub>75</sub> ratio of 2, demonstrating that the first complex contains one SsbB tetramer and the second complex contains two tetramers bound to the dT<sub>75</sub> nucleotide. Stoichiometric binding was observed at 8 nM for both the dT<sub>35</sub> and dT<sub>75</sub> oligonucleotides, which is a higher affinity than is generally reported for other SSBs in EMSAs [164],[165]. We therefore performed a similar experiment with a radioactively labeled dT<sub>75</sub> oligonucleotide (Fig. 2-6 C). Again two different complexes, representing one and two SsbB

tetramers bound to the  $T_{75}$  oligomer were observed. The complexes were however formed at a concentration of approximately 100 nM  $(SsbB)_4$ , which is similar to affinities observed for other SSBs, but 10-fold lower than the affinity observed for the fluorescently labeled oligonucleotide. This demonstrates that the presence of a fluorescent label on an oligonucleotide can strongly influence the binding properties. Since the observed affinity was affected by the presence of the fluorescent probe, we also studied the effects of other components on the observed affinity. No large differences were observed when the binding reactions were performed using either SBA, Tris-HCl or Tris-Acetate based buffers supplemented with either 0 or 10 mM  $MgCl_2$  and/or 10, 200 or 500 mM NaCl. To compare the effects of N-terminal tags on ssDNA binding, the EMSAs described above were also performed with native SsbB, His-tagged SsbB and OneSTrEP-tagged SsbB. No differences were found between native SsbB and OneSTrEP-tagged SsbB, but His-tagged SsbB bound ssDNA with a lower affinity (Figure 2-7).

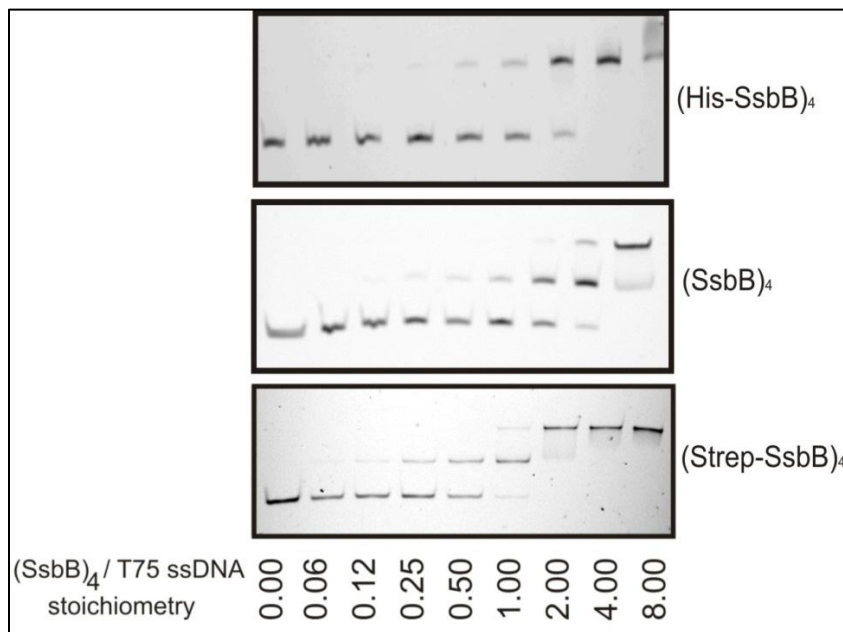


**Figure 2-7: EMSA with His-SsbB, SsbB and Strep-SsbB bound to Cy3 labeled  $T_{75}$ .** Increasing concentrations of SsbB proteins (His-tagged, Strep-tagged and tag-less) were incubated with 8nm Cy3 labeled  $T_{75}$ -mer. The reactions were separated by polyacrylamide gel electrophoresis and were visualized using a LAS-4000 imager (Fujifilm).

Therefore, the following experiments were only performed using native or OneSTrEP-tagged SsbB.

#### 2.2.4 Quenching of intrinsic tryptophan fluorescence

SsbB has two tryptophane residues (Trp56 and Trp62) in the OB fold domain, allowing an analysis of DNA binding by tryptophan fluorescence quenching.

Fluorescence titrations with poly(dT) under low (20 mM NaCl), medium (200 mM NaCl) and high (500 mM NaCl) salt conditions and in the presence of 10 mM MgCl<sub>2</sub> are shown in Figure 14A). The average length of the poly(dT) was approximately 1000 bases as estimated by agarose gel electrophoresis. When binding to poly(dT), the intrinsic tryptophan fluorescence of SsbB decreases with only 35 %. Remarkably, the fluorescence quenching is lower than normally seen for other SSBs and the quenching is not dependent on either the salt (see Fig. 2-8 A) or the Mg<sup>2+</sup> concentration (data not shown).

No suitable fit was obtained when the binding curves were fitted to the model of Schwarz and Watanabe [166], (Personal communication, Peter Lens, Philipps-Universität Marburg).

In a subsequent experiment, titrations were performed with dTn oligomers of fixed lengths. Titrations nucleotides with lengths (n) of 25, 35 and 45 are shown in Figure 2-8 B. These data show a biphasic curve. The initial phase shows that SsbB binds with high affinity to these oligonucleotides with a stoichiometry of 1 oligonucleotide per SsbB tetramer. The initial phase results in approximately 35 % quenching, similar to what was observed for the poly(dT). The second phase represents a second binding event with much lower affinity. These data thus demonstrate that SsbB binds these oligonucleotides with one oligonucleotide per SsbB tetramer, most likely in a (SSB)<sub>35</sub> like manner. This binding is non-cooperative and independent of salt and Mg<sup>2+</sup> concentrations.

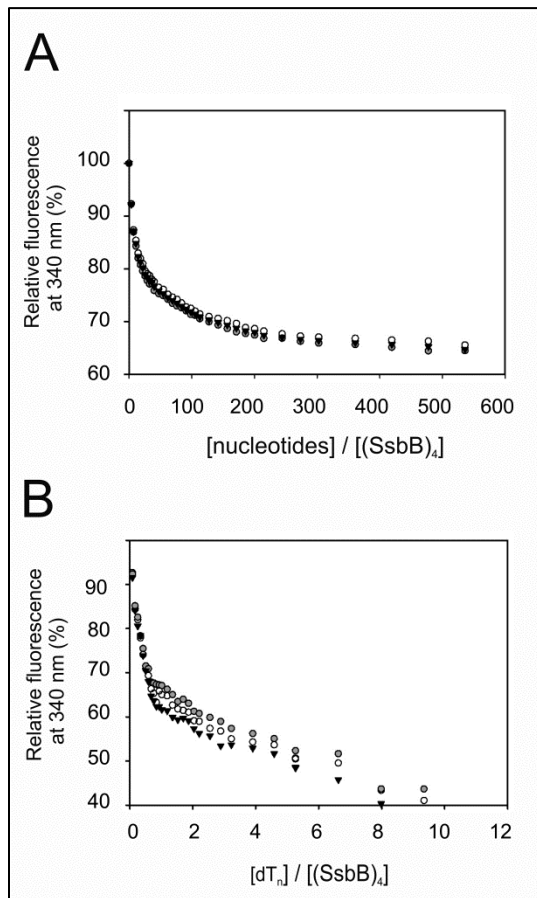


**Figure 2-8: Fluorescence titrations of SsbB**

A) 0.4  $\mu$ M SsbB was titrated with increasing concentrations of poly(dT) in a buffer containing 20 mM Tris pH 7.5 and either 20 mM NaCl (open circles), 200 mM NaCl (close circles) and 500 mM NaCl (closed triangles). B) 0.4  $\mu$ M SsbB was titrated with increasing concentrations of dT<sub>n</sub> of 25 (closed circles), 35 (open circles) and 45 (closed triangles) nucleotides in a buffer containing 20 mM Tris pH 7.5 and 200 mM NaCl.

### 2.2.5 Determination of the minimal binding frame for one or two SsbB tetramers

Since we were unable to determine the binding frame using fluorescence titrations, EMSAs were performed with poly(dT) oligonucleotides with different lengths (Figure 2-9 A). In these experiments, the gels were coomassie stained to detect the SsbB protein. These experiments were performed in an excess of oligonucleotides and showed a small mobility shift for 15 nucleotides and larger shifts for oligonucleotides of increasing lengths. This demonstrated that SsbB can bind to oligonucleotides of 15 nucleotides and longer. To determine the minimal length required to bind two SsbBs, EMSAs were performed with even longer oligonucleotides (Figure 2-9 B). When these EMSAs were performed at low protein to nucleotide ratios ( $(\text{SsbB})_4/\text{dT}_n < 1$ ) only binding of one tetramer per dT<sub>n</sub> was observed. Further experiments were performed at a tetrameric SSB to nucleotide ratio of 4 ( $(\text{SsbB})_4/\text{dT}_n = 4$ ). Upon

increasing the length of the added oligonucleotide, lengths smaller than 70 nucleotides resulted in a shift to a faster mobility as compared to the free protein indicating binding of one SsbB tetramer. In contrast, at oligonucleotide lengths larger than 70 nucleotides a small shift was observed to a slower mobility, indicating the binding of two SsbB tetramers. These experiments demonstrated that the minimal binding frame for two SsbB tetramers is 70 nucleotides.

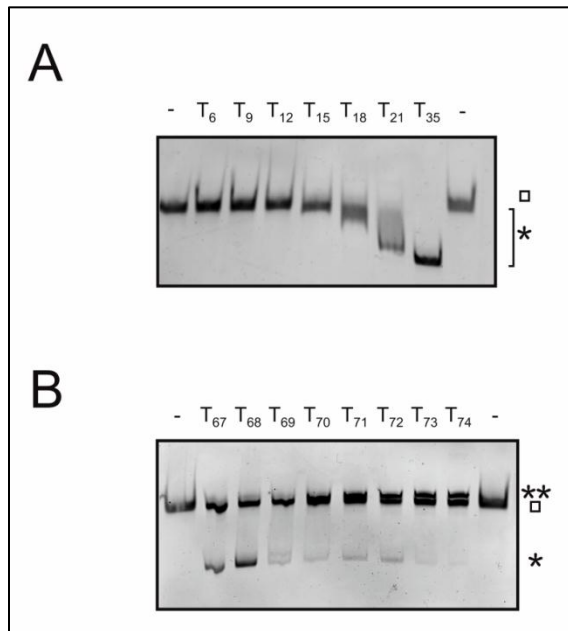


**Figure 2-9: Analysis of the minimal binding frame of SsbB by electrophoretic mobility shift assays**

A) Determination of the minimal binding frame of one SsbB tetramer. Each binding reaction contained 1  $\mu\text{M}$   $(\text{SsbB})_4$  and 5  $\mu\text{M}$   $\text{dT}_n$  of different lengths (6-35 nucleotides) and was performed in SBA buffer. The reactions were analyzed by polyacrylamide gel electrophoresis and SsbB was later visualized by Coomassie staining. B) Determination of the minimal binding frame of two SsbB tetramers. The binding reaction contained 1  $\mu\text{M}$   $(\text{SsbB})_4$  and 0.25  $\mu\text{M}$   $\text{dT}_n$  of different lengths (67-74 nucleotides) and was performed in SBA buffer. The reactions were analyzed by polyacrylamide gel electrophoresis and SsbB was later visualized by Coomassie staining. The square ( $\square$ ) indicates the free SsbB tetramer, while one (\*) or two (\*\*) asterixes represent an oligonucleotide bound to one or two SsbB tetramers.

### 2.2.6 SsbB binding to ssDNA visualized by atomic force microscopy

The AFM experiments were performed together with Dr. Eveline Peeters, University Brussels.

Atomic Force Microscopy (AFM) experiments were performed in air to analyze the architecture of SsbB-ssDNA complexes at a single molecule-level (Figure 2-10). SsbB protein was incubated with M13 ssDNA, which is a 6407 nt-long circular DNA molecule. Images were recorded of deposited reactions with concentration ratios (R) ranging from 1/707 to 1/44 (corresponding to tetramer/nucleotides). In order to

improve the adsorption of the ssDNA molecules and complexes, the trivalent cationic polyamine spermidine was included in the reaction mixtures, as described before [167]. Adsorbed unbound ssDNA molecules visualized with AFM, appear condensed because of hairpins and other secondary structures that are formed between complementary regions (Figure 2-10 A). At low ratios, SsbB tetramers bind the DNA apparently randomly, observed as individual “blobs” on the nucleoprotein complexes (Figure 2-10 B and C). Tetramers do not bind in arrays or clusters, but are rather distributed independently over the ssDNA molecules. This might suggest that under these conditions SsbB binds preferentially to DNA regions without secondary structure, and is initially excluded from condensed regions. At higher R, DNA molecules are saturated by SsbB protein, thereby resolving the condensed ssDNA structures (Fig. 2-10 D and 2-10 E). As observed for *E.coli* SSB, the co-existence of different types of structures (quasi-naked ssDNA, more or less saturated complexes) was observed in the same deposition. This indicates that there might be some limited cooperativity in the SsbB-ssDNA interaction, upon binding to longer ssDNA molecules [167]. Evidence is also provided that SsbB binds specifically to ssDNA, and not to dsDNA. A deposition of a reaction mixture containing both types of DNA visualized a saturated SsbB-ssDNA complex adsorbed next to an unbound dsDNA molecule (Fig. 2-10 F).

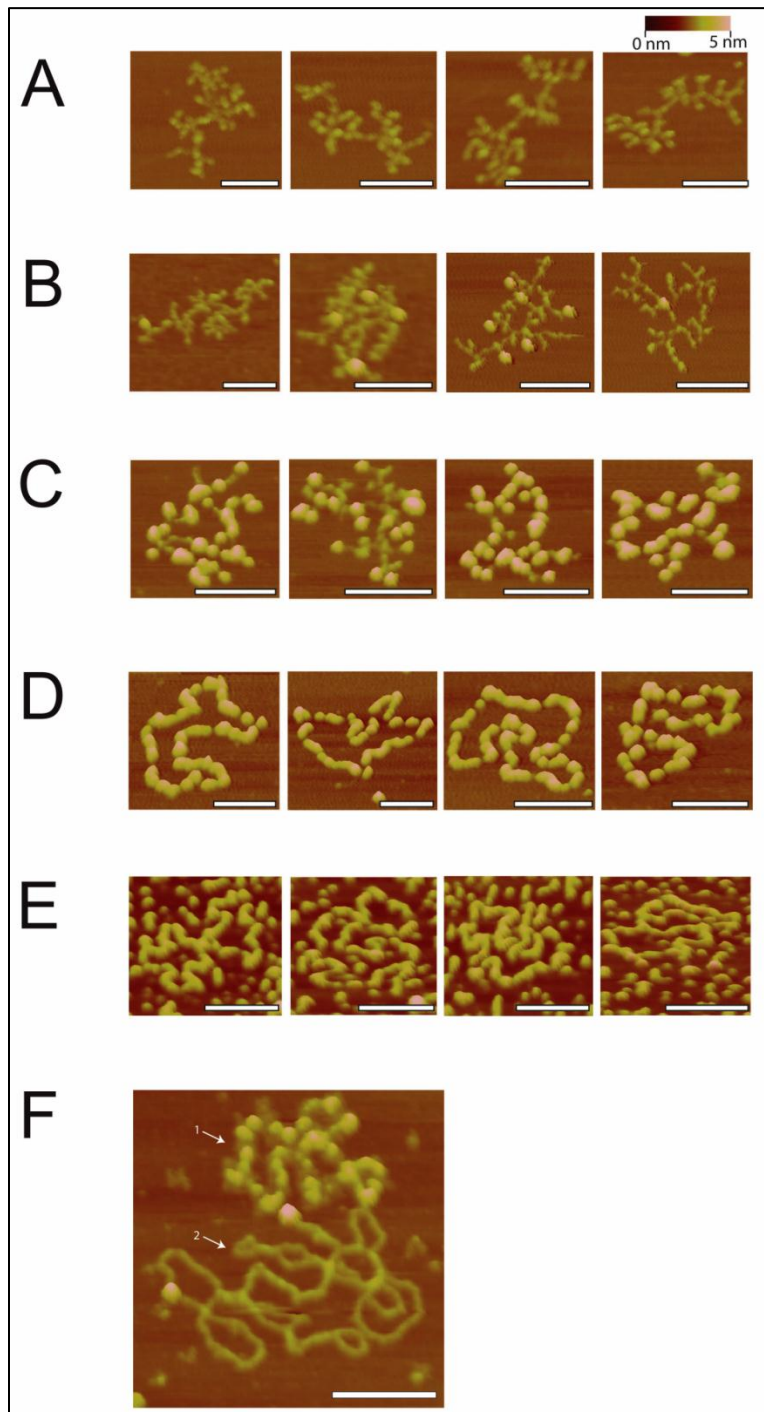


**Figure 2-10: SsbB binding to M13 ssDNA visualized by atomic force microscopy.**

A selection of AFM images, zoomed to display one DNA molecule or complex per image. The scale bar in all pictures equals 100 nm. These images were made for SsbB-ssDNA complexes at concentration ratios ( $R$ , corresponding to tetramer/nucleotides) of (A) 0, (B) 1/707, (C) 1/354, (D) 1/88 and (E) 1/44. (F) SsbB binds only to ssDNA (indicated by 1) and not to dsDNA (indicated by 2). The two bound proteins on the dsDNA are probably not SsbB, as indicated by their larger apparent volume, but impurities present in the M13 preparation.



### 2.2.7 The physiological characterization of the SsbB

DNA secretion studies demonstrated that neither deletion of *ssbB* (Pachulec, manuscript in preparation), nor overexpression of SsbB (Samta Jain, see appendix) had any effect on ssDNA secretion. SsbB could also not be detected in the medium or in outer membrane blebs, suggesting that the SsbB is also not secreted (Samta Jain, see appendix). Finally, it was tested whether SsbB had an effect on DNA uptake. Addition of high concentrations of SsbB (3.5  $\mu\text{M}$ ) to the medium had no effect (Samta Jain, see appendix), but when SsbB was overexpressed in the acceptor strain, a lower transformation rate was observed. Therefore overexpression of SsbB either affects DNA uptake, DNA stability in the acceptor strain, or the efficiency of recombination. It has previously been shown that SSB overexpression could have a negative effect on RecA recombinase activity [168]. Thus these data most likely show that SsbB has no influence on ssDNA secretion and/or DNA uptake.

### 2.2.8 SsbB stimulates topoisomerase activity

Since SsbB does not affect DNA secretion or uptake, further possible functions of SsbB were studied. In the GG1, *ssbB* is co-transcribed with the topoisomerase I, *topB*. It has been previously shown that other SSBs, like the SSBs of *E. coli* and of *Mycobacterium tuberculosis* could stimulate *E. coli* topoisomerase I activity [169]. It was shown that these stimulating effects occurred by enhancing DNA binding to topoisomerase I, and not via any direct interaction between the SSB and the topoisomerase I. SsbB strongly stimulated the activity of *E. coli* topoisomerase in a concentration dependent manner (Figure 2-11). This demonstrates that SsbB can stimulate a heterologous DNA processing enzyme.

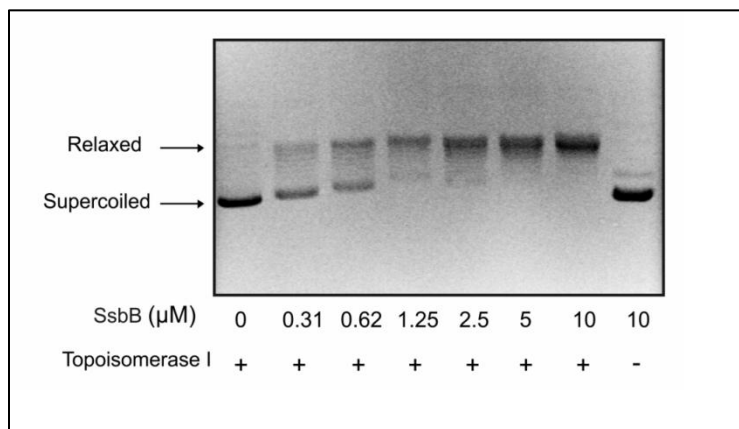


**Figure 2-11: SsbB stimulates *E. coli* Topoisomerase I activity.**

Supercoiled plasmid DNA was incubated with 0.12 units of topoisomerase and with increasing amounts of purified SsbB, as indicated. Reactions were carried out at 37°C for 30 min. DNA was resolved on a 1% agarose gel and stained with ethidium bromide. Arrow heads indicate the relaxed and supercoiled forms of plasmid.

### 2.3 Discussion

Within this study we have found that the GGI encodes a conserved cluster of genes also found in other genetic islands. This cluster is often found in integrated conjugative elements like the PGI-3(SG), PGI-2(C) and the *clc*-like genetic islands found in *Pseudomonas aeruginosa* and other organisms, and consists of a core set of 8 genes, which are generally transcribed in the same direction, and consists of the partitioning proteins ParA and ParB, four conserved hypothetical proteins containing respectively a DUF2857, no DUF, a DUF1845 and a DUF 3158 domain, a ssDNA binding protein and a topoisomerase I. Similar to what is observed for the GGI, these clusters are often located near the border of the integrated element. Two of the eight proteins, the protein that did not contain a conserved DUF and the protein with a DUF3158 domain could not be identified within the GGI. The integrated conjugative elements in which this cluster is found often contain a type IV secretion system involved in conjugation of the integrated element. This occurs after excision of the element from the chromosome, and the generation of a circular intermediate. Indeed it has been proposed that such a cluster found in the *clc* genetic island of *Pseudomonas* sp. strain B13 might play a role in preparing the DNA for conjugal transfer [170], possibly by stabilization of the circular intermediate or targeting the DNA to the type IV secretion system. The GGI is maintained within the chromosome of *N. gonorrhoeae*. It is flanked by a perfect and an imperfect *dif* site. When repaired, the presence of two correct *dif* sites causes excision of GGI from the chromosome by the XerCD recombinase [41]. The excised circular GGI can only be detected transiently, but even the transiently present circular GGI might transfer from one cell to another. Mutagenesis of ParA within the GGI abolished the secretion of ssDNA [33] further suggesting a role for the ParA-TopB genetic cluster in the maintenance or transport of ssDNA.

To further functionally characterize SsbB, it was purified to homogeneity. Similar to many other SSBs, SsbB was shown to form a stable tetramer. The tetramer bound ssDNA with high affinity, characterized by an equilibrium dissociation constant of 100 nM. Remarkably, SsbB bound with at least 10-fold higher affinity to Cy3-labeled oligonucleotides, demonstrating that fluorescent labels can strongly influence the binding affinity. Fluorescently labeled oligonucleotides are currently widely used, and our data shows special care should be taken when they are used to directly determine binding affinities.

A combination of EMSAs, fluorescence titrations and atomic force microscopy were used to characterize the binding of SsbB to ssDNA. This demonstrated that the oligonucleotide length required for SsbB binding was approximately 15 nucleotides, which is similar to the binding frames of the SSBs of *E. coli* and *Mycobacterium tuberculosis* that vary between 15 and 17 nucleotides [171,172]. Fluorescence

titrations demonstrated that SsbB binds first to one oligonucleotide after which a second oligonucleotide can only bind to the same SsbB with lower affinity. A similar negative cooperativity was observed for *E.coli* SSB [85], [173]. Titrations to determine the oligonucleotide length to which two SsbBs could bind showed that a second SsbB tetramer could only bind if the ssDNA was longer than 70 nucleotides. Indeed, many different SSBs can bind with 2 SSB tetramers to an oligonucleotide of 75 nucleotides at low salt or low  $Mg^{2+}$  concentrations [85]. Generally, these SSBs, like for example the *E. coli* SSB, bind DNA with two of the OB folds occluding approximately 35 nucleotides in a highly cooperative mode. At higher salt or  $Mg^{2+}$  concentrations, the binding mode changes to a mode with lower co-operativity where the ssDNA is bound to four OB folds occluding approximately 65 nucleotides. In this mode only one SSB tetramer can bind to an oligonucleotide of 75 nucleotides [85]. Remarkably, within our experiments we have not observed that SsbB binding to ssDNA was sensitive to either salt or  $Mg^{2+}$  concentrations. Using atomic force microscopy, we have also studied binding to longer DNA fragments. SsbB tetramers bound distributed independently over the ssDNA molecules. This might suggest that SsbB binding is initially excluded from condensed regions and that SsbB initially only binds to DNA regions without secondary structure. Regions with higher secondary structure are only resolved at higher SsbB concentrations. SsbB was expressed only at low levels under normal growth conditions, suggesting that SsbB under these conditions either binds distributed evenly over exposed ssDNA stretches, or is specifically targeted to certain regions by other proteins.

Although SsbB functions in many respects similar to other SSBs, SsbB could not complement the *E.coli* *ssb* mutant, even when overexpressed to high levels. We therefore set out to find a specific function for SsbB. First, the role of SsbB in ssDNA secretion was studied. VirE2, a ssDNA binding protein encoded on the *A. tumefaciens* Ti plasmid is necessary for transport of the T-DNA to the plant cell nucleus. VirE2 is transported directly to the target cell, where it binds and protects the ssDNA [174]. It was demonstrated that the binding of the transported VirE2 to the ssDNA pulls the DNA into the target cell [83]. Before transport to the target cell, VirE2 is kept transport competent by VirE1 [175].

No homolog of VirE1 could however be detected within the GGI, and neither deletion of the *ssbB* gene nor the overexpression of SsbB affected ssDNA secretion. SsbB could not be detected in the medium isolated from strains involved in ssDNA secretion via the type IV secretion system. Also the addition of purified SsbB to the culture supernatant at concentrations 1000 fold higher than detected in the medium did not affect the GGI dependent transfer of chromosomal markers. This makes it unlikely that SsbB either function inside the cell to assist the transport of DNA, or is secreted into the medium where

it could assist the transport of the ssDNA. Another possibility studied is that SsbB functions not in the process of export of ssDNA, but in the process of the uptake of ssDNA. If SsbB is involved in competence, it is expected that the presence of SsbB increases the transformation efficiency. Surprisingly, when SSB was overexpressed in the recipient cell, the transformation efficiency was reduced. Most likely the overexpression of SsbB interferes with the activity of RecA in the recombination process [168,176]. It is therefore concluded that SsbB is not involved in DNA secretion and uptake.

In general, these SSBs found in genetic islands might together with the topoisomerase I homologs serve to stabilize the circular form of the GGI when it has excised from the chromosome before it is re-integrated or exported. We demonstrate that SsbB, together with TopB forms an operon separately from the other genes found in the conserved cluster. This suggests that, although the partitioning protein ParA and the SSB are found in the same cluster they might function in different processes. The possible interaction with other proteins encoded within the GGI should be studied to further characterize the role of the SSBs within the genetic islands.

## Chapter 3

### **Biosensor development for the visualization of single-stranded DNA and double-stranded DNA in the biofilms and planktonic cultures**

**Maria Zweig** and Chris van der Does

Parts of the chapter are submitted to Environmental Microbiology as Supplementary Data of the manuscript: Role and Visualization of Extracellular Single-stranded DNA involved in Biofilm Formation by *Neisseria gonorrhoeae*.

### 3.1 Aim of the study

Currently many different methods and stains are available to fluorescently detect DNA, such as Ethidium bromide, Propidium iodide, DDAO (7-hydroxy-9H-(1,3-dichloro-9,9-dimethylacridin-2-one), SYTO 60, SYBR Green, OliGreen and many others. However, to our knowledge, all currently available stains detect both ssDNA and dsDNA.

As described in the introduction and chapter 2, cells have evolved a specialized class of ssDNA-binding (SSB) proteins that bind to ssDNA with high affinity and in a sequence-independent manner. Oligonucleotide/oligosaccharide-binding (OB) domains bind ssDNA through a combination of electrostatic and base-stacking interactions with the phosphodiester backbone and nucleotide bases, respectively.

I aimed to use this highly specific DNA binding reaction of SSBs to specifically detect ssDNA in the medium and in biofilms, by fluorescently labelling and detecting these SSBs, and I set-out to develop a system in which we can reduce the background fluorescence of non-bound SSB by using an approach in which the fluorescence of the SSB increases upon DNA binding. It has been previously shown that the fluorescence of *E.coli* SSB (G24C) labelled with IDCC (7-diethylamino-3-(((2-oidacetoamido)ethyl)amino)carbonyl)coumarin) was increased 6-fold upon binding DNA.

The final aim of this study was to determine the role of single stranded DNA (ssDNA) in biofilm formation, and to visualize ssDNA in biofilms of different species.

### 3.2 Results

#### 3.2.1 Expression and purification of the SsbB from *Neisseria gonorrhoeae*

In the genome of *N. gonorrhoeae*, a second SSB (SsbB), besides the chromosomal SSB, is encoded within the Gonococcal Genetic Island (GGI). Since SsbB was characterized in detail (see Chapter 1), I set up experiments to test whether this protein could be used as a biosensor for the detection of the ssDNA. Within these experiments I set-out to fluorescently label SsbB using cysteine specific fluorescent probes. The mutagenesis of the only native cysteine of SsbB (Cys56) to serine led to the incorrect folding of the protein and to inclusion body formation (Figure 2-5).

A structural model obtained by modeling SsbB on the crystal structures of *E.coli* *ssb* (<http://swissmodel.expasy.org/>), suggested that the native Cys56 is located on the inside of the protein and was most likely inaccessible for the labeling (Figure 3-1 A). Since the native cysteine could not be exchanged, it was tested whether the native Cys56 was accessible to the cysteine specific fluorescent

maleimide probes (Figure 3-1 B,C). This demonstrated that the native cysteine was not accessible for maleimide probes.

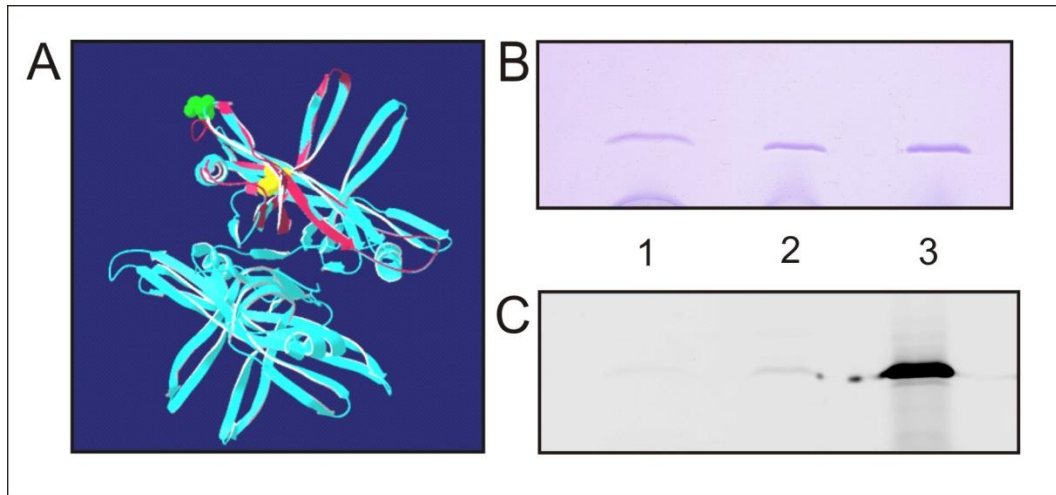


**Figure 3-1:** A) SsbB (in pink) structure prediction based on SSB from *E. coli* (in blue). The native Cysteine56 is presented in yellow, serine128 is presented in green. B) SDS-Page Analysis of 1 = SsbB, 2 = heat denatured SsbB and 3 = SsbBD26C. Proteins were later visualized by Coomassie staining (in B) or by fluorescent detection (in C).

Two different positions, Asp26 and Ser128, were selected and these residues were mutated to cysteines. Both proteins were overexpressed and purified to homogeneity (Data not shown). Both proteins eluted from the gel filtration column as tetramers. The labelling conditions for both proteins were optimized by testing different coumarin-maleimide probes. Since the SsbBS128C mutant was less stable than wt SsbB and aggregated over time, the SsbBD26C mutant was used for further experiments.

### 3.2.2 Detection of ssDNA with labeled SsbB

To demonstrate ‘proof of principle’, an attempt was made to detect ssDNA bound to beads using fluorescence microscopy. The size of the beads was 1 nm in diameter which is a comparable size as *N. gonorrhoeae* cells. DNA was first immobilized on the magnetic beads. Initially beads with the silica-like structure and beads with Oligo-T-tails, which can catch poly-A-DNA were used. After addition of the labeled SsbB a fluorescent signal was observed mainly in the medium. This observation indicated that most likely SsbB was able to strip DNA away from the beads. To immobilize DNA stronger on the beads, the streptavidin-biotin interaction was used. The streptavidin-covered beads were first incubated with Biotinylated-DNA. The labeled SsbB was added to the pre-incubated beads and fluorescent microscopy was performed. It was shown that the fluorescent signal increased more than 10 times after addition of the labeled SsbB for the beads covered with DNA in comparison with the beads without DNA (Figure 3-2), demonstrating that using this method we are indeed able to detect ssDNA.

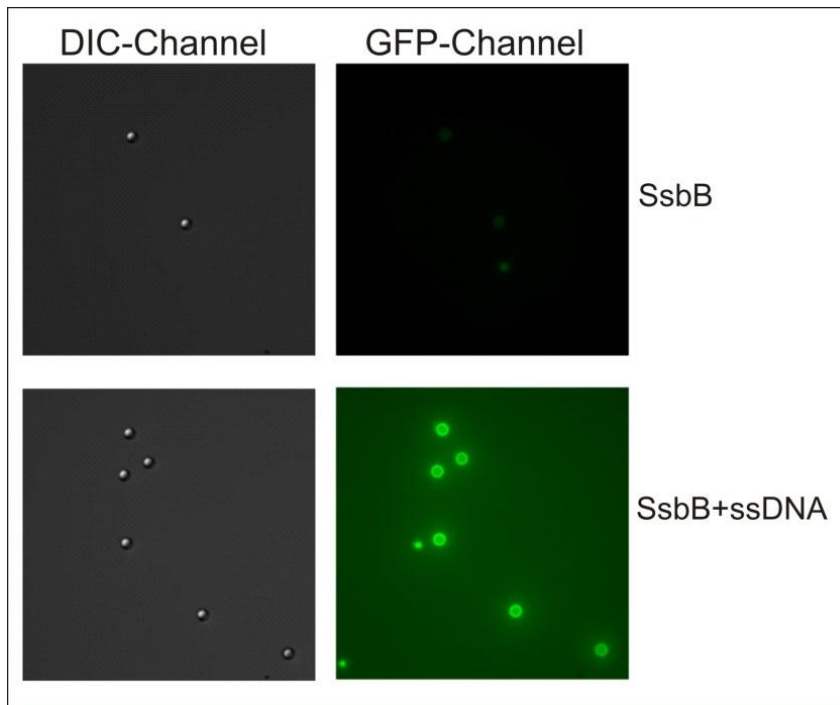


**Figure 3-2:** A biotinylated T<sub>100</sub> oligonucleotide was bound to streptavidin covered beads and incubated with Fluorescein-labelled SsbBS128C. Beads are 1nm in diameter. The upper panel shows the image obtained after addition of the labelled SsbBS128C to the streptavidin covered beads. The lower panel represents beads which were incubated with the biotinylated T100 oligonucleotide and with fluorescein-labeled SsbBS128C. The beads were visualized by DIC or Fluorescent Microscopy (GFP-channel)

To test whether the fluorescence was sensitive to DNA binding, the fluorescence intensity of the labeled protein as tested as a function of the ssDNA added. Remarkably, for both proteins the fluorescence intensity of the coumarin-maleimide labeled proteins decreased upon addition of ssDNA (data not shown). This is in contrast to previous studies performed with the *E. coli* SSB G24C mutant, which showed a 6 fold increase in fluorescence after binding to ssDNA when the protein was labeled with IDCC [177]. Unfortunately the IDCC fluorescent probe is currently no longer commercially available. The fluorescence experiments also revealed that the labeled proteins were not stable for prolonged periods at 37 °C. Since e.g. study of the localization of DNA in biofilms using Confocal Laser Scanning Microscopy are performed at 37 °C and might take several hours, it was decided to also test other SSBs which might be more stable.

### 3.2.3 Expression and purification of the SulSSB from *Sulfolobus solfataricus*

Since SsbB was found to be instable at 37 C, it was decided to test SSB proteins of several (hyper)thermophiles. In a first attempt, the SSB of *Sulfolobus solfataricus* (SulSSB) was tested. The SSB from *S. solfataricus* is an abundant protein with a unique structural organization, which exists as a



monomer in solution and multimerizes upon DNA binding [105]. Remarkably, the crystal structure of SulSSB protein shows similarity to eubacterial homotetrameric proteins, since its OB-domain is flanked by a C-terminal negatively charged region with conserved aspartate residues [108].

SulSSB was overexpressed and purified to homogeneity (data not shown). Agarose gel electrophoretic analysis demonstrated that DNA binding of SulSSB is not highly co-operative (data not shown).

The SSB from *S. solfataricus* does not contain any cysteines. SulSSB was labelled with different coumarine probes, but for all the fluorescence intensity of the coumarin-maleimide labeled proteins decreased upon addition of ssDNA (data not shown). Since SulSSB binds ssDNA in non-cooperative manner and no suitable coumarine-maleimide probes could be found, we looked for further alternative stable SSB proteins.

#### **3.2.4 Expression and purification of the TteSSB2 from *Thermoanaerobacter tengcongensis***

In the next attempt, TteSSB2 of *Thermoanaerobacter tengcongensis* was used. This protein binds ssDNA with high affinity and remained fully active even after 6 h incubation at 100 °C [178]. TteSSB2 was overexpressed and purified (Figure 3-3). Gelfiltration experiments confirmed that TteSSB2 forms a tetramer (Figure 3-3 B) and electrophoretic mobility shift assays demonstrated that TteSSB2 binds ssDNA with an affinity of approximately 100 nM (Figure 3-3 C), whereas it does not bind to dsDNA even at concentrations of 5 µM (Figure 3-3 D).

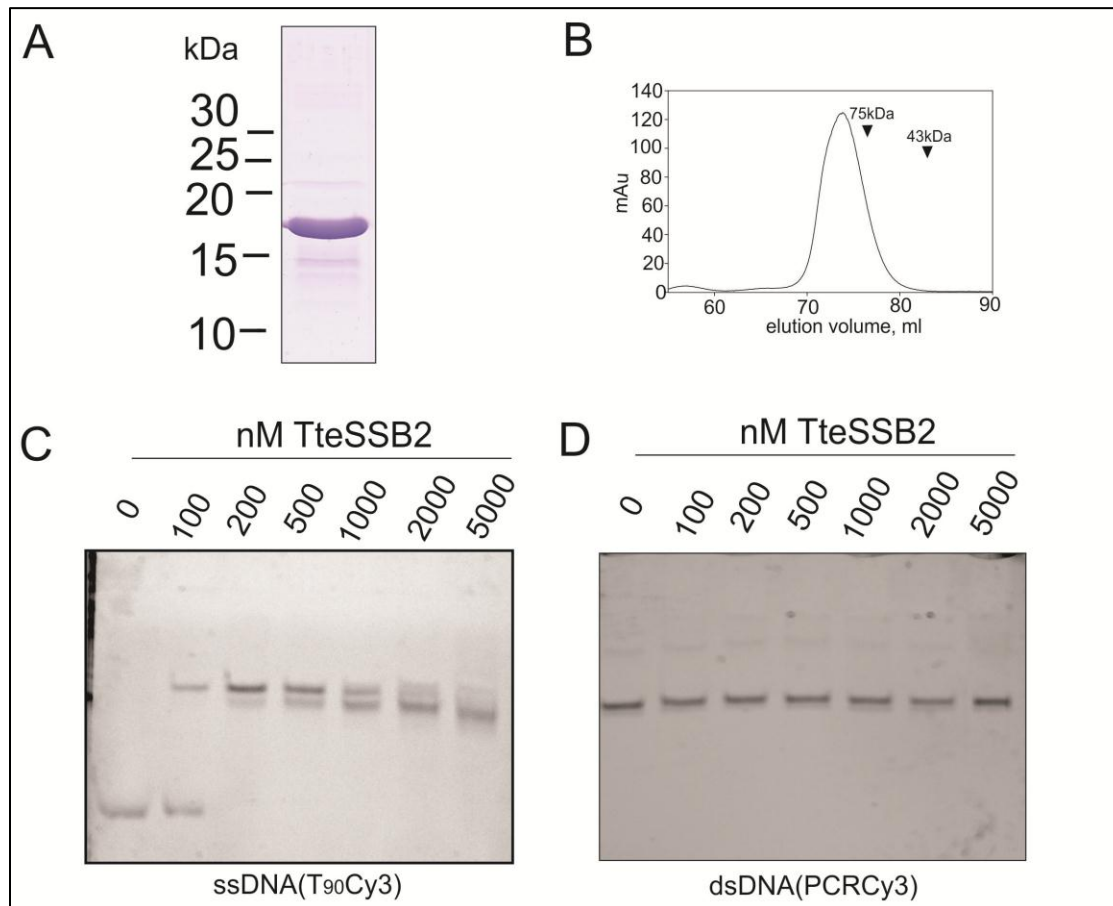


**Figure 3-3: Purification and specificity of the single-stranded DNA binding protein TteSSB2.**

TteSSB2 was overexpressed in *E. coli* and purified by a heat-step followed by anion exchange and gel filtration chromatography. (B) TteSSB2 eluted as a tetramer from the SD200 gel filtration column and was essentially pure as assayed by (A) Coomassie staining of an SDS-PAGE of the purified protein. The positions of the various markers for both the gel filtration and the SDS-PAGE are indicated. Electromobility shift assays were performed with incubating either a Cy3 labeled dT<sub>90</sub> oligonucleotide (C) or a Cy3 labeled PCR product (D) with increasing concentration of TteSSB2. The fluorescently labeled DNA was analyzed after separation on 7.5 % polyacrylamide gels using a LAS-4000 imager.

As a control for DNA binding, also the thermostable Sac7d protein from *Sulfolobus acidocaldarius* was overexpressed and purified to homogeneity (Figure 3-4 A). Sac7d is a 7 kDa chromatin protein that is highly conserved in the Crenarchaeota. The protein was purified as a monomer (Figure 3-4 B) and shows higher affinity for double-stranded DNA than for single-stranded DNA [179]. Purified Sac7d bound to ssDNA and dsDNA with approximately equal affinities of 2  $\mu$ M (Figure 3-4 C and 3-4 D). This indicates that fluorescently Sac7d could be used as protein that binds both single stranded and double stranded DNA.

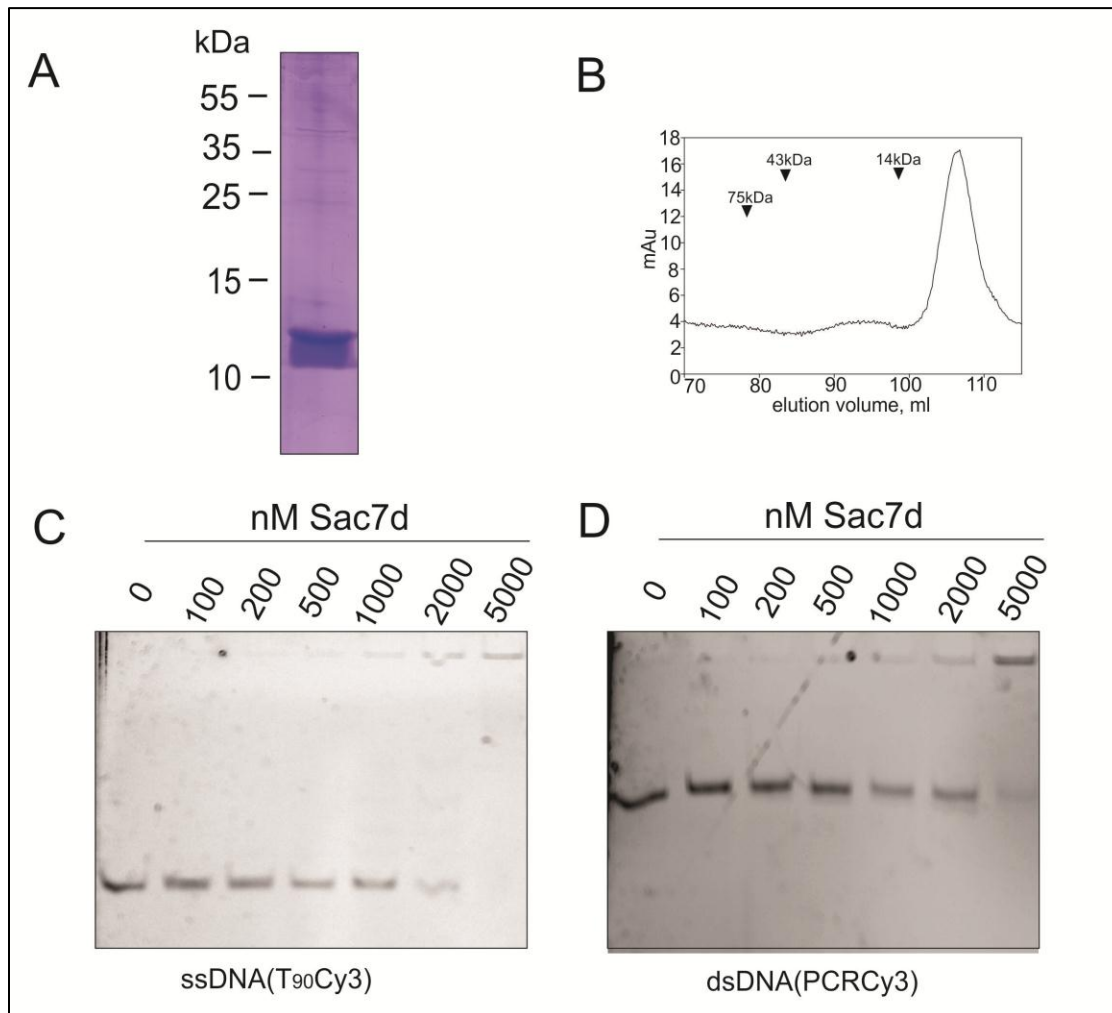


**Figure 3-4: Purification and specificity of the DNA binding protein Sac7d.**

His-tagged Sac7d was overexpressed in *E. coli* and purified by Ni-NTA affinity, anion exchange and gel filtration chromatography. (B) Sac7d eluted as a monomer from the SD200 gel filtration column and was essentially pure as assayed by (A) Coomassie staining of an SDS-PAGE of the purified protein. The positions of the various markers for both the gel filtration and the SDS-PAGE are indicated. Electromobility shift assays were performed with incubating either a Cy3 labeled dT<sub>90</sub> oligonucleotide (C) or a Cy3 labeled PCR product (D) with increasing concentrations of Sac7d. The fluorescently labeled DNA was analyzed after separation on 7.5 % polyacrylamide gels using a LAS-4000 imager.

To detect TteSSB2 and Sac7d, we aimed to label the proteins with fluorescent dyes by coupling these dyes to cysteine residues in the proteins. Neither TteSSB2 nor Sac7d contains any native cysteines. Previously, *E. coli* SSB labelled with an extrinsic environmentally sensitive fluorophore was shown to be a sensitive probe for ssDNA binding [180]. The fluorescence of *E. coli* SSB labelled at position G26C with IDCC (*N*-[2-(iodoacetamido)ethyl]-7-diethylaminocoumarin-3-carboxamide) increase up to 6.1 fold upon binding to ssDNA [180]. To test whether similar results could be obtained with TteSSB2 and Sac7d, four

cysteine mutants (G24C, W55C, Q79C and R81C) were created in TteSSB2 and 2 cysteine mutants (S18C and L48C) were created in Sac7d (Figure 3-5).

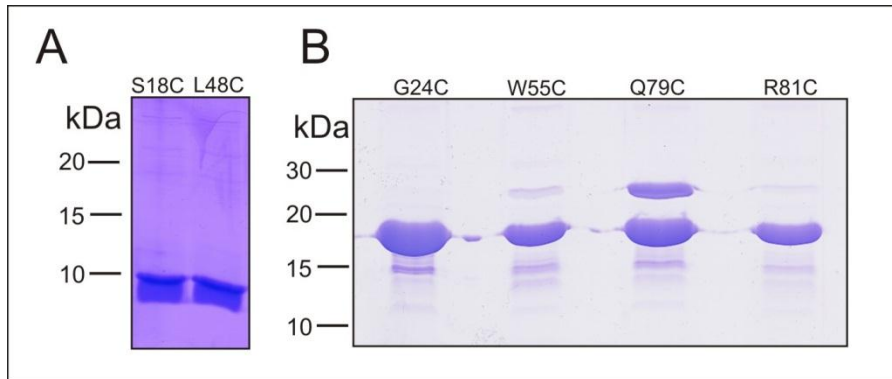


**Figure 3-5: Purification of thermostable Sac7d and TteSSB2 proteins.**

A) His-tagged Sac7d mutants were overexpressed in *E.coli* and purified by Ni-NTA affinity, anion exchange and gel filtration chromatography. B) TteSSB2 was overexpressed in *E.coli* and purified by a heat-step followed by anion exchange and gel filtration chromatography.

The G24C mutation in TteSSB2 is homologous to the G26C mutation in *E. coli* SSB. The other positions were chosen in such a manner that, predicted by either homology modelling of TteSSB2 or by the Sac7d crystal structure, labelling at these positions would most likely not interfere with DNA binding, but that the positions would still be close to the bound DNA such as that the DNA binding might influence fluorescence. All proteins were purified to homogeneity (Figure 3-5). The proteins were labelled with fluoresceine. Equal labelling of the proteins was confirmed by loading the labelled protein on a gel and by imaging the gel using a LAS-4000 imager (data not shown). The different labelled mutants were tested for DNA binding by fluorescent imaging of Streptavidin incubated beads Biotinylated-DNA and fluorescent microscopy was performed. It was shown that the fluorescent signal increased more than 10 times after addition of the labeled SsbB for the beads covered with DNA in comparison with the beads without DNA. Labelling of TteSSB2 at positions Q79C and R81C, completely abolished binding to ssDNA, but ssDNA binding was not affected in the other mutants (Figure 3-6).

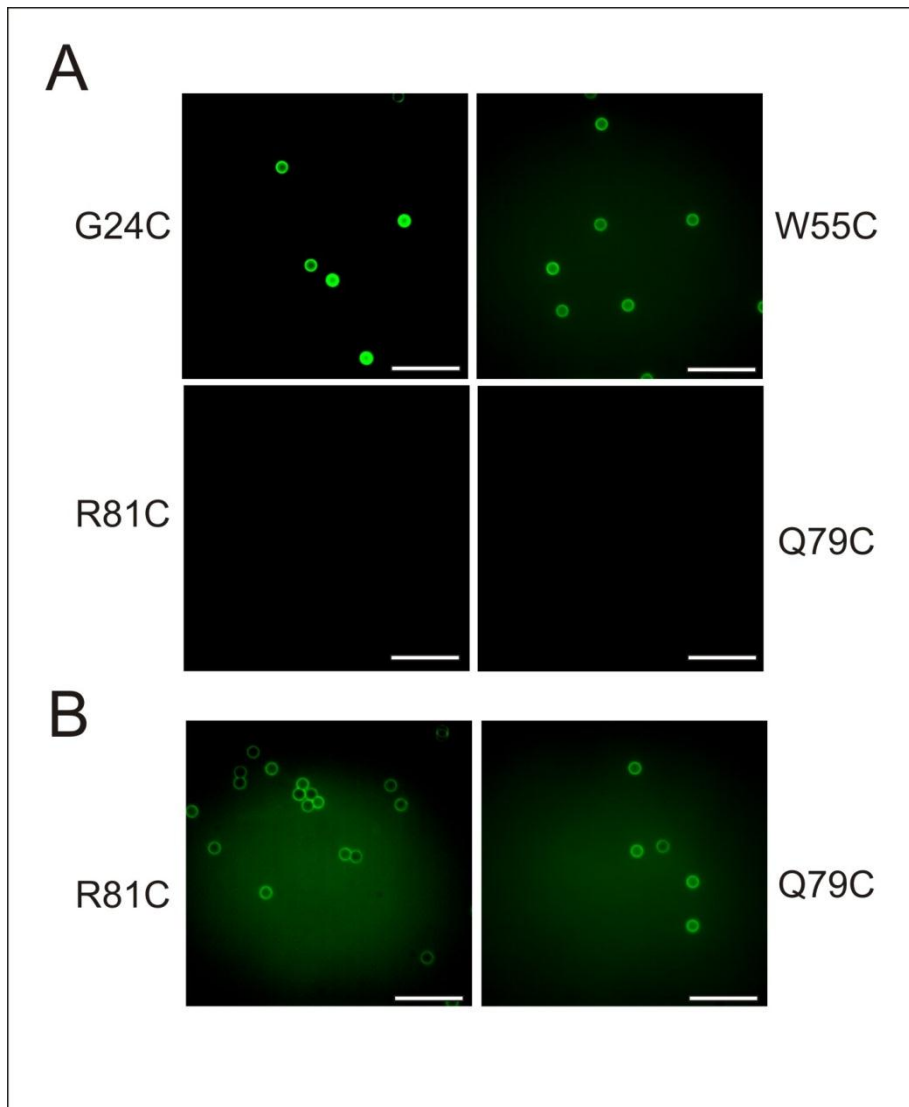


**Figure 3-6: Detection of the biotynated  $T_{100}$ -mer on the magnetic Streptavidine-beads with different TteSSB2 mutants.** A) Streptavidine covered magnetic beads were first incubated with biotynated  $T_{100}$ mer. Next fluoresceine-labelled TteSSB2 cysteine mutants were added to the beads and bead-protein-complexes were immobilized on the agarose covered slides. B) Represents the TteSSBR81C and TteSSBQ79C proteins at an increased sensitivity. The beads were visualized by Fluorescent Microscopy (GFP-channel). The bars are 5  $\mu$ m length.

The influence on the fluorescent intensity upon binding to DNA was studied for different combinations of cysteine mutants and fluorophores (Table 1).

Of the labels tested, the TteSSB2-W55C mutant labelled with IANBD gave the largest (4-fold) increase in fluorescence. No increase or decrease was detected for the labelled Sac7d mutants. The TteSSB2 W55C mutant and the Sac7d S18C mutant labelled either with IANBD or Texas Red were selected for further experiments.

**Table 1: Fluorescence changes upon DNA binding for various mutant: fluorophore combinations.**

<b>Protein</b>	<b>Fluorophore</b>	<b>Excitation (nm)</b>	<b>Emission (nm)</b>	<b>Fluorescence ratio (<math>\pm</math> DNA)</b>
<b>TteSSB2 G24C</b>	IANBD	472	536	1,6
	Fluorescein	492	515	1,1
	Texas Red	583	603	1
	MIANS	322	417	1,6
<b>TteSSB2 W55C</b>	IANBD	472	536	4
	Fluorescein	492	515	1,2
	Texas Red	583	603	1
	MIANS (M8)	322	417	1,8
<b>TteSSB2 R81C</b>	Fluorescein	492	515	No binding to DNA
<b>TteSSB2 Q79C</b>	Fluorescein	492	515	No binding to DNA
<b>Sac7d S18C</b>	IANBD	472	536	1
	Texas Red	583	603	0,8
<b>Sac7d L48C</b>	IANBD	472	536	1
	Texas Red	583	603	0,8

Titration were performed with 50 nM TteSSB2 or Sac7d with increasing concentrations ssDNA or DNA. Experiments were performed at 8 °C in a buffer containing 20 mM Tris pH 7.5 and 1 mM dithiothreitol. The excitation and emission wavelengths and the increase of fluorescence at saturating DNA concentration are indicated. IANBD is N-((2-(iodoacetoxy)ethyl)-N-Methyl)amino-7-Nitrobenz-2-Oxa-1,3-Diazole, Fluorescein is Fluorescein-5-Maleimide, Texas Red is 5-(chlorosulfonyl)-2-(2,3,6,7,12,13,16,17-octahydro-1H,5H,11H,15H-pyrido[3,2,1-ij]quinolizino[1',9':6,7,8]chromeno[2,3-f]quinolin-4-ium-9-yl)benzenesulfonate C2 maleimide and MIANS is 2-(4'-Maleimidylanilino)Naphthalene-6-Sulfonic Acid.

### **3.2.5 ssDNA and dsDNA can be visualized in biofilms of the thermoacidophilic archaea *Sulfolobus acidocaldarius* using fluorescently labelled TteSSB2 and Sac7d**

We aimed to demonstrate that ssDNA and dsDNA could indeed be visualized in biofilms using CSLM and fluorescently labelled ssDNA and dsDNA binding proteins. To demonstrate this, the presence of ssDNA and dsDNA in biofilms of the thermoacidophile *Sulfolobus acidocaldarius* was studied. It has previously been shown that three day old biofilms of *S. acidocaldarius* contain extracellular DNA [181]. This DNA is found at positions where cellular aggregates are visible. This DNA was sensitive to DNase I treatment, but removal of the DNA had no effect on the structure of the biofilms, which suggested that extracellular DNA does not play a structural role in biofilms of *S. acidocaldarius* [181]. Based on the conditions under which the *S. acidocaldarius* biofilms were grown (76°C and pH 3.0) it was assumed, that the DNA would be present as a mixture of denaturated ssDNA and dsDNA. Before imaging the biofilm was washed with Brock media of pH 5 and imaged by CLSM after incubation with DAPI (to visualize the cells), DDAO (to visualize the external DNA), IANBD labelled TteSSB2-W55C (to visualize ssDNA) and Texas Red labelled Sac7d S18C (to visualize both ssDNA and dsDNA). Since the fluorescence spectra of DDAO and Texas Red overlap, these fluorephores could not be used at the same time. In a first experiment a three day old static biofilm of *S. acidocaldarius* was imaged by CLSM after incubation with DAPI, DDAO and IANBD labelled TteSSB2-W55C. As has been described previously, *S. acidocaldarius* readily formed biofilms which contained a high density of cells and large aggregates, forming towering structures above the surface of attached cells. Labelling with DDAO showed the presence of external DNA which was associated with the large aggregates forming towering structures above the surface (Figure 3-7 A).

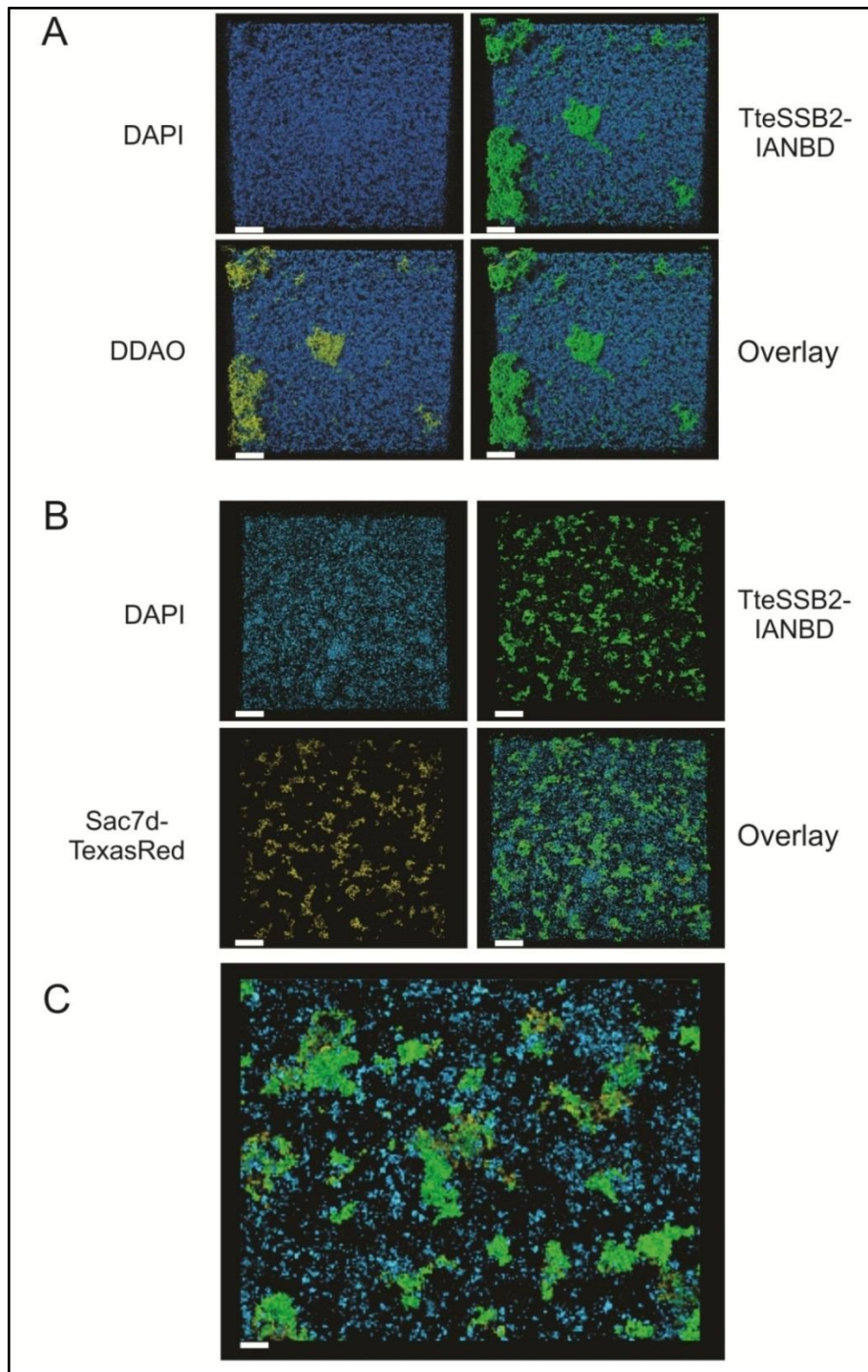


**Figure 3-7: Visualization of DNA in static biofilms formed by *S. acidocaldarius***

Three day old biofilms formed by *S. acidocaldarius* were labelled with (A) DAPI, DDAO and IANBD labelled TteSSB2-W55C or with (B) DAPI, Texas Red labelled Sac7d-S18C and IANBD labelled TteSSB2-W55C and visualized by CLSM. The lower right panels show an overlay of the signals. In (C) a zoom-in of the overlay shown in (B) is shown. Micrographs represent three-dimensional images. The bar in (A) and (B) is 20  $\mu\text{m}$  in length, while the bar in (C) is 5  $\mu\text{m}$  in length.



The labelling with IANBD labelled TteSSB2-W55C showed a very similar labelling pattern as DDAO, demonstrating that IANBD labelled TteSSB2-W55C was co-localizing with the DNA. The highly specific binding of TteSSB2 to ssDNA demonstrates that in biofilms of *S. acidocaldarius* large amounts of ssDNA can be detected. In a second experiment a three day old static biofilm of *S. acidocaldarius* was imaged after incubation with DAPI, Texas Red labelled Sac7d-S18C and IANBD labelled TteSSB2-W55C ( Figure 3-7 B). Both Texas Red labelled Sac7d-S18C and IANBD labelled TteSSB2-W55C specifically stained the large aggregates forming towering structures above the surface. Remarkably, although the labelling patterns of Texas Red labelled Sac7d-S18C and IANBD labelled TteSSB2-W55C overlapped in many positions, several positions were only labelled Texas Red labelled Sac7d-S18C or IANBD labelled TteSSB2-W55C demonstrating that three day old static biofilm of *S. acidocaldarius* contain both ssDNA and dsDNA (Figure 3-7 C). It also demonstrates that ssDNA and dsDNA can be detected in biofilms using CSLM with fluorescently labelled TteSSB2 and Sac7d.

### 3.3 Discussion

In this study we developed a method to specifically and separately detect ss- and dsDNA using fluorescently labeled (thermo)stable ssDNA and dsDNA binding proteins. Both proteins bind to DNA in an essentially sequence aspecific manner. The fluorescent detection of the labeled proteins was optimized by introducing the fluorescent probes at positions where their fluorescence increases upon ssDNA binding. This reduces the signal of the proteins that are not bound to DNA. Detection of ssDNA using TteSSB2 of *Thermoanaerobacter tengcongensis* was highly specific, and ssDNA could be specifically detected in biofilms of *Sulfolobus acidocaldarius*. This technique can be applied to various bacteria growing at different conditions, since the TteSSB2 is an extremely stable protein, which does not bind to the cell surface.

The Sac7d protein from *Sulfolobus acidocaldarius* bound with slightly higher affinity to dsDNA, but most likely will detect both ssDNA and dsDNA, especially since even secreted ssDNA will contain many positions where the ssDNA will anneal and form stretches of dsDNA. Indeed the Sac7d specifically detected DNA in biofilms of *Sulfolobus acidocaldarius*.

This technique enables the visualisation of the secretion and uptake of DNA *in vivo*. The combination of the fluorescently labelled ssDNA binding proteins and the remarkable property of our system to transport DNA directly into the medium instead of into other cells will enable us to follow this process in real time on the level of single molecules. It will be possible to determine the timing and the localisation of the secretion process. These experiments can be performed both on planktonic cells as on biofilms. We will also use it to detect the fate of the secreted DNA within culture.

## Chapter 4

### **Role and Visualization of Extracellular Single-stranded DNA involved in Biofilm Formation by *Neisseria gonorrhoeae*.**

**Maria A. Zweig**<sup>1</sup>, Sabine Schork<sup>1</sup>, Andrea Koerdt<sup>2</sup>, Katja Siewering<sup>1</sup>, Claus Sternberg<sup>3</sup>, Kai Thormann<sup>1</sup>, Sonja-Verena Albers<sup>2</sup>, Soren Molin<sup>3</sup>, and Chris van der Does<sup>1#</sup>.

<sup>1</sup> Department of Ecophysiology, Max-Planck-Institute for terrestrial Microbiology, Marburg, Germany.

<sup>2</sup> Molecular Biology of Archaea, Max-Planck-Institute for terrestrial Microbiology, Marburg, Germany.

<sup>3</sup> Technical University of Denmark, Department of Systems Biology, Denmark.

Submitted to Environmental Microbiology Journal

## 4.1 Aim of the study

*N. gonorrhoeae* is an obligate human pathogen which normally colonizes the genital tract and causes the disease gonorrhea. Gonococci are capable to form biofilms during natural cervical infection and both over glass and in continuous flow-chamber systems. Many clinical isolates contain a gonococcal genetic island (GGI) which encodes a novel Type IV Secretion System (T4SS). The T4SS of *N. gonorrhoeae* secretes single-stranded DNA (ssDNA) in a contact independent manner directly into the medium. *N. gonorrhoeae* biofilm contains large amounts of extracellular DNA. Like for many well studied bacterial biofilms also *N. gonorrhoeae* biofilm was shown to contain large amounts of DNA which is a major matrix component [137]. We suggest that the actively secreted ssDNA could play an important role in gonococcal biofilm formation.

Currently many different methods and stains are available to fluorescently detect nucleic acids. Not a single stain or method is known for separate visualization of double- and single-stranded DNA. In this study we take advantage of the unique technique we developed (see Chapter 3), which utilizes the highly specific DNA binding reaction of SSBs.

The aim of this study was to study visualize the secreted ssDNA and double-stranded DNA in the biofilms and in the planktonic cultures of *N. gonorrhoeae*.

## 4.2 Results

### 4.2.1 Exonuclease I inhibits the initial stages of biofilm formation

DNA is an important structural component of biofilms of many microorganisms. DNA plays an important role in the initial attachment [130], but also the amount of DNA within biofilms determines the final structure and thickness of the biofilm [130]. Whether this DNA is present as ss- or dsDNA and whether other components are bound to this DNA is currently still unknown. Biofilms formed by *N. gonorrhoeae* contain large amounts of DNA [137]. It has been proposed that this DNA is either released via autolysis or via membrane blebs and that an endogenous nuclease controls its incorporation into the biofilm. Many clinical isolates of *N. gonorrhoeae* contain a GGI, which encodes a T4SS [38]. *N. gonorrhoeae* strain MS11 was shown to secrete ssDNA via this T4SS [33].

To study the effect of secreted ssDNA on biofilm formation in *N. gonorrhoeae*, two approaches were taken. In the first approach, the effect of the addition of Exonuclease I, which highly specifically degrades ssDNA, on biofilm formation was tested. Therefore, Exonuclease I was over-expressed and purified to homogeneity (Figure 4-1 A). As expected, Exonuclease I eluted from the gelfiltration column

as a monomer. The specificity of the purified Exonuclease I in the medium used for the biofilm experiments was tested in an assay where increasing concentrations of the enzyme were incubated with either Cy3 labeled dT<sub>90</sub>-oligomers (to test for nuclease activity on ssDNA) or a PCR product generated with Cy3 labeled primers (to test for nuclease activity on dsDNA) were incubated in the medium used for the continuous flow experiments for 1 hour at 37 °C (Figure 4-1 C and D). This demonstrated that Exonuclease I is highly specific for ssDNA (Figure 4-1).

In contrast, purified Exonuclease III digested dsDNA efficiently, but also showed significant activity against ssDNA in the medium used for the continuous flow experiments, and therefore was not further used. Purification and characterization of Exonuclease III are presented in the Figure 4-1 EIII.

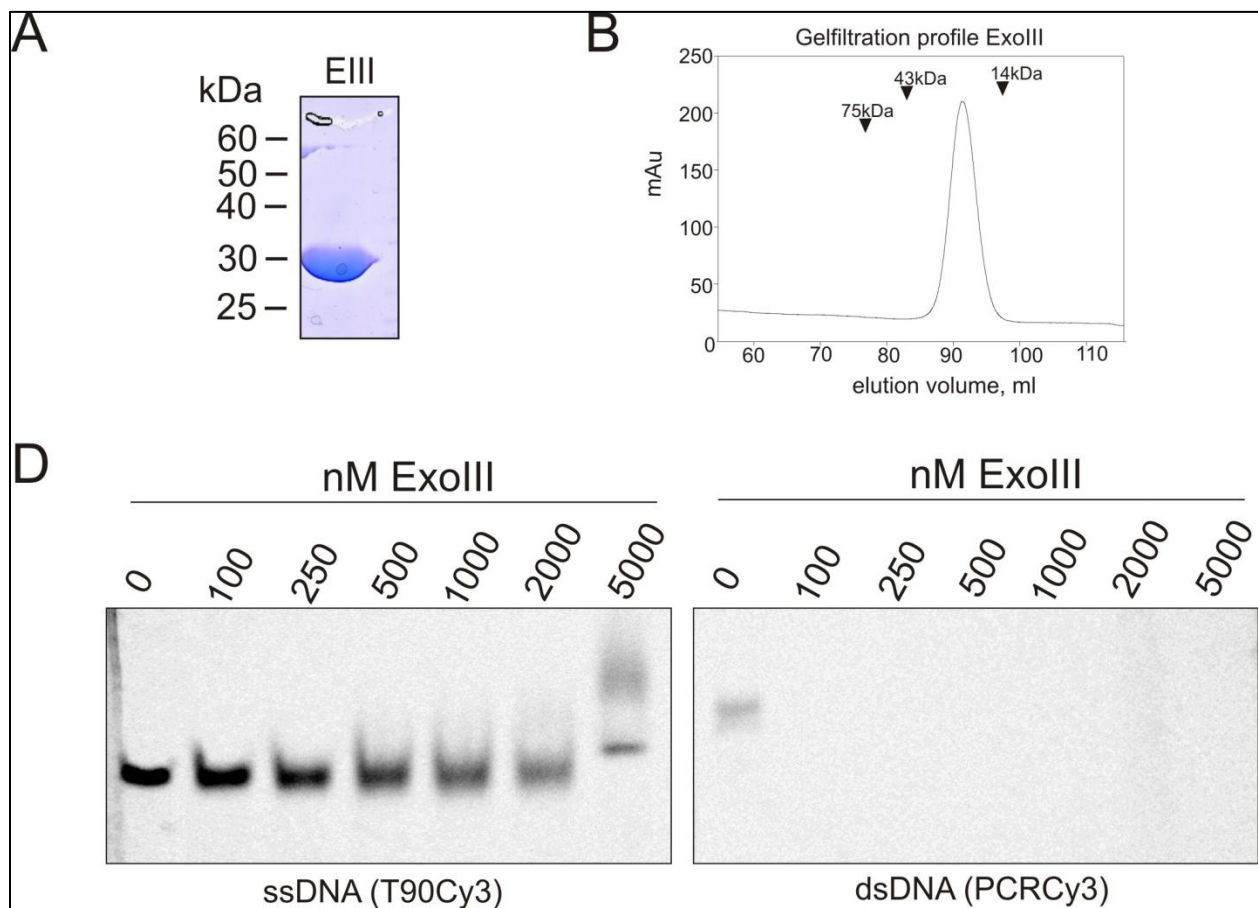


**Figure 4-1 EIII: Purification and characterization of Exonuclease III**

His-tagged Exonuclease III was purified by Ni-NTA affinity, anion exchange and gel filtration chromatography. (B) His-tagged Exonuclease III eluted as a monomer from the SD200 gelfiltration column and was essentially pure as assayed by (A) Coomassie staining of an SDS-PAGE of the purified protein. The positions of the various markers for both the gelfiltration and the SDS-PAGE are indicated. To test the specificity of the purified Exonuclease III, 150 ng of a Cy3 labeled dT<sub>90</sub> oligonucleotide (C) or 150 ng of a Cy3 labeled PCR product (D) were incubated with increasing

concentrations of Exonuclease I for 1 h at 37 °C. The fluorescently labeled DNA was analyzed after separation on a 7.5 % polyacrylamide gels using a LAS-4000 imager.

After the purification and characterization of Exonuclease I, the initial biofilm formation of *N. gonorrhoeae* strain MS11 was investigated in a continuous flow chamber system. The system was perfused at a rate of 0.2 mm s<sup>-1</sup> with Graver-Wade medium supplemented with Kellogg's supplements and 0.042% NaHCO<sub>3</sub> diluted 1:5 with phosphate buffered saline (PBS) or with the same medium containing purified Exonuclease I (Figure 4-2). The quantification of the relative biofilm formation is shown in Figure 4-2 B.

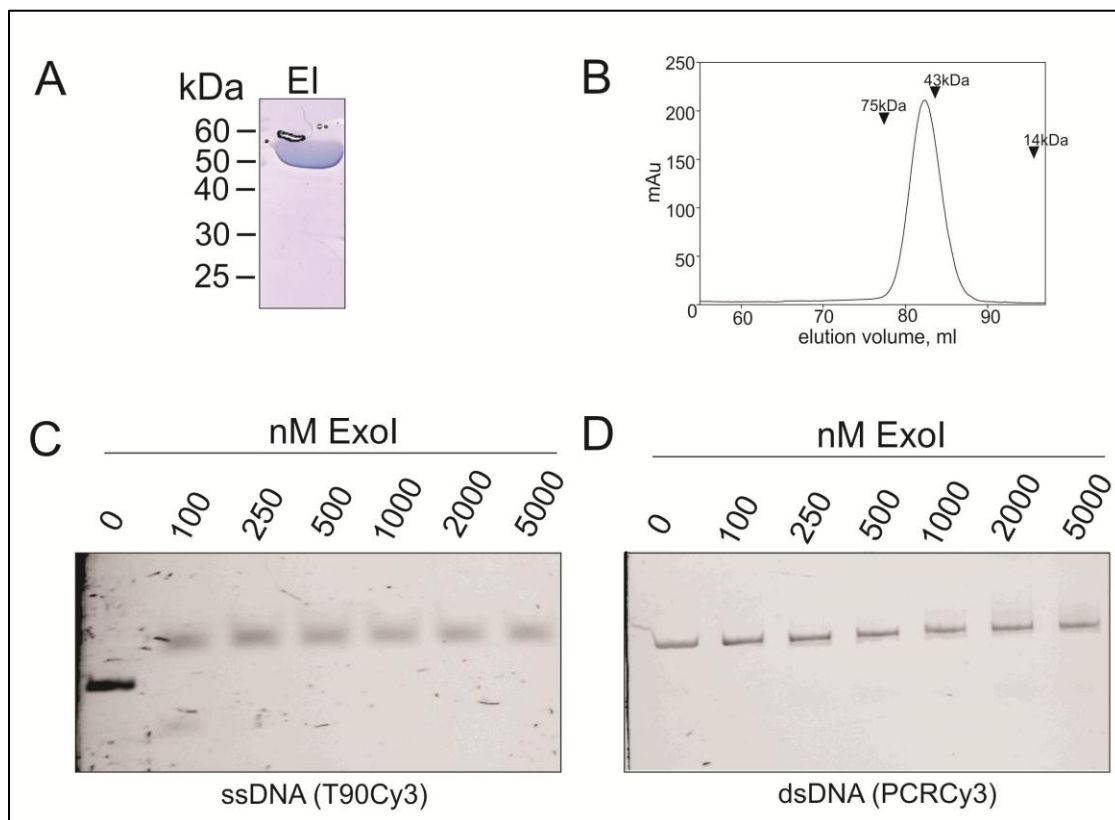


**Figure 4-1: Purification and characterization of Exonuclease I**

His-tagged Exonuclease I was purified by Ni-NTA affinity, anion exchange and gel filtration chromatography. (B) His-tagged Exonuclease I eluted as a monomer from the SD200 gelfiltration column and was essentially pure as assayed by (A) Coomassie staining of an SDS-PAGE of the purified protein. The positions of the various markers for both the gelfiltration and the SDS-PAGE are indicated. To test the specificity of the purified Exonuclease I, 150 ng of a Cy3 labeled dT<sub>90</sub> oligonucleotide (C) or 150 ng of a Cy3 labeled PCR product (D) were incubated with increasing concentrations of Exonuclease I for 1 h at 37 °C. The fluorescently labeled DNA was analyzed after separation on a 7.5 % polyacrylamide gels using a LAS-4000 imager.

The system was inoculated with an exponentially growing *N. gonorrhoeae* culture and biofilm development was monitored by Confocal Laser Scanning Microscopy (CLSM) after 3 and 6 hrs. Almost no attached cells could be detected when Exonuclease I was added (Figure 4-2). This suggested that ssDNA is important for initial attachment of *N. gonorrhoeae*.

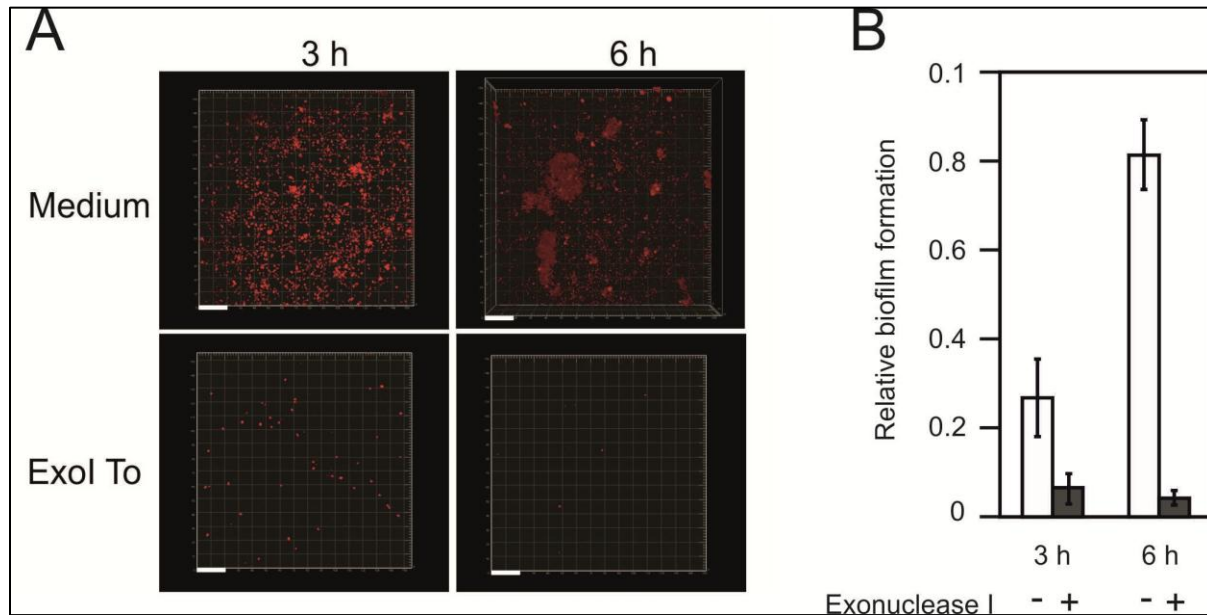


**Figure 4-2: The effect of Exonuclease I on initial attachment.**

Confocal microscopy of continuous flow chambers inoculated with *N. gonorrhoeae* strain MS11 imaged 3 (left panels) and 6 hrs (right panels) after inoculation. The flow chambers contained either minimal medium (upper panels) or minimal medium containing Exonuclease I (lower panels). The enzymes were refreshed every 2 hrs. (A) The biofilm was stained with Syto62 and visualized by CLSM. Micrographs represent three-dimensional images. The bar is 20  $\mu$ m in length. (B) Quantification of the amount of biofilm formed in (A). Biofilm formation is depicted relative to the amount of biofilm formed by MS11 after 24 hours.

#### 4.2.2 DNA secretion facilitates biofilm formation

Since initial attachment of *N. gonorrhoeae* strain MS11 was influenced by the addition of Exonuclease I, and thus most likely by the presence of ssDNA, it was tested whether the ssDNA secreted via the T4SS encoded with the GGI facilitates biofilm formation.

Therefore, biofilm formation of *N. gonorrhoeae* strain MS11 and an MS11 strain containing a deletion of the *traB* gene (MS11 $\Delta$ *traB*) were compared. The *traB* gene encodes a component of the T4SS core complex spanning the inner and outer membrane and deletion of this gene results in the abolishment of DNA secretion [40]. The *traB* mutation does not affect the growth rate (data not shown). To demonstrate that any observed effects were caused by the deletion of the *traB* gene, a strain was

created in which the *traB* gene was restored (*MS11ΔtraB::traB*). Since biofilm formation is strongly affected by the presence and absence of Type IV pili [182], and the Type IV pili of *N. gonorrhoeae* can undergo both phase and antigenic variation [183], piliation of the three strains was compared by comparing colony morphology after growth on plates, by sequencing the *pilE* gene, and by determining the expression levels of PilE by Western blotting of isolated membranes with a PilE antibody. No differences between the three mutants were observed in these three aspects (Figure 4-3).

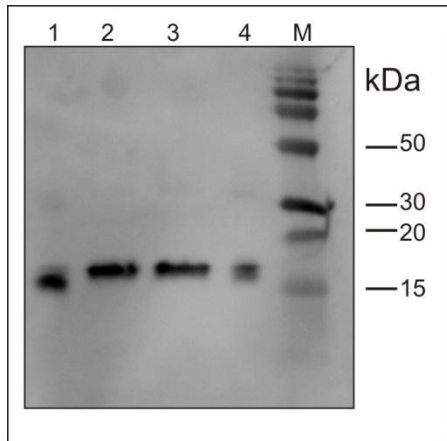


**Figure 4-3: Western Blott Analysis on isolated membranes with PilE-AB.**

1 = ND500 (negative control, has different *pilE*), 2 = MS11, 3 = MS11ΔTraB, 4 = MS11ΔTraB:TraB, M = Marker.

Biofilms of the three strains were grown for 3 days in a continuous flow chamber system. After 48 and 72 hrs, most of the surface was covered by strain MS11 and the formation of distinct three-dimensional structures was observed (Figure 4-4 A). The *MS11ΔtraB* strain showed strongly reduced biofilm formation after 48 and 72 hrs. Also the formation of the distinct three-dimensional structures was strongly reduced. The *MS11ΔtraB::traB* complementation strain showed similar biofilm formation as was observed for strain MS11 after 48 and 72 hrs, with coverage of most of the surface and formation of distinct three-dimensional structures (Figure 4-4). The quantification of biofilm formation is shown in Figure 4-4 B. Increasing the flow rate two-fold showed that the biofilm of the *MS11ΔtraB* strain could be easily washed away and was less stable than the biofilms of the MS11 and the *MS11ΔtraB::traB* strains. This demonstrated that the deletion of the *traB* gene strongly influences biofilm formation.

The observation that the *traB* deletion affects biofilm formation suggests that either the presence of the T4SS or a substrate secreted by the T4SS facilitates biofilm formation and contributes to the stabilization of the biofilm. Since ssDNA is secreted via the T4SS [33], and biofilm formation was strongly influenced

by the presence of Exonuclease I, we propose that ssDNA secreted via the T4SS plays an important role in biofilm development and stabilization.

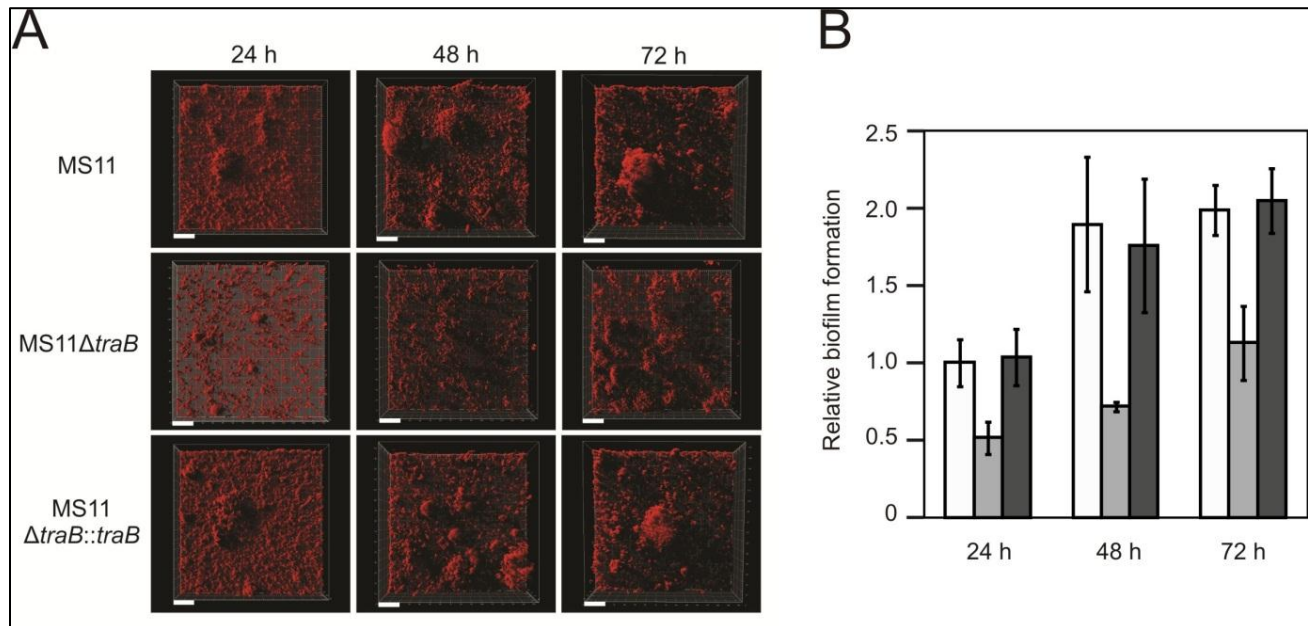


**Figure 4-4: Deletion of the *traB* gene results in a strong decrease of biofilm formation.**

Confocal microscopy of continuous flow chambers inoculated with *N. gonorrhoeae* strain MS11, MS11ΔtraB and MS11ΔtraB::traB imaged 24, 48 and 72 hrs after inoculation. (A) The biofilm was stained with Syto62 and visualized by CLSM. Micrographs represent three-dimensional projections. The bar is 20 μm in length. (B) Quantification of the amount of biofilm formed in (A). Biofilm formation is depicted relative to the amount of biofilm formed by MS11 after 24 hours.

#### 4.2.3 Treatment of biofilms with Exonuclease I only affects strains that secrete ssDNA

To test the effect of the specific degradation of ssDNA, 24 hrs old biofilms of MS11 and the non-secreting mutant MS11ΔtraB were perfused for 1 hour with medium containing Exonuclease I (Figure 4-5 A). The quantification of biofilm formation is shown in Fig. 4-5 B. Treatment of biofilms formed by strain MS11 demonstrated that single cells attached to the glass surface were washed away, but that the distinct three-dimensional structures were not affected by treatment with Exonuclease I. The observation that attached cells of the MS11ΔtraB strain were not affected by treatment with Exonuclease I suggested that ssDNA plays an important role in the initial attachment of the single cells to the surface, but that this putative role is taken over by other components at later stages of biofilm



formation. Indeed, DNA has previously been proposed to function as a cell-to-surface and/or cell-to-cell adhesin during the initial phase of biofilm formation[184].

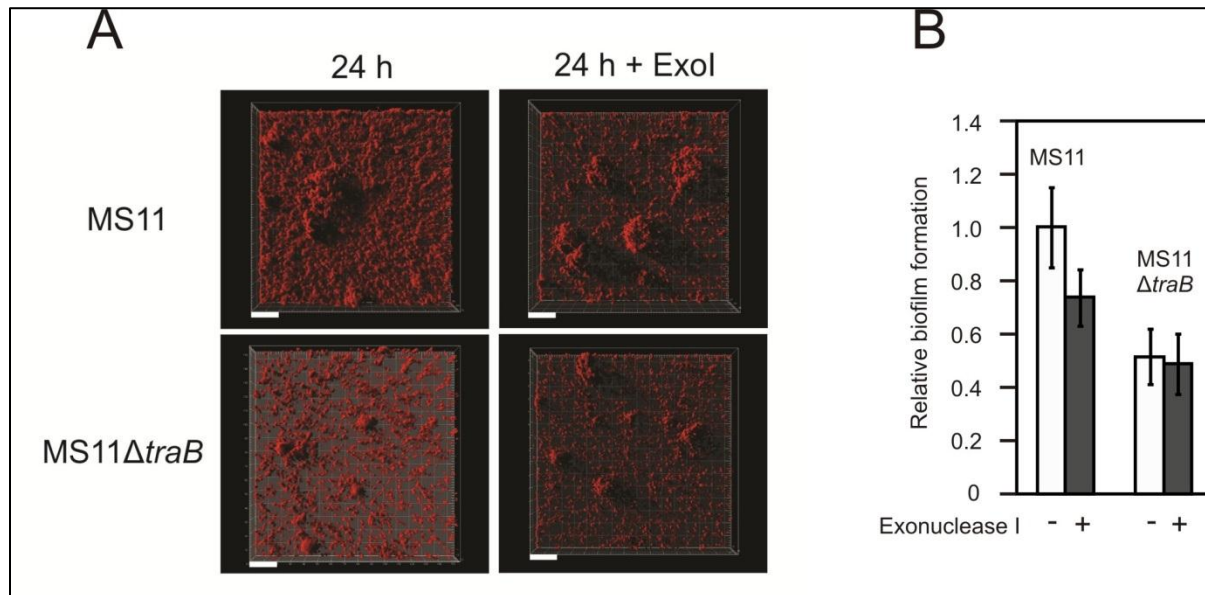


**Figure 4-5: The effect of Exonuclease I on 24 hrs old biofilms.**

Confocal microscopy of continuous flow chambers inoculated with *N. gonorrhoeae* strain MS11 and MS11ΔtraB imaged 24 hrs after inoculation either after 1 hour perfusion with medium, or 1 hour perfusion with medium containing Exonuclease I. (A) Biofilm was stained with Syto62 and visualized by CLSM. Micrographs represent three-dimensional images. The bar is 20 μm in length. (B) Quantification of the amount of biofilm formed in (A). Biofilm formation is depicted relative to the amount of biofilm formed by MS11 after 24 hours.

#### 4.2.4 Visualization of single-stranded DNA

Since our experiments provided strong evidence for a role of ssDNA in biofilm formation of *N. gonorrhoeae* strains, we developed a technique to specifically visualize ssDNA. Currently, many different methods and stains are available to fluorescently detect DNA, such as Ethidium bromide, Propidium iodide, DDAO (7-hydroxy-9H-(1,3-dichloro-9,9-dimethylacridin-2-one), SYTO 60, SYBR Green, OliGreen and many others. To our knowledge, all currently available stains detect however both ssDNA and dsDNA. ssDNA binding proteins (SSBs) bind to ssDNA with high specificity but without clear sequence specificity, and bind to dsDNA only with much lower affinity. We used fluorescently labelled TteSSB2 of *T. tengcongensis* to specifically detect ssDNA. This protein binds specifically to ssDNA with high affinity and remained fully active even after 6 hrs incubation at 100°C [185]. As a control for dsDNA binding, also the thermostable Sac7d protein from *S.s acidocadarius* was overproduced and purified to homogeneity. In the medium used for the continuous flow experiments, Sac7d bound only slightly better to dsDNA

than to ssDNA and therefore could only be used to image both ssDNA and dsDNA. A detailed description of the purification, characterization, DNA binding specificity and optimization of fluorescent labelling of TteSSB2 and Sac7d is provided in the Chapter 3.

#### **4.2.5 The majority of eDNA in biofilms of *N. gonorrhoeae* MS11 is double-stranded**

Since ssDNA might play an important role in the initial attachment of single cells to the surface, we tried to visualize ssDNA and dsDNA in a 10 hrs old biofilm of MS11 (Figure 4-6). Specifically, 10 hrs old biofilms were used, since at that time point the formation of the distinct three-dimensional structures has started, but also single attached cells were still observed. In 10 hrs old biofilms, the single attached cells were still sensitive to Exonuclease I. To enable comparison of the amounts of ssDNA and total external DNA, biofilms were incubated with Texas Red-labelled Sac7d-S18C or Texas Red-labelled TteSSB2-W55C (Fig. 4-6). Both proteins showed approximately equal fluorescence intensity. Interestingly, dsDNA, but not ssDNA could be detected in the 10 hrs old biofilms of MS11. The dsDNA co-localized with the distinct three-dimensional structures. Thus, the amounts of ssDNA which can be detected are very small in comparison to the dsDNA present in the biofilm. Since we were not able to detect ssDNA under the continuous flow conditions, we attempted to visualize ssDNA in planktonic cultures. Texas Red-labelled Sac7d-S18C or Texas Red-labelled TteSSB2-W55C were added to planktonic cultures (Figure 4-7). Again, under these conditions, external DNA could be easily detected with Sac7d-S18C, but no ssDNA was detected with TteSSB2-W55C. When labelled Sac7d-S18C was used, closer inspection revealed that two different intensities of fluorescence were associated with different cells, most likely indicating lysed and non-lysed cells. To confirm that Texas Red-labelled TteSSB2-W55C could in fact be used to detect ssDNA, M13 derived ssDNA was added to the culture and the culture was imaged again. Indeed ssDNA attached to the cells could now be detected (Figure 4-7). We therefore concluded that, compared to the amounts of external dsDNA, only minor amounts of ssDNA were present in cultures of *N. gonorrhoeae*. These minor amounts, however, stimulated the initial attachment of the cells.

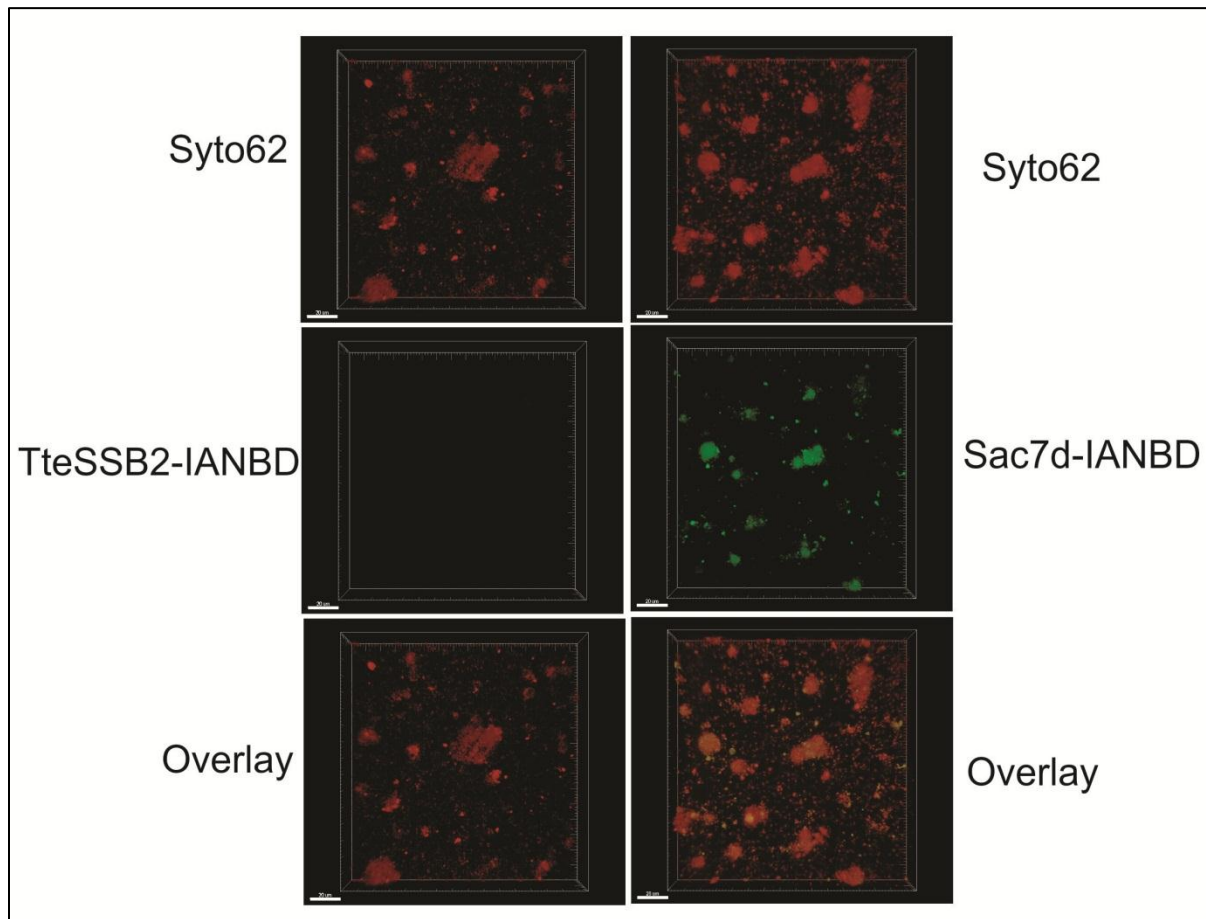


**Figure 4-6: Detection of ssDNA and dsDNA in 10 hrs old continuous flow biofilms of *N. gonorrhoeae*.**

Confocal microscopy of continuous flow chambers inoculated with *N. gonorrhoeae* strain MS11 imaged 10 hrs after inoculation. The biofilm was stained with Syto62 and IANBD- labelled TteSSB2-W55C (left side) and Syto62 and IANBD-labelled Sac7d-S18C (right side) and visualized by CLSM. Micrographs represent three-dimensional projections. The bar is 20 µm in length.

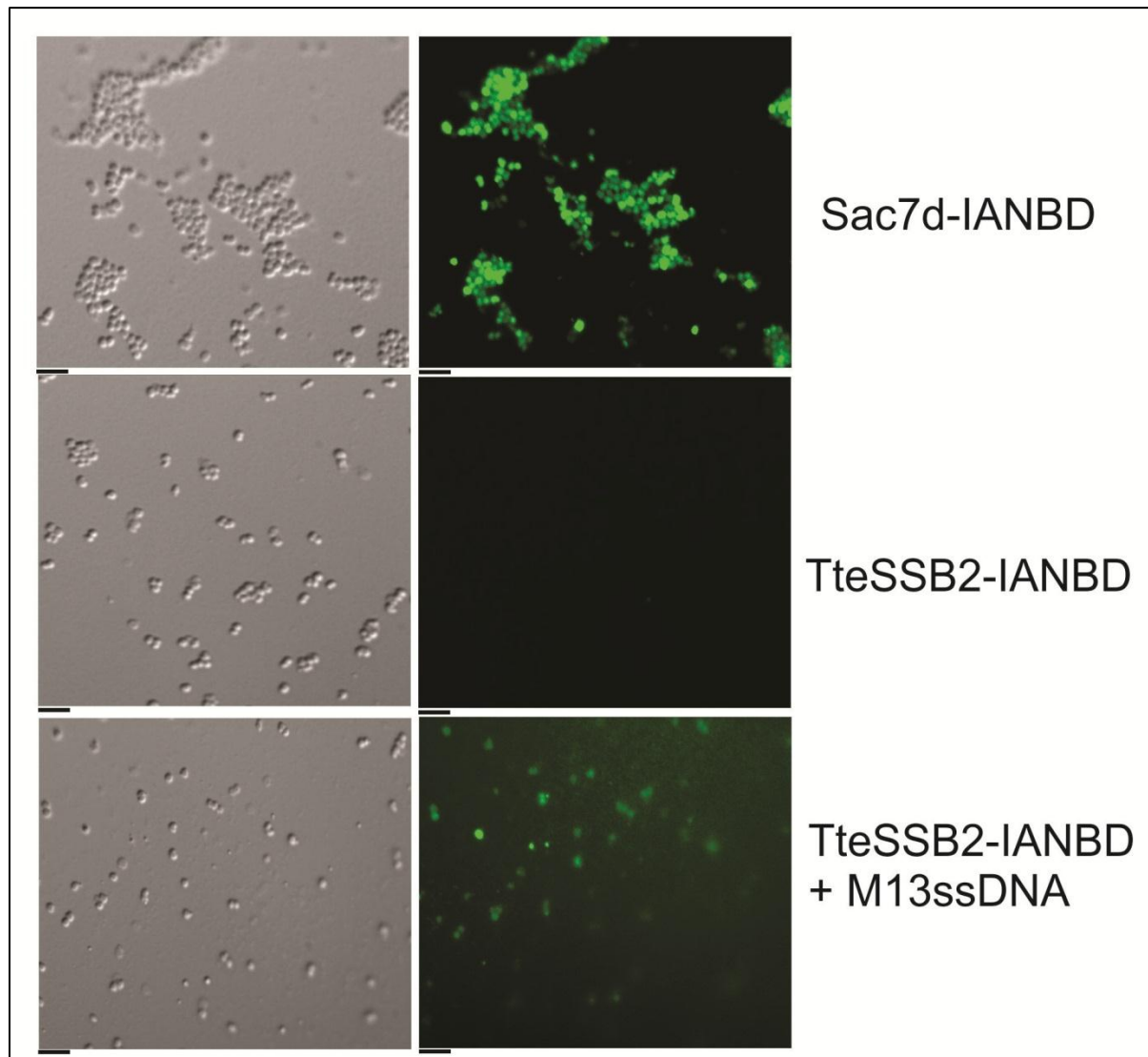


**Figure 4-7: Detection of ssDNA and dsDNA in an exponentially growing culture of *N. gonorrhoeae*.**

*N. gonorrhoeae* MS11 was grown exponentially in minimal medium. The cells were incubated with IANBD-labelled Sac7d-S18C (upper row) or IANBD-labelled TteSSB2-W55C (second row), or was first incubated with ssDNA and then incubated with IANBD-labelled TteSSB2-W55C (third row). The cells were visualized by DIC (left side) or CLSM (right side). Micrographs represent three-dimensional projections. The bar is 5  $\mu\text{m}$  in length.

### 4.3 Discussion

Since the study of Whitchurch *et al.* [130] eDNA is known as one of the major structural components of many bacterial biofilms [129,186,187]. The presence of eDNA was demonstrated using different fluorescent probes that bound to DNA and the importance of eDNA was demonstrated mainly by assessing the effect of DNase I treatment. This often results in release of biomass from grown biofilms, and significantly inhibited biofilm formation [130], [136], [188]. None of the fluorescent probes used in these studies like e.g. propidium iodide, DDAO [138], SYTOX Orange [188], ethidium bromide [138], and PicoGreen [189], can however discriminate between ssDNA and dsDNA. Also DNase I treatment degrades both ssDNA and dsDNA. Thus, it is currently unknown whether different forms of DNA, such as e.g. ssDNA or dsDNA or specific components bound to the eDNA play a specific and/or different role in biofilm. The amounts of the different forms of DNA have also not been assessed before.

eDNA was also shown to play an important role in biofilm formation in *N. gonorrhoeae* [137]. Cultures of *N. gonorrhoeae* strain MS11 were found to contain ssDNA, which is secreted directly into the medium via the T4SS encoded within the GGI [33]. The biofilm formation of *N. gonorrhoeae* has previously not only been studied in MS11, a strain that contains the GGI, but also in *N. gonorrhoeae* strains 1291 and FA1090 which do not contain a GGI. All three of these strains were able to form biofilms [150]. Biofilm formation of *N. gonorrhoeae* is affected by many different factors, like the ability to release blebs [149], the expression of Nuc, the extracellular thermonuclease [137], and the presence of Type IV pili. Many gonococcal genes, like the PilE gene undergo rapid variation [183], which complicates a direct comparison of different isolates. Therefore, we have studied the effects of ssDNA secretion by comparing biofilm formation in MS11 with biofilm formation in a mutant and a complementation mutant directly derived from MS11.

We show in this study that actively secreted ssDNA facilitates biofilm formation of *N. gonorrhoeae*. Our data suggest that ssDNA plays an important role in the initial attachment of single cells to the surface and that this role is taken over by other components at later stages of biofilm formation. The  $\Delta traB$  mutant that does not secrete ssDNA showed strongly reduced biofilm formation. The formation of the distinct three-dimensional structures observed in the wild type (WT) and complementation mutant was strongly reduced in the  $\Delta traB$  mutant, and the stability of the formed biofilm was also strongly reduced. This is the first time that an effect of ssDNA on biofilm formation is demonstrated.

Lappann *et al.* demonstrated that in *N. meningitidis* the capability to form biofilms differs between different lineages [136]. In the most prevalent lineages, biofilm formation is dependent on eDNA. These lineages form stable biofilms and show a very stable interaction with the host. Several less prevalent lineages do not use eDNA for biofilm formation, and form much less stable biofilms. It was proposed that the lineages that do not use eDNA for biofilm formation and show poor colonization properties compensate for their poor colonization properties by higher transmission rates. Possibly, the secretion of ssDNA via the T4SS modulates the colonization and transmission rates of *N. gonorrhoeae* strains.

In this study we developed a method to specifically detect ss- and dsDNA, using fluorescently labelled thermostable ssDNA and dsDNA binding proteins. Both proteins bind to DNA in an essentially sequence unspecific manner. The fluorescent detection of the labelled proteins was optimized by introducing the fluorescent probes at positions where their fluorescence increases upon ssDNA binding. This reduces the signal of the proteins that are not bound to DNA. Detection of ssDNA using TteSSB2 of *Thermoanaerobacter tengcongensis* was highly specific, and ssDNA could be specifically detected in biofilms of *S. acidocaldarius*. TteSSB2 could also be used to detect ssDNA bound to *N. gonorrhoeae* strains, when ssDNA had been added to the culture. The Sac7d protein from *S. acidocaldarius* bound to dsDNA with higher affinity, but most likely will detect both ssDNA and dsDNA, especially since even secreted ssDNA will contain many positions where the ssDNA will anneal and form stretches of dsDNA. Indeed the Sac7d specifically detected DNA in biofilms of *S. acidocaldarius* and of *N. gonorrhoeae*.

In this study we attempted to detect both ss- and dsDNA within biofilms of *N. gonorrhoeae*. During the initial phase in which cells attach to the surface, and where experiments with Exonuclease I demonstrated that ssDNA plays an important role, neither ssDNA nor dsDNA could be detected. Most likely the amounts of ss- and dsDNA are too low for detection at these stages using the fluorescently labelled proteins. At later stages, large amounts of dsDNA could be easily detected. DNA has been found in different patterns for different organisms. For example, the eDNA of *Pseudomonas aeruginosa* is present in the micro-colonies and organized as a grid-like structure on the substratum [138], whereas the eDNA in *Bacillus cereus* biofilms is evenly distributed over the surface, and in biofilms of *Haemophilus influenzae* and the gamma proteobacterium F8 eDNA occurs as filamentous strands [190,191]. In *N. gonorrhoeae* the DNA was primary localized inside the mature mushrooms-like structures. The localization of the DNA using the fluorescently labelled Sac7d resembled the localization patterns found for *N. gonorrhoeae* using other DNA stains. It was remarkable that no ssDNA could be detected in the biofilms of gonococci. This suggests that either only low amounts of ssDNA are present

at these stages compared to dsDNA, or that the ssDNA is shielded from detection by the TteSSB2 protein.

In conclusion, the data presented here show that ssDNA secreted via the T4SS with the GGI facilitates initial attachment of *N. gonorrhoeae* to surfaces. This ssDNA is present only in low amounts. In the mature biofilm, much larger amounts of eDNA are found. This DNA is mostly double stranded and does not play an important structural role within the biofilm.

**Chapter 5****Materials and Methods****5.1 Reagents and equipment****5.1.1 Reagents**

All reagents used in this work were purchased from Difco (Heidelberg), Fermentas (Sankt-Leon Rot), Merck (Darmstadt), Carl Roth (Karlsruhe) and Sigma-Aldrich (Steinheim), if not indicated otherwise.

**5.1.2 Enzymes and Kits****Table 2: Enzymes and Kits used in this study**

<b>Enzyme or Kit</b>	<b>Manufacturer</b>
<b>DnaseI</b>	Roche, Mannheim
<b>Ribonuclease A</b>	Sigma Alrich, Steinheim
<b>Phusion Hot Start High-Fidelity DNA Polymerase</b>	Finnzymes, Hess. Oldendorf
<b>2x DyNAzyme™ II Polymerase Master Mix</b>	Finnzymes, Hess. Oldendorf
<b>T4-Ligase</b>	New England Biolabs, Frankfurt a. M.
<b>Restriction enzymes</b>	New England Biolabs, Frankfurt a. M.
<b>CloneJET™ PCR Cloning Kit</b>	Fermentas, St. Leon-Rot
<b>2x Maxima™ SYBR Green/ROX qPCR Master Mix</b>	Fermentas, St. Leon-Rot
<b>GenElute™ PCR Clean-Up Kit</b>	Sigma Aldrich, Steinheim
<b>Zyppy™ Plasmid Miniprep Kit</b>	Zymo Research, Freiburg
<b>Zymoclean™ Gel DNA Recovery Kit</b>	Zymo Research, Freiburg
<b>ZR Genomic DNA II Kit</b>	Zymo Research, Freiburg
<b>FireSilver Staining Kit</b>	Proteom Factory, Berlin
<b>Dig High Prime DNA Labeling and Detection Kit</b>	Roche, Mannheim



**Table 3: DNA and protein ladders used in this study**

Ladder	Manufacturer
<b>DNA ladder:</b> GeneRuler™ 1kb Plus DNA Ladder	Fermentas GmbH, St. Leon-Rot
<b>Protein ladder:</b> PageRuler™ Protein Ladder (10kDa to 200kDa)	Fermentas GmbH, St. Leon-Rot

**Table 4: Equipment used in this study**

Application	Device	Manufacturer
<b>Cell disruption</b>	Branson sonifier	Heinemann (Schwäbisch Gmünd)
<b>Centrifugation</b>	RC 5B plus, Ultra Pro 80, Multifuge 1 S-R, Biofuge frasco, Biofuge pico	Sorvall/Thermo Scientific (Dreieich), Heraeus/Thermo Scientific (Dreieich),
<b>PCR</b>	MasteCycler personal MasteCycler egradient	Eppendorf (Hamburg)
<b>Electroporation</b>	GenePulser Xcell	Bio-Rad (Munche)
<b>Protein electrophoresis</b>	Mini-PROTEAN® 3 cell	Bio-Rad (Munche)
<b>Western blotting</b>	TE77 semi-dry transfer unit	Amersham Biosciences (Munche)
<b>Chemiluminescence detection</b>	Fuji Photo Film FPM 100A Luminescent image analyzer LAS-4000	Fujifilm (Düsseldorf)
<b>Immunofluorescence microscopy</b>	Diagnostic microscope slides 12 well	Thermo Scientific (Dreieich)

<b>Electron microscopy</b>	Carbon-film covered grids	PLANO (Wetzlar)
<b>Imaging</b>	Leica DM6000B and DM IRE2 light microscopes  Nikon Eclipse TE 2000-E light microscope	
<b>Determination of optical densities</b>	Ultrospec 2100 pro spectrophotometer	Amersham Biosciences (Munche)
<b>Determination of nucleic acids absorption</b>	Nanodrop ND-1000 UV-Vis spectrophotometer	Nanodrop (Wilmington)

---

## 5.2 Microbiological methods

### 5.2.1 Cultivation of bacteria

#### 5.2.1.1 Cultivation of *E. coli*

*E. coli* strains (see table 1) were used for cloning and overexpression and were grown in Luria-Bertani (LB) medium at 37°C with the appropriate antibiotics; ampicillin (100 µg/ml), erythromycin (500 µg/ml) or chloramphenicol (34 µg/ml).

#### 5.2.1.2 Cultivation of *N. gonorrhoeae*

*N. gonorrhoeae* strains were plated from glycerol stocks on GC agar (BD Difco, Heidelberg, Germany) containing Kellogg's supplements[192] and grown overnight under 5% CO<sub>2</sub> at 37 °C. When necessary, chloramphenicol and/or erythromycin were added at the final concentration 10 µg/ml

#### 5.2.1.3 Cultivation of *Sulfolobus ssp.*

*Sulfolobus* strains were grown in Brock medium at 76 °C, with pH adjusted to 3 using sulphuric acid, and supplemented with 0.1% (w/v) tryptone [193].

## 5.2.2 Strains used in this study

**Table 5:** *E.coli* strains used in this study

Strain	Description	Source or reference
<b>DH5<math>\alpha</math></b>	F- endA1 glnV44 thi-1 recA1 relA1 gyrA96 deoR nupG $\Phi$ 80dlacZ $\Delta$ M15 $\Delta$ (lacZYA- argF)U169, hsdR17(rK- mK+), $\lambda$ -	Invitrogen
<b>Tuner (DE3)</b>	F- ompT hsdSB(rB- mB-) gal dcm lacY1 (DE3)	Novagen
<b>C43 (DE3)</b>	F' ompT hsdS <sub>B</sub> (r <sub>B</sub> <sup>-</sup> m <sub>B</sub> <sup>-</sup> ) gal dcm (DE3)	[194]
<b>RDP268</b>	F- thr-J leuB6 proA2 his4 argE3 thi-J ara-14 lacYJ galk2 xyl-5 mtl-I rpsL31 tsx-33 supE4422 ssb:Km, $\lambda$ -	[162]

**Table 6:** *N. gonorrhoeae* strains used in this study

Strain	Description	Source or reference
<b>MS11</b>	<i>Neisseria gonorrhoeae</i> strain	[22]
<b>ND500</b>	MS11A $\Delta$ GGI	[33]
<b>SJ001</b>	MS11 strain with <i>pilQ</i> truncation	[195]
<b>SJ023</b>	MS11 strain transformed with plasmid pSJ023. N-terminal one strep tagged <i>SSB</i> <sup>OE</sup> behind a <i>lac</i> promoter inserted between <i>lctP</i> and <i>aspC</i> on the chromosome, (Cm <sup>R</sup> )	This study
<b>SJ038</b>	MS11 strain transformed with plasmid pSJ038; <i>SSB</i> <sup>OE</sup> behind a	This study

	<i>lac</i> promoter inserted between <i>lctP</i> and <i>aspC</i> on the chromosome, (Cm <sup>R</sup> )	
EP005	MS11ΔTraB, (Erm <sup>R</sup> )	[196]
EP006	MS11 ΔrecA, (Erm <sup>R</sup> )	[196]
EP030	ND500 ΔrecA, (Erm <sup>R</sup> )	[196]
EP015	MS11 strain transformed with plasmid pKH35 vector between <i>lctP</i> and <i>aspC</i> region on the chromosome, (Cm <sup>R</sup> )	[196]
EP029	ND500 strain transformed with plasmid pKH35 vector between <i>lctP</i> and <i>aspC</i> region on the chromosome, (Cm <sup>R</sup> )	[196]
KS001	MS11ΔTraB:TraB	This study

**Table 7:** *Sulfolobus* spp used in this study

Strain	Description	Reference or source
<i>S.solfataricus</i> P2 (DSM1617)		[197]
<i>S.acidocaldarius</i> (DSM639)		[197]
<i>S.tokodaii</i> (DSM16993)		[197]

### 5.3 Molecular biological methods

#### 5.3.1 Polymerase Chain Reaction (PCR)

Amplification of DNA sequences for preparative purposes was done by using Phusion Hot Start High-Fidelity DNA Polymerase (Finnzymes, Hess. Oldendorf).

**Table 8: Composition of PCR reaction mixture and thermal cycling protocol used for standard PCR reactions**

50 µl PCR reaction mixture	Thermal cycling protocol		
35,5 µl sterile H <sub>2</sub> O <sub>dd</sub>	Initial denaturation	98°C 30 sec	1x
10 µl 5x HF-Phusion buffer	Denaturation	98°C 10 sec	30 cycles
1 µl dNTPs	Annealing	50-65 °C* 20 sec	
1 µl Primer 1 (10 µM)	Extension	72°C (30sec/kb)	
1 µl Primer 2 (10µM)	Final extension	72°C 10 min	1x
1 µl Template DNA			
0,5 µl Phusion polymerase			

\*annealing temperature was chosen between 50 and 65°C, depending on the melting temperature of the primer pair

#### 5.3.2 Primers and plasmids used in this study

**Table 9: Primers used in this study**

Primer	5-3 Sequence	Used for
400F-GGI	CACACCTCGAGTTACAATGGGATGTCATCATCAGC	NgSsbB amplification
401R-GGI	CTCTCCATATGCACCATCACCATCACCATCACCACATGTCAGTTCAACTTTTTGTTCCG	NgSsbB amplification; introduces 10 x His and NdeI site exchange
402F-GGI	GGGCAGCATCACGATTCCAGTACTCGCTAGAAATCCACTCC	Cysteine 59 to Serine of NgSsbB
403R-GGI	TGGAATCGTGATGCTGCCATCTCCATAAAATATTACAGG	exchange Cysteine 59 to Serine of NgSsbB
404F-GGI	GCTCACGTTTAGGACGCAACTTGATAGCTTCTACAC	exchange Serine 128 to Cysteine

		of NgSsbB
<b>405F-GGI</b>	CGGTCCTAAACGTGAGCAGTGTGAGGACAATAATC	exchange Serine 128 to Cysteine of NgSsbB
<b>406R-GGI</b>	ACCCGAGGTCTCTGCGCCATGTCAGTTCAACTTTTGTTCG	NgSsbB amplification; introduces BsaI site for cloning in pPR-IBA102
<b>407F-GGI</b>	AGGGAAGGTCTCGTATCATTACAATGGGATGTCATCATCAGC	NgSsbB amplification; introduces BsaI site for cloning in pPR-IBA102
<b>423F-GGI</b>	AGGCCACTCGAGTTACAATGGGATGTCATCATCAGC	amplification of NgSsbBWT-tag-less, introduces XhoI site, forward
<b>424R-GGI</b>	AGGCCACATATGTCAGTTCAACTTTTGTTCG	amplification of NgSsbBWT-tag-less, introduces NdeI site, reverse
<b>427R-GGI</b>	GTACGATTGAGGCTTCACAGTTTTTAGGGCTAGCTACAGGACGC	exchange Asparagin 26 to Cysteine of NgSsbB
<b>428F-GGI</b>	TGAAGCCTCAATCGTACTGAATTTTTCAGTTGCCCTACC	exchange Asparagine 26 to Cysteine of NgSsbB
<b>429R-GGI</b>	AAGATGTATTCATTGTTTAAGATCCGGCTGCTAACAAAGCC	amplification of Trun-NgSsbB, reverse
<b>430F-GGI</b>	TTAAACAATGAATACATCTTGAACACG	amplification of Trun-NgSsbB, forward
<b>611</b>	AAGTGAACCACCGGATGACAGCTCGGGGTAATCAG	exchange Glycine 24 to Cysteine in TteSSB2
<b>612</b>	CATCCGGTGGTTCACTTTTCTCTGCCGTGGATCG	exchange Glycine 24 to Cysteine in TteSSB2
<b>613</b>	TTCCAGGATTTCTGCCAGGCGATTACAGGCAACCACCGGAATG	exchange Tryptophan 55 to Cysteine in TteSSB2
<b>614</b>	CTGGCAGAAATCCTGGAACAGTATGCGGTGAAAGGC	exchange Tryptophan 55 to Cysteine in TteSSB2
<b>615</b>	TCCGTGTAGCGACGGGTACACAGACGACCAACCACGG	exchange Glutamine 79 to Cysteine in TteSSB2
<b>616</b>	CCCGTCGCTACACGGATGGCAGTGGTAAAAACGTTTCG	exchange Glutamine 79 to Cysteine in TteSSB2
<b>617</b>	TGCCATCCGTGTAGCGACAGGTCTGCAGACGACCAAC	exchange Arginine 81 to Cysteine in TteSSB2

618	CGCTACACGGATGGCAGTGGTAAAAACGTTTCGCATTCTGG	exchange Arginine 81 to Cysteine in TteSSB2
678	CTCTCCATATGCACCATCACCATCACCATCACCATCACCACCGAATGGAAGAAAAAGTAGGTAATC	SulSSB1
679	CACACCTCGAGTCACTCCTCTTACCTTCTTCG	SulSSB2
680	CTTCGTTTTCTTGTCTCCTACCACATCTTCTCCATAACC	SulSSB3
681	GGAGACAAGAAAACGAAGAAGGTGAAGAGGAGTGAC	SulSSB4
985	CTCTCCATATGCACCATCACCATCACCATCACCATCACCACATGATGAATGACGGTAAGC	ExoI amplification
986	CACACCTCGAGTTAGACAATCTTTCGCGCTAC	ExoI amplification
1016	CTCTCCATATGCACCATCACCATCACCATCACCATCACCACATGAAATTTGTCTCTTTAATATC	ExoIII from BL21 for
1017	GTATCTCGAGTTAGCGGCGGAAGGTCG	ExoIII from BL21 rev
1040	AGACACTTGAAGATAAAGAAGGTTTGAGAG	Ser18-Cys mutagenesis for Sac7d
1041	TTATCTTACAAGTGTCTACTTCTTCTCTTCAACC	Ser18-Cys mutagenesis for Sac7d
1042	ACGCACATATGGTGAAGGTAAAGTTC	Amplification of Sac7d
1043	AGCCACTCGAGTCAGTGATGGTATGGTATGGTATGGTATGTTTCTTCTCTTTCTGC	Amplification of Sac7d
1044	CTTTTGAGCATCACACTCGCTTACAGCTCCTCTACC	Lys48-Cys mutagenesis for Sac7d
1045	AAGCGAGTGTGATGCTCCAAAAGAATTATTAGACATG	Lys48-Cys mutagenesis for Sac7d
pHJ002_For	5'-GCGGTAGGTCTCAGCGCCATGTCAGTTCAACTTTTTGTTCTGTG-3'	
pHJ002_Rev	5'-CGCGGTAGGTCTCATATCACAATGGGATGTCATCATCAGCGT-3'	
pSJ038_For	5'-GCGGCCATATGATATGTCAGTTCAACTTTTTGTTCTGTGG-3'	
pSJ038_Rev	5'-GCGCCTCGAGCGTGGCCATATATTACAATGGG-3'	
ssb-Hind	5'-GCTAAGCTTTCAGCCATAATGCAGCAAG-3'	
ssb-Xho	5'-ACTCGAGATGACTGTCCGTGGGCATTT-3'	
ForwardDus	CCGAAGCTTGAGCTTGCCGTCTGAAATGG	
ReverseDus	TATCGAATTCCTGCAGCCCGGGGATCCAC	
ForwardErmC	TACTGCCGGCCGCTCTAGAACTAGTG	
ReverseErmC	TCGGAATTCGCTGCATGCCGTCTGAAACC	
GGI-89F	CGCGAATTCTCAGAACGCGCTTACATCAG	
GGI-90R	CGCGAGCTCCAGTACGACATCGACTTGAC	
GGI-87F	GCGGAAGCTTGGAGGTTGAGATGAGGGTGAAAG	
GGI-88R	CTGCGGTACCGATAACCGCTAATTGCAGGCG	

Table 10: Plasmids used in chapter 2

Plasmids	Description	References
pET-20b(+)	Cloning/expression vector, (Amp <sup>R</sup> )	Novagen
pPR-IBA-102	N-terminal OneStrep vector pPR-IBA-102(Amp <sup>R</sup> )	IBA GmbH
pIDN3	IDM vector (Erm <sup>R</sup> )	[198]
pKH35	Complementation vector (Cm <sup>R</sup> ), 6.5kb	[33]
pKH37	Complementation vector (Cm <sup>R</sup> ), 6.5kb	[199]
pMV009	<i>SsbB</i> gene cloned in the pET-20b(+) vector. PCR product of the full length <i>ssbB</i> gene created with primers 423F-GGI and 424R-GGI, (Amp)	This study
pHJ002	<i>ssb</i> gene with N-terminus OneSTrEP tag cloned in the pBR-IBA102 vector. PCR product of the full length <i>ssb</i> gene created with primers pHJ002_For and pHJ002_Rev using MS11A genomic DNA as template and cloned in the BsaI site of pBR-IBA102.	<b>This study</b>
pSJ023	N-terminal one strep tagged <i>ssb</i> gene cloned in pKH37 vector. <i>ssb</i> gene cloned from pHJ002 in the XbaI and HindIII sites of pKH37.	<b>This study</b>
pSJ038	<i>ssb</i> gene cloned in pKH37	<b>This study</b>



	vector. PCR product of the full length <i>ssb</i> gene created with primers pSJ038_For and pSJ038_Rev using MS11A genomic DNA as template and cloned in the XhoI and NdeI sites of pKH37.
<b>pKH113</b>	<i>ssb</i> gene cloned in pIDN3 vector. PCR product of the full length <i>ssb</i> gene created with primers <i>ssb</i> -Hind and <i>ssb</i> -Xho using MS11A genomic DNA as template and cloned in the HindIII and XhoI sites of pIDN3.
<b>pKH114</b>	<i>ermC</i> and <i>ssb</i> gene cloned from pKH113 in pRPZ146 using PstI and SphI; replacing the <i>E. coli</i> <i>ssb</i> and <i>tet</i> from pRPZ146.

Table 11: Plasmids used in chapter 3

Plasmids	Description	References
<b>pMV001</b>	N-terminal fusion of 10-His to <i>ssb</i> gene from <i>S. solfataricus</i> cloned in the pET-20b(+) vector, PCR was performed on gDNA of <i>S. solfataricus</i> using primers 678 and 678 and cloned in in the NdeI and XhoI sites of pET-20b(+), (Amp)	This study
<b>pMV002</b>	SSB2-Cys from <i>S. solfataricus</i> cloned in the pET-20b(+) vector, Mutagenesis PCR was performed on pMV001 using primers 680 and 681, (Amp)	This study

<b>pMV003</b>	N-terminal fusion of 10-His to <i>ssbB</i> gene cloned in the pET-20b(+) vector. PCR product of the full length <i>ssbB</i> gene created with primers 401R-GGI and 400F-GGI on MS11A genomic DNA cloned in the <i>NdeI</i> and <i>XhoI</i> sites of pET-20b(+), (Amp)	This study
<b>pMV010</b>	N-10xHis- <i>ssbBD26C</i> from <i>N. gonorrhoeae</i> cloned in the pET-20b(+) vector, Mutagenesis PCR was performed on pMV003 using primers 427R-GGI and 428F-GGI, (Amp)	This study
<b>pMV011</b>	TteSSB2 from <i>T. thencongensis</i> cloned in the pET-20b(+) vector, the <i>NdeI/XhoI</i> fragment of pMV002 containing the <i>ttessb2</i> gene was cloned in the <i>NdeI</i> and <i>XhoI</i> sites of pET-20b(+), (Amp)	This study
<b>pMV012</b>	TteSSB2G24C from <i>T. thencongensis</i> cloned in the pET-20b(+) vector, Mutagenesis PCR was performed on pMV011 using primers 611 and 612, (Amp)	This study
<b>pMV013</b>	TteSSB2W55C from <i>T. thencongensis</i> cloned in the pET-20b(+) vector, Mutagenesis PCR was performed on pMV011 using primers 613 and 614, (Amp)	This study
<b>pMV014</b>	TteSSB2Q79C from <i>T. thencongensis</i> cloned in the pET-20b(+) vector, Mutagenesis PCR was performed on pMV011 using primers 615 and 616,	This study

---

	(Amp)	
<b>pMV015</b>	TteSSB2W55C from <i>T. thencongensis</i> cloned in the pET-20b(+) vector. Mutagenesis PCR was performed on pMV011 using primers 617 and 618, (Amp)	This study
<b>pMV023</b>	Overexpression of His <sub>10</sub> -tagged Sac7d from <i>S.acidocaldarius</i> PCR product of the <i>sac7d</i> gene created with primers 1042 and 1043 on genomic DNA of <i>S.acidocaldarius</i> cloned in the <i>Nde</i> I and <i>Xho</i> I sites of pET-20b(+), (Amp)	This study
<b>pMV024</b>	Overexpression of His <sub>10</sub> -Sac7dSer18Cys from <i>S. acidocaldarius</i> . Mutagenesis PCR was performed on pMV023 using primers 1040 and 1041, (Amp)	This study
<b>pMV025</b>	Sac7dL48C from <i>S. acidocaldarius</i> cloned in the pET-20b(+) vector, Overexpression of His <sub>10</sub> -Sac7dLys48Cys from <i>S.acidocaldarius</i> . Mutagenesis PCR was performed on pMV023 using primers 1044 and 1045. Amp	This study

Table 12: Plasmids used for chapter 4

Plasmids	Description	References
<b>pET-20b(+)</b>	Cloning/expression vector, (Amp <sup>R</sup> )	Novagen
<b>pSH001</b>	Cloning vector, (Erm <sup>R</sup> )	[196]

<b>pIND1</b>	IDM vector (Erm <sup>R</sup> )	[198]
<b>pEP015_2</b>	<i>traB</i> replacement	[196]
<b>pEP015_1</b>	<i>traB</i> replacement	[196]
<b>pMV019</b>	Overexpression of His <sub>10</sub> -tagged Exonuclease I. PCR product of the full length <i>sbcB</i> gene of <i>E.coli</i> created with primers 986 and 985 on BL21 genomic DNA cloned in the <i>NdeI</i> and <i>XhoI</i> sites of pET-20b(+), (Amp)	This study
<b>pMV020</b>	ExonucleaseIII overexpression N-terminal fusion of 10-His to <i>xthA</i> gene from <i>E. coli</i> cloned in the pET-20b(+) vector, PCR product of full length <i>xthA</i> gene of <i>E.coli</i> created with primers 1016 and 1017 on BL21 gDNA cloned in the <i>NdeI</i> and <i>XhoI</i> sites of pET-20b(+), (Amp)	This study
<b>pMV023</b>	Overexpression of His <sub>10</sub> -tagged Sac7d from <i>S.acidocaldarius</i> PCR product of the <i>sac7d</i> gene created with primers 1042 and 1043 on genomic DNA of <i>S.acidocaldarius</i> cloned in the <i>NdeI</i> and <i>XhoI</i>	This study

---

	sites of pET-20b(+).	
<b>pMV024</b>	Overexpression of His <sub>10</sub> -Sac7dSer18Cys from <i>S. acidocaldarius</i> . Mutagenesis PCR was performed on pMV023 using primers 1040 and 1041, (Amp)	This study
<b>pMV025</b>	Overexpression of His <sub>10</sub> -Sac7dLys48Cys from <i>S. acidocaldarius</i> . Circular PCR was performed on pMV023 using primers 1044 and 1045, (Amp)	This study
<b>pMV022</b>	TteSSB2 in pUC57	GenScript

### 5.3.3 Colony lysis for colony PCR

The colony PCR method was performed to screen recombinant clones for the presence of the correct insert. To perform a PCR on a lysed colony, the DyNAzym II Polymerase Master Mix was used. Therefore single colonies were picked with a sterile pipette tip and transferred to a tube containing 25 µl lysis buffer (1% Triton X-100, 20 mM Tris-HCl, 2 mM EDTA (pH 8.0)). After that the samples were heat-denatured at 95°C for 20 min. 2 µl of the cell lysates were directly used as DNA templates for PCR.

### 5.3.4 Agarose gel electrophoresis

In order to analyze PCR products, plasmids and other DNA fragments, they were separated according to their size via agarose gel electrophoresis. Therefore, samples were mixed with 6x loading dye (50% sucrose solution; 0,1% bromphenol blue) before loading on a 1% (w/v) agarose gel containing 1 µg/ml ethidium bromide. 1xSBA-buffer (Table 13) was used as gel and electrophoresis buffer. Voltage and running time were adjusted according to the demanded separation characteristics. GeneRuler 1kb Plus DNA Ladder (Fermentas, St. Leon Roth) was used as molecular size marker and DNA fragments were visualized by illuminating UV-light (wavelength 365 nm), photographed by the Bio-Doc Imaging System and printed by the Mitsubishi Electronic P93 printer. To isolate a DNA fragment from the agarose gel,

the piece with the desired band was cut by a lancet on a UV-table and was purified using the Zymoclean Gel DNA Recovery Kit (Zymo Research, Freiburg).

**Table 13: Composition of 20x SBA buffer**

20x SBA buffer (pH 8,5)	200 mM NaOH  40 mM EDTA (pH 8,0)  Adjust with boric acid to pH 8,5
-------------------------	--

### 5.3.5 DNA restriction

To digest DNA fragments, restriction enzymes from New England Biolabs (Frankfurt a.M.) were used. Buffer and incubation temperature were chosen according to the manufacturers recommendations. To prepare samples for preparative purposes, a total volume of 50 µl was used and incubated over night. For analytical purposes, 10 µl reactions were prepared and incubated for 1 h. The volume of the restriction enzyme was about 0,1% of the total volume. Digested products were purified with GenElute PCR Clean-Up Kit (Sigma Aldrich, Steinheim).

### 5.3.6 Ligation

In order to ligate two DNA fragments, which were treated before with the same restriction enzyme, T4-ligase (New England biolabs, Frankfurt a.M.) was used. This enzyme catalyzes the formation of phosphodiester bonds between neighboring 3'-OH and 5'-phosphate ends. To ligate two DNA fragments, equal concentrations of both were mixed and T4-Ligase buffer (New England biolabs, Frankfurt a.M.) and 5 units of the enzyme were added. The reaction mix was then incubated for 2 h at room temperature.

### 5.3.7 Transformation of competent *E.coli* cells

After thawing a 50 µl aliquot of competent *E.coli* TOP10F' cells on ice, 50 ng of plasmid DNA was added and incubated on ice for 30 min. Subsequently the cells were placed at 42°C for 90 sec and were then immediately placed on ice. Then 700 µl of LB medium was added to the tube and the cells were incubated at 37°C for 30 to 45 min while shaking vigorously. The transformed cells were either used to inoculate liquid LB-medium or were used to be grown on LB agar plates. For the latter a volume of 50 µl but also the residual cells, which were concentrated by centrifugation, were plated on two different LB

plates containing the appropriate antibiotic. After incubation over night at 37°C, single colonies could be picked for further use.

### **5.3.8 Transformation of *N. gonorrhoeae***

A volume of 20 µl from the purified and concentrated (200 ng/µl) PCR product was denatured at 95°C for 5 min and was then immediately put on ice. After cooling down the transformation construct was pipetted on a GCB agar plate and was put in the laminar flow cabinet until the DNA solution was dried. Next the plate was pre-warmed at 37°C and a piliated colony from an overnight plate of *N. gonorrhoeae* MS11A was picked with a sterile loop and was swept over the dried DNA solution. The plate was incubated overnight at 37°C in a 5% CO<sub>2</sub> atmosphere. The next day the cell material was taken by a sterile swab and plated on a pre-warmed GCB plate containing chloramphenicol (10 µg/ml) as selection marker. The plate was again incubated for 48 h. Single colonies were picked and screened for the presence of the correct insert. Positive clones were plated again on a new plate and incubated over night at 37°C to make glycerol stocks for long term storage.

### **5.3.9 DNA Sequencing**

DNA constructs, used for preparative purposes in this study, were sequenced by Eurofins MWG Operon's DNA sequencing service (Hamburg).

### **5.3.10 Co-culture assay for DNA uptake and transformation**

The assay was performed as described previously [33]. *N. gonorrhoeae* strains EP006 or EP030 which have an erythromycin marker inserted within the *recA* gene to ensure one directional transfer were used as donors, while *N. gonorrhoeae* strains EP015, EP029 and SJ038 which contain a chromosomal chloramphenicol marker were used as acceptor strains. Shortly, piliated *N. gonorrhoeae* strains were grown overnight on GCB agar plates at 37 °C under 5 % CO<sub>2</sub> and transferred to 3 ml of GCBL medium supplemented with Kellogg's supplements and 0.042 % NaHCO<sub>3</sub>. Cultures were grown for 2.5 hrs at 37 °C with shaking under 5% CO<sub>2</sub>. 1 ml of both donor and recipient cultures were centrifuged and pellets were resuspended in 3 ml of GCBL. 0.5 ml of donor and recipient cells were mixed in 3 ml of GCBL, and growth was continued. After 5 hrs, serial dilutions were spread on selective media containing erythromycin and chloramphenicol. Transfer frequencies were calculated as CFU of transformants per CFU of donor. To study the effect of SsbB on DNA transformation, a similar assay was performed after addition of 50 µl of 2 mg/ml purified OneSTrEP-tagged SsbB directly after mixing the strains and again after 2.5 hrs.

### 5.3.11 Complementation of *E. coli* SSB

To determine if SsbB could substitute for *E. coli* SSB, we attempted to replace pRDP146 with pKH114 in *E. coli* SSB mutant RDP268. pKH114 carries *ermC* and the GGI *ssb* in place of *tet* and the *E. coli* *ssb* that are on pRPZ146 [162]. RDP268 carries the *aphA* gene in place of *ssb* on the chromosome and is unable to grow unless complemented with an *ssb* gene [162]. pRDP146 is capable of complementing the mutation as is a similar plasmid carrying the *E. coli* F-plasmid single-stranded binding protein gene *ssf*. Electroporation was used to introduce pKH114 into RDP268, and transformants were selected on LB agar plates containing erythromycin. Fifty  $\text{Erm}^{\text{R}}$  colonies were replica plated to plates containing tetracycline or erythromycin. All fifty transformants grew on both selective media. Plasmid screening by the method of Kado and Liu [200]. demonstrated that the  $\text{Erm}^{\text{R}}$   $\text{Tet}^{\text{R}}$  colonies carried both plasmids, pKH114 and pRDP146. Since these two plasmids carry the same origin of replication, they should be incompatible, and growth without selection for the antibiotic resistance markers would allow for loss of one plasmid if it were not essential for growth [162]. To determine if pRDP146 could be lost, two transformants were grown overnight in Luria broth with erythromycin, but without tetracycline. Dilutions of the culture were plated on LB agar containing erythromycin. 856  $\text{Erm}^{\text{R}}$  colonies were replica-plated to LB agar containing tetracycline. All  $\text{Erm}^{\text{R}}$  colonies maintained  $\text{Tet}^{\text{R}}$ , suggesting that pRDP146 was required for growth and that the GGI SSB could not substitute for *E. coli* SSB in the SSB mutant RDP268.

### 5.3.12 Transcriptional Mapping

*N. gonorrhoeae* strains were grown in GCBL liquid medium containing 0.042 %  $\text{NaHCO}_3$  and Kellogg's supplements until  $\text{OD}_{600} \sim 0,6$  was reached. Total RNA of 1 ml culture was isolated using the peqGOLD TriFast® reagent (peqLab). To remove contaminating DNA, total RNA was treated with 1 unit RNase-free DNaseI (Fermentas) for 30 min at 37 °C. RNA was quantified spectrophotometrically, and quality assessed by agarose gel electrophoresis. The MuLV transcriptase and the random hexamer primer of the first strand cDNA synthesis kit (Fermentas) were used to generate cDNA. A control of cDNA synthesis was performed without MuLV transcriptase. Transcripts were mapped using the following primers: for *yaf-ssbB*, 705R-GGI and 767F-GGI, for *ssb-topB*, 703R-GGI and 702F-GGI, for *topB-yeh*, 708R-GGI and 709F-GGI, for *yeh-yegB*, 701R-GGI and 499F-GGI and for *yegA-yef*, 498R-GGI and 726F-GGI.



### 5.3.13 Quantitative PCR

Transcript levels of *ssbB*, *topB*, *tral* and *traD* and the reference gene *secY* were determined for RNA isolated from piliated (EP006) and non piliated (SJ001) *N. gonorrhoeae* strains by quantitative Real-Time PCR (qRT-PCR). Oligonucleotide primers were designed using clone manager 9 professional edition (Sci-Ed Software). The primers used were as follows: for *ssbB*, 766R-GGI and 767F-GGI, for *topB*, 769F-GGI and 770R-GGI, for *tral*, 474R-GGI and 475F-GGI, for *traD*, 472R-GGI and 473F-GGI and for *secY*, 697 and 698. cDNA was isolated as described above. qRT-PCRs were performed using the SYBR Green/ ROX qPCR Master Mix (Fermentas) in a 7300 Real Time PCR System of Applied Biosystems. Reaction mixtures were prepared in a 25  $\mu$ l volume and run in triplicate for each gene. *N. gonorrhoeae* strain MS11 chromosomal DNA was used to establish the primer efficiency. Six biological replicates were performed. Results were depicted as the level of transcript compared with the *secY* gene ( $2^{-\Delta\text{Ct}}$ ).

### 5.3.14 DNA secretion assays

*N. gonorrhoeae* strains MS11, ND500 and SJ038 were grown overnight on GCB agar plates at 37 °C under 5 % CO<sub>2</sub> and inoculated in 3 ml of defined medium (Graver-Wade medium) [26] supplemented with Kellogg's supplements and 0.042 % NaHCO<sub>3</sub> [201]. These cultures were grown while shaking for 1.5 hrs at 37 °C under 5 % CO<sub>2</sub> and then diluted to an OD<sub>600</sub> ~ 0.2. To remove DNA derived from the initial starting culture, the cultures were diluted to OD<sub>600</sub> ~ 0.1 and growth was continued for 2 hrs. After three dilutions, samples were collected directly after the dilution and after 2 hrs. At these times also the OD<sub>600</sub> was determined. Cells were directly removed by centrifugation for 5 mins in a table top centrifuge at 14.000 rpm. Supernatants were assayed for the amount of DNA using PicoGreen (Invitrogen). The amount of secreted DNA was calculated by comparison to a DNA standard curve. The amount of secreted DNA was expressed as amount of  $\mu$ gr secreted DNA/ $\Delta$ OD<sub>600</sub>. In all assays *N. gonorrhoeae* ND500 (MS11: $\Delta$ GGI) was included as a background.

### 5.3.15 Isolation of secreted fraction

To analyze the secreted fraction of *N. gonorrhoeae*, a 250 ml culture of SJ023 was grown to OD<sub>600</sub> of 0.5 in GCBL medium. Cells were then harvested by centrifugation at 8000 rpm for 10 mins. The medium supernatant was filtered through a 0.2  $\mu$ m filter to remove the cell debris. The supernatant was centrifuged at 40.000 rpm in a Ti45 rotor for 1 hour at 4 °C to obtain the pellet containing the blebs. The pellet was resuspended in 250  $\mu$ l 2X sample buffer (SB) with 0.5 M Tris-HCl pH 6.8, 10 % (w/v) SDS, 0.1 % (w/v) bromophenol blue, 20 % glycerol and 10 mM DTT. After removal of the pellet, the supernatant fraction was concentrated 100 fold by trichloroacetic acid precipitation. At higher concentrations the

pellets could not be fully resuspended anymore. The harvested cell pellet was resuspended into 20 ml of buffer A (50 mM Tris-HCl pH 7.5) and disrupted using a French press at 15 psi. Cell debris was removed by centrifugation at 6000 rpm for 10 mins and 40  $\mu$ l supernatant was dissolved with 40  $\mu$ l of 2X SB and 20  $\mu$ l was loaded ( ) on the gel. Alternatively, either the cytoplasmic supernatant or the medium supernatant obtained from 120 ml culture of SJ023 were applied to a Strep-tactin Sepharose column (IBA) equilibrated with buffer D. Bound proteins were eluted with buffer D containing 2.5 mM desthiobiotin, separated on a 15 % SDS-PAGE gel and analyzed by Coomassie staining and Western blotting using an Strep-Tactin AP conjugate antibody (IBA).

## **5.4 Biochemical methods**

### **5.4.1 Induction and overexpression of recombinant proteins in *E.coli***

In order to overexpress and isolate proteins in *E.coli* BL21 pLysS cells were transformed with the overexpression vector, containing the desired gene. Then 30 ml of LB medium containing the appropriate antibiotic was inoculated with transformed cells and incubated over night at 37°C in the shaking incubator. From the overnight culture 10 ml was used to inoculate 1 l LB-medium with the appropriate antibiotic. The culture was incubated at 37°C while shaking until an OD<sub>600</sub> of 0,5-0,6 was reached. Then the cells were induced by the addition of 0,5 M IPTG to a final concentration of 5 mM and were grown again for 2-3 h under the conditions mentioned before. After that the cells were collected by centrifugation at 6000 rpm at 4°C for 20 min. Finally the pellet was washed with cold LEW buffer (50 mM NaH<sub>2</sub>PO<sub>4</sub>, 300 mM NaCl, pH 8.0) and was collected again by centrifugation under the same conditions as done before. In the end the pellet was shock frozen with liquid nitrogen and kept at -20°C until further use.

### **5.4 2 Cell disruption and purification of recombinant proteins**

In order to isolate recombinant cytoplasmic proteins, transformed and induced cells were thawed on ice and resuspended on 30 ml cold LEW buffer containing a pinch DNaseI (Roche, Mannheim) and a tablet of Protease Inhibitor Cocktail (Complete-Mini; Roche, Mannheim). Cell disruption was performed using French Pressure Cell Press, SLM Aminco (SLM Instruments Inc., Rochester, NY, USA) at a pressure of 1100 pounds per square inch ( $\approx$  75bar). This procedure was repeated three times. Then the disrupted cells were centrifuged at 4°C at 8000 rpm for 20 min in a Fiberlite F10-6x500y rotor (Thermo Scientific) and the supernatant, containing the cytoplasmic proteins, was harvested. For purification of the isolated proteins, an ÄKTA purifier (GE Healthcare, USA) was used. His tagged proteins were purified by loading the supernatant on a HiTrap Chelating 1 ml column (GE Healthcare, USA), which was preloaded with 0,1

M NiSO<sub>4</sub> and equilibrated in LEW buffer. The column was washed with 10 volumes of LEW buffer and eluted with a linear gradient of LEW buffer supplemented with 400 mM imidazole. Peak fractions were collected and used for further analysis.

### 5.4.3 TCA precipitation

To concentrate proteins in a solution a TCA precipitation was performed. Therefore an equal volume of 25 % TCA was added to the sample and left on ice for at least 30 min. After that the sample was centrifuged for 5 min at 13000 rpm at 4°C. Subsequently the pellet was washed with 1 ml of acetone and was centrifuged again under the same conditions as before. The acetone wash step was repeated once more and the pellet was resuspended in a small volume of TE-buffer.

### 5.4.4 SDS-PAGE

A polyacrylamide matrix, consisting of a 4% stacking gel (Table 16) and a 15% separating gel (Table 17) was used to separate the samples. Before loading on the gel the proteins in the samples had to be denatured by the addition of 5x SDS loading buffer (Table 14) and adjacent exposure to heat at 95°C for 10 min. SDS-PAGE was performed in 1x TBE buffer (Table 15) using the Bio-Rad Mini-PROTEAN Electrophoresis System at a voltage of 150 mV for 80 min (Electrophoresis Power Supply, Consort EV265). The gels were either stained with Coomassie Brilliant Blue R-250 (10% acetic acid, 45% methanol, 1 g Coomassie R250, 45% H<sub>2</sub>O<sub>add</sub>) or with Silver Solution, comprised in the FireSilver Staining Kit (Proteome Factory, Berlin). For destaining of the gel, destaining solution (5% CuSO<sub>4</sub>, 7% acetic acid, 10 % 2-propanol) was used.

**Table 14: Composition of 5x SDS loading buffer**

5x SDS loading buffer	10 % (w/v) SDS
	50 % glycerol
	0,04 % bromphenol blue
	500 mM DTT
	300 mM Tris/HCl

**Table 15: Composition of 10x TBE buffer**

10x TBE buffer	440 M Tris base  440 M Boric acid  2% EDTA (0,5 M; pH8,0)
----------------	---

**Table 16: Composition of 4% polyacrylamide stacking gel**

4 % polyacrylamide stacking gel	3 ml H <sub>2</sub> O <sub>dd</sub>  1,25 ml stacking gel buffer (0,5 M Tris; 0,4 % SDS; pH 6.8)  0,65 ml acrylamide 30%  60 µl APS 10%  6 µl TEMED
---------------------------------	---

**Table 17: Composition of 15% polyacrylamide separating gel**

15 % polyacrylamide separating gel	3,65 ml H <sub>2</sub> O <sub>dd</sub>  2,5 ml separating gel buffer (1,5 M Tris; 0,4 % SDS; pH 8.8)  3,75 ml acrylamide 40%  80 µl APS 10%  8 µl TEMED
------------------------------------	---

#### 5.4.5 Expression and purification of TteSSB2, Sac7d, ExoI and ExoIII

All proteins were overexpressed in *E. coli* strain BL21pLysS. Cells were grown in 1 L of LB medium supplemented with 1% glucose at 37 °C to an OD<sub>600</sub> of 0.5 and induced with 0.5 mM isopropyl β-D-1-thiogalactopyranoside (IPTG). After 3 hrs the cells were harvested by centrifugation, resuspended in 30

ml of buffer A (50 mM NaPO<sub>4</sub>, 300 mM NaCl, pH 8.0) and stored at -80 °C. Prior to purification, frozen cell pellets were thawed on ice. After thawing, the solution was supplemented with 1 Tablet of Protease Inhibitor Cocktail (Roche) and 1 mg of DNase I (Roche), and the cells were disrupted by passing them 3 times through a high-pressure Cell Disrupter (Constant Cell Disruption Systems) at 2,300 bar. Cell debris was removed by centrifugation at 10,000 rpm in an F10-6x500y rotor (FiberLite) and the supernatant was filtered through a 0.45 µm filter. Purifications were performed on an ÄKTA-Purifier system (GE Healthcare).

His-tagged ExoI, ExoIII and Sac7d were purified by loading the clarified supernatant on a 1 ml Hi-Trap Chelating column (GE Healthcare) preloaded with 0.1 M NiSO<sub>4</sub> and equilibrated in buffer A. The column was washed with 10 column volumes of buffer A and bound proteins were eluted with a linear gradient of buffer A supplemented with 400 mM imidazol. Peak fractions containing proteins were pooled and diluted with two volumes of buffer B (10 mM Tris-HCl pH 8.0, 10 mM NaCl). This sample was loaded on a Hi-Trap Q column (GE Healthcare) equilibrated with buffer B, and the protein was eluted with a linear gradient up to 1 M NaCl in buffer B. Fractions containing proteins were concentrated to 2 ml using Amicon Ultra – 10K Concentrators (Millipore). Finally, these fractions were loaded on a Superdex SD200 gelfiltration column (GE Healthcare), equilibrated with buffer C containing 150 mM NaCl and 20 mM Tris-HCl pH 8.0. Fractions containing proteins were pooled and frozen in liquid N<sub>2</sub> until further use.

To purify TteSSB2, the disrupted cell suspension was heated for 15 min at 75 °C, followed by centrifugation at 10,000 rpm in an F10-6x500y rotor (FiberLite). The supernatant was filtered through a 0.45 µm filter. The filtrate was loaded on Hi-Trap Q column (GE Healthcare) equilibrated with buffer B, and the protein was eluted with a linear gradient up to 1 M NaCl in buffer B. Fractions containing proteins were concentrated to 2 ml using Amicon Ultra – 10K Concentrators (Millipore). Finally, these fractions were loaded on a Superdex SD200 gelfiltration column (GE Healthcare), equilibrated with buffer C containing 150 mM NaCl and 20 mM Tris-HCl pH 8.0. Fractions containing proteins were pooled, and frozen in liquid N<sub>2</sub> until further usage.

#### **5.4.6 Expression and purification of SsbB**

SsbB proteins were overexpressed in *E. coli* strain C43 (DE3). Cells were grown in 1 L of Luria-Broth medium at 37 °C to an OD<sub>600</sub> of 0.5 and induced with 0.5 mM isopropyl β-D-1-thiogalactopyranoside (IPTG). After 3 hrs the cells were harvested by centrifugation, resuspended in 30 ml of buffer A (50 mM NaPO<sub>4</sub>, 300 mM NaCl, pH 8.0) and stored at -80 °C. Before purification, frozen cell pellets were thawed on ice. After thawing, the solution was supplemented with 1 tablet of Protease Inhibitor Cocktail (Roche)

and 1 mgr of DNase I (Roche), and the cells were disrupted 3 times in a high-pressure Cell Disrupter (Constant Cell Disruption Systems) at 2.300 bar. Cell debris was removed by centrifugation at 10.000 rpm in an F10-6x500y rotor (FiberLite) and the supernatant was filtered through a 0.45  $\mu\text{m}$  filter. Purifications were performed on an AKTA-Purifier system (GE Healthcare). His-tagged SsbB was purified by loading the clarified supernatant on a 1 ml Hi-Trap Chelating column (GE Healthcare) preloaded with 0.1 M  $\text{NiSO}_4$  and equilibrated in buffer A. The column was washed with 10 column volumes of buffer A and bound proteins were eluted with a linear gradient of buffer A supplemented with 400 mM imidazol. Peak fractions containing SsbB were pooled and diluted with two volumes of buffer B (10 mM Tris-HCl pH 8.0, 10 mM NaCl). This sample was loaded on a Hi-Trap Q column (GE Healthcare) equilibrated with buffer B, and the protein was eluted with a linear gradient up to 1 M NaCl in buffer B. Fractions containing SsbB were concentrated to 2 ml using Amicon Ultra – 10K Concentrators (Millipore). Finally these fractions were loaded on a Superdex SD200 gelfiltration column (GE Healthcare), equilibrated with buffer C containing 150 mM NaCl and 20 mM Tris-HCl pH 8.0. Fractions containing tetrameric SsbB were pooled, and frozen in liquid  $\text{N}_2$  until further use. OneSTrEP-tagged SsbB was purified by loading the clarified supernatant on a Strep-tactin Sepharose column (IBAGO) equilibrated with buffer D (150 mM NaCl, 1 mM EDTA, 100 mM Tris-HCl pH 8.0). SsbB was eluted with buffer D containing 2.5 mM desthiobiotin. Peak fractions containing SsbB were pooled and diluted with two volumes of buffer B and purified over Hi-Trap Q and Superdex SD200 columns as described above. Native SsbB was purified over a Hi-Trap Q column, as described above. Peak fractions were loaded on a 5 ml Hi-Trap Desalting column (GE Healthcare) equilibrated with buffer E (50 mM NaCl, 1 mM EDTA, 1 mM TCEP, 20 mM Tris-HCl, pH 8.0), fractions containing SsbB were collected. Desalted SsbB fractions were loaded on the DNA-cellulose column (Amersham Bioscience) equilibrated in buffer E and eluted over night at 4  $^\circ\text{C}$  with buffer E containing 1 M NaCl. Finally SsbB was further purified on a Superdex SD200.

#### **5.4.7 Polyacrylamide Gel Electrophoresis Mobility Shift Assays**

The ssDNA binding reactions were performed in SBA buffer (10 mM NaOH, 2 mM EDTA, titrated to pH 7.5 with Boric acid) which was when indicated supplemented with 10 mM  $\text{MgCl}_2$  and/or 200 or 500 mM NaCl. To determine the binding mode of SsbB, 5' Cy3 labeled labeled  $\text{dT}_n$  primers were used. 8 nM of  $\text{dT}_{35}$  or  $\text{dT}_{75}$  primers were mixed with increasing concentrations of  $(\text{SsbB})_4$  [ 0 – 64 nM]. The reaction solutions were incubated at 4  $^\circ\text{C}$  for 15 min after which the reaction was mixed with 5X gel loading solution (0.25 % bromphenol blue, 40 % sucrose). The aliquots were analyzed by electrophoresis on 7.5 % native polyacrylamide gels using a buffer system consisting of the SBA buffer supplemented with the same  $\text{MgCl}_2$  concentration as used in the binding reaction. The fluorescently labeled primers were

visualized on a LAS-4000 imager (Fujifilm). To determine the minimal binding frame of one SsbB tetramer, 1  $\mu\text{M}$  (SsbB)<sub>4</sub> was incubated with 5  $\mu\text{M}$  of unlabeled dT<sub>n</sub> oligonucleotide. To determine the minimal binding frame of two SsbB tetramers, 1  $\mu\text{M}$  (SsbB)<sub>4</sub> was incubated with 0.25  $\mu\text{M}$  of unlabeled dT<sub>n</sub> oligonucleotide. A similar incubation and separation protocol as described above was used, except that the bands corresponding to the SsbB protein were visualized by G-250 BioSafe Coomassie Brilliant Blue staining.

#### **5.4.8 Fluorescence titrations**

Titrations were performed on a temperature-controlled PC1 spectrofluorometer (ISS Inc) with a cooled photomultiplier. The excitation wavelength was set to 285 nm and the emission wavelength to 340 nm. The slit widths for the excitation and the emission beam were set to 1 and 2 nm respectively. Experiments were performed at 8°C in a buffer containing 20 mM Tris pH 7.5 and 1 mM dithiothreitol. When applicable, 20, 200 or 500 mM NaCl or 10 mM MgCl<sub>2</sub> was added. Samples were allowed to equilibrate for 90 s between measurements.

#### **5.4.8 Protein isolation from Neisseria cells for Western Blotting**

Neisseria cells were inoculated from the o.n plates in 3 ml prewarmed GCB medium and grown at 37 °C with continuous shaking for 2 hours. Those cultures were used to start fresh culture, the starting OD<sub>600</sub> was 0,2. The cultures were grown till OD<sub>600</sub>=0,7-0,8. Cells were collected by centrifugation. TriFast reagent (peqlab) was used for total protein isolation. Protein isolation was performed like described in the manual without any modifications. Isolated protein fractions were solubilized in 100  $\mu\text{l}$  protein-loading-buffer (SDS, bromphenol) at 75°C for 15 min and loaded on the SDS-Gel for further analysis.

#### **5.4.9 Western Blotting**

15% polyacrylamide SDS-PAGE gels were run for all the analysis with SsbB. Western blotting was performed by electroblotting the gels on PVDF membranes and incubating with 1:4000 dilution of Streptactin AP conjugate antibody (IBA). The chemiluminescence signal was obtained using the CDP-star substrate (Roche) on a LAS-4000 imager (Fujifilm).

#### **5.4.10 Site-specific labeling of proteins via cysteines**

Prior to labelling of the cysteines, purified proteins were reduced by incubation with 10 mM tris[2-carboxyethyl]phosphine (TCEP) for 10 min on ice. 2  $\mu\text{l}$  of 50 mM stock solution of the fluorescent probe was added to a total volume of 200  $\mu\text{l}$  containing the protein of interest at a concentration of 100  $\mu\text{M}/\text{ml}$  in buffer C. Labelling was performed in the dark for 2 hrs at room temperature. The reaction was

stopped by addition of 10 mM glutathion. Access of dye and glutathion was removed by separation of the reaction solution on a 2 ml PD-column (GE Healthcare) equilibrated with buffer C. Fractions containing the labelled protein were frozen in liquid N<sub>2</sub> until further use.

#### **5.4.11 Activity assays for specificity of ExoI and ExoIII**

The specificity of the enzymes for ssDNA and dsDNA was tested using a dT<sub>90</sub> oligonucleotide labelled with Cy3 at the 5' end, and a 468 bp PCR product obtained with an unlabelled primer 407R-GGI and a Cy3-labelled primer. The reactions were performed in the growth medium used in the continuous flow experiments (Graver-Wade medium diluted 1:5 with PBS). Shortly, 150 ng of the dT<sub>90</sub> oligonucleotide or the PCR product was mixed with increasing concentrations of ExoI or ExoIII [0 – 5,000 nM] in a total volume of 12 µl. The reaction was incubated at 37 °C for 1 hr after which the reaction was mixed with 3 µl 40 % sucrose. The aliquots were analyzed by electrophoresis on 7.5 % native polyacrylamide gels using a buffer system consisting of the SBA buffer. The fluorescently labelled DNA was visualized on a LAS-4000 imager (Fujifilm).

#### **5.4.12 Topoisomerase DNA relaxation assay**

For the DNA relaxation assay, supercoiled plasmid DNA was prepared using the Nucleobond kit (Bioké). 500 ng of supercoiled plasmid DNA was incubated with 0.12 units of Topoisomerase I (New England Biolabs) in the buffer supplied by the manufacturer with increasing amounts of SsbB. A total reaction volume of 25 µl was incubated at 37 °C for 30 mins and stopped by the addition of 10 mM EDTA and incubation at 65 °C for 20 mins. The samples were run on a 1 % agarose gel at 100 V for 1 hr and then stained in buffer containing ethidium bromide for 30 mins and visualized using an UV gel documentation system (Bio-Rad).

#### **5.4.13 Visualisation of ssDNA/dsDNA in the biofilms**

For visualization of DNA in the biofilms, either 500 nM labelled TteSSB2 or 500 nM labelled Sac7d was inoculated in to the channels. After 10 min the flow was resumed to wash away unbound protein.

### **5.5 Bioinformatics**

Sequence alignments of different SSBs were performed by Clustal X 2.0.

The synteny of SsbB homologs was determined using Absynte (<http://archaea.u-psud.fr/absynte>) [202].



## 5.6 Microscopy

### 5.6.1 Fluorescent light microscopy

To perform light microscopy, *N. gonorrhoeae* colonies were scraped from overnight grown plates and diluted in Graver-Wade medium [26] supplemented with Kellogg's supplements and 0.042 % NaHCO<sub>3</sub>. Cultures were grown at 37 °C constantly shaken at 140 rpm. Cells were grown to an OD<sub>600</sub> of 0.8, collected by centrifugation and diluted in fresh medium. This procedure was repeated at least three times, until most DNA derived from lysed cells was removed. Samples were collected directly after the last dilution. When the indicated enzymes (1 µM ExoI) or M13ssDNA (final concentration 0.0625 µgr/ml) were added, incubation was continued for 15 minutes. 2 µl of the cell suspension was loaded on the glass slide covered with 1 %-agarose. Microscopy and image acquisition was performed on a Zeiss Imager M1. Image data obtained were processed with MethaMorph software.

### 5.6.2 Confocal Laser Microscopy

For continuous-flow chamber experiments with *N. gonorrhoeae* a Graver-Wade medium supplemented with Kellogg's supplements and 0.042% NaHCO<sub>3</sub> diluted 1:5 with PBS was used. Colonies from 3 plates grown overnight were collected and inoculated in 3 ml prewarmed Graver-Wade medium. Cultures were grown to an OD<sub>600</sub> of 0.8, diluted 1:1,000 with fresh Graver-Medium and 200 µl of the diluted cell suspension was inoculated in the continuous-flow chamber. Flow chamber experiments were performed as described previously [203]. Strains were grown in three separate channels. From each channel at least six image stacks were acquired. When indicated 1 µM of ExoI was injected into the channels for 1 hour. The flow rate was stopped during the incubation time. To exclude the effect of stopped flow, one channel was inoculated with medium not containing enzymes and compared afterwards with the channels containing enzymes. Microscopy and image acquisition was performed on a Leica TCS SP5 (Leica Microsystems, Wetzlar). Images were processed and quantified using the IMARIS software package (Bitplane AG, Zürich, Switzerland). At least two fully independent experiments were performed. Biofilm experiments with different *Sulfolobus* spp. were performed as described previously [181].

## 6 Appendix

### Physiological characterization of SsbB

Physiological characterization of SsbB was performed by Katja Siewering and Samta Jain.

#### 6.1 SsbB is expressed in *N. gonorrhoeae*

The *ssbB* gene is located between several genes transcribed in the same direction (Figure 5-1 A).

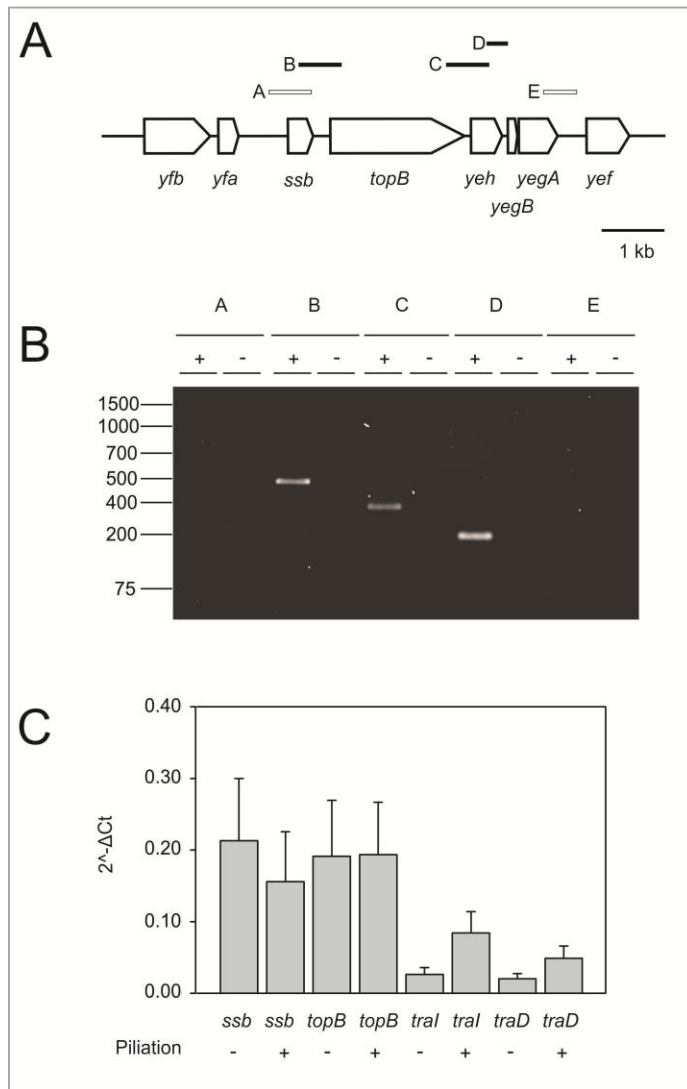


**Figure 5-1:** Analysis of the transcription of the *yfa-yef* region. Reverse transcriptase was used to map the operon structure of the *ssb-yegA* region within the GGI of *N. gonorrhoeae* strain MS11. A) Schematic representation of the *yfa-yef* region of the GGI. Genes are indicated by arrows and the expected PCR products by lines over the genes. Primer combinations for which a PCR product was obtained are indicated by black boxes and primer combinations for which no PCR product was obtained are indicated by white boxes. B) Operon mapping of the *ssb-yegA* operon. Transcripts were determined by PCR. (+) indicates reactions on cDNA created in the presence of reverse transcriptase and (-) indicates reactions on cDNA created in the absence of reverse transcriptase. C)

Quantitative gene expression levels of *ssbB*, *topB*, *tral* and *traD* of piliated and non-piliated *N. gonorrhoeae* strains were determined by qRT-PCR. The graph shows the mRNA levels as comparative gene expression after normalizing each gene to *secY*. Values depict means  $\pm$  standard deviation of six biological replicates.

Homologs of the ParA and ParB proteins, the topoisomerase, and the proteins with the DUF2857 (YfeB) and the DUF1845 (Yfb) domains are conserved within the SsbB homologs encoded within genetic islands. The *yegA* gene is followed by a previously unnamed gene (annotated as NgonM\_04872 in the MS11 whole genome shotgun sequence) which encodes a 149 amino acids long conserved hypothetical protein with a DUF3577 domain. This gene was named *yef*. In general, intergenic regions between the open reading frames (ORFs) of these genes are small, suggesting transcription in polycistronic messengers. To analyze the transcriptional linkage of these genes, reverse transcription PCR (RT-PCR) was performed with primer pairs spanning different intergenic regions (Figure 5-1 A,B). Successful amplification by these primer pairs was confirmed on chromosomal DNA (data not shown). No amplification products were detected in control reactions in the absence of reverse transcriptase (Figure 5-1 B). The RT-PCR analysis demonstrated that the *ssbB*, *topB*, *yeh*, *yegB* and *yegA* genes form an operon (Figure 5-1 B). It further showed that the *para*, *parB*, *yfeB* and *yfb* genes, although they are often found genetically linked to *ssb*, are not encoded in the same operon. In a next step we set-out to determine whether any possible regulation of the operon could be identified. The first operon of the GGI containing the *tral* and *traD* genes which encode proteins involved in targeting the secreted DNA to the secretion apparatus is upregulated in piliated cells compared to non-piliated cells [74]. To determine the expression levels of the *ssbB* gene and to test whether a similar difference could be observed in the expression of the *ssbB-yegA* operon, a qualitative real time PCR (qRT-PCR) using primers designed against the *ssbB*, *topB*, *tral* and *traD* genes and against the *secY* gene as a control was performed on mRNA isolated from piliated and non-piliated strains (Figure 5-1 C). The qRT-PCR revealed relatively low levels of transcription compared to the transcript containing the *secY* gene but higher levels of transcription than the *tral* and *traD* genes. However, no differences in the expression levels of the *ssbB* and *topB* genes were observed between piliated and non-piliated cells.

## 6.2 SsbB has no effect on DNA secretion or uptake

Since it was demonstrated that SsbB is expressed and forms an active ssDNA binding protein, we commenced to study possible functions of SsbB. SsbB is encoded within the GGI that encodes a T4SS involved in the secretion of ssDNA into the medium. The ssDNA binding protein VirE2 encoded by the *A. tumefaciens* T4SS is transported to the recipient cells [175] where it helps in importing the bound single stranded DNA [204]. It also has previously been proposed that the SSB encoded within *clc*-like elements

might be involved in DNA transport [170]. DNA secretion studies demonstrated that deletion of *ssbB* had no effect on the secretion of ssDNA (Pachulec, manuscript in preparation). To test whether overexpression of SsbB had any effect on ssDNA secretion, WT or OneSTrEP-tagged SsbB expressed from an inducible *lac* promoter was inserted into the chromosome of *N. gonorrhoeae* strain MS11. DNA secretion assays showed that there was no significant effect of SsbB overexpression on DNA release (Figure 5-2 A). To test whether SsbB might be secreted, different fractions were isolated, and compared to an isolated cytosolic fraction. The medium was concentrated by trichloroacetic acid (TCA) and the outer membrane derived vesicles, called blebs [205], were concentrated by ultracentrifugation respectively. OneSTrEP-tagged SsbB could only be detected in the cytoplasmic fraction (Figure 5-2 B). Western blotting with purified OneSTrEP-tagged SsbB showed that the detection limit is 50 fmol (corresponding to 1 ng or 10  $\mu$ l of 5 nM solution (Figure 5-2 B right panel). In a further attempt to detect SsbB, OneSTrEP-tagged SsbB was purified from cells and medium using a Strep-tactin Sepharose column, but again significant amounts of SsbB could be purified only from the cytosolic fraction, but not of the medium fraction (data not shown). It is concluded that One-Strep-tagged SsbB is not secreted via the T4SS at significant levels.

Several SSBs like YwpH of *Bacillus subtilis* [116] and SsbB of *Streptococcus pneumoniae* [119] play an important role in DNA uptake and competence. To test whether SsbB might play a similar role, the effect of SsbB on the efficiency of DNA uptake by *N. gonorrhoeae* was tested in co-culture experiments (Figure 5-2 C). In these experiments, strains in which the *recA* gene is disrupted by an erythromycin marker to ensure unidirectional transfer of DNA were used as donor strains, whereas strains with a chloramphenicol marker were used as acceptor strains. Similar to previous observations, transfer of chromosomal markers increased strongly in strains containing the GGI, whereas the transfer decreased in strains not containing the GGI [38]. Similar transfer rates were observed when the transfer frequencies of chromosomal markers to either acceptor strains with or without the GGI were determined. Transfer of the markers was abolished when DNase I was added to the medium, but the addition of high concentrations of SsbB (3.5  $\mu$ M) to the medium had no effect. When SsbB was overexpressed in the acceptor strain, a lower transformation rate was observed. Therefore overexpression of SsbB either affects DNA uptake, DNA stability in the acceptor strain, or the efficiency of recombination. It has previously been shown that SSB overexpression could have a negative effect on RecA recombinase activity [168]. Thus these data show that SsbB has no influence on ssDNA secretion and/or DNA uptake.

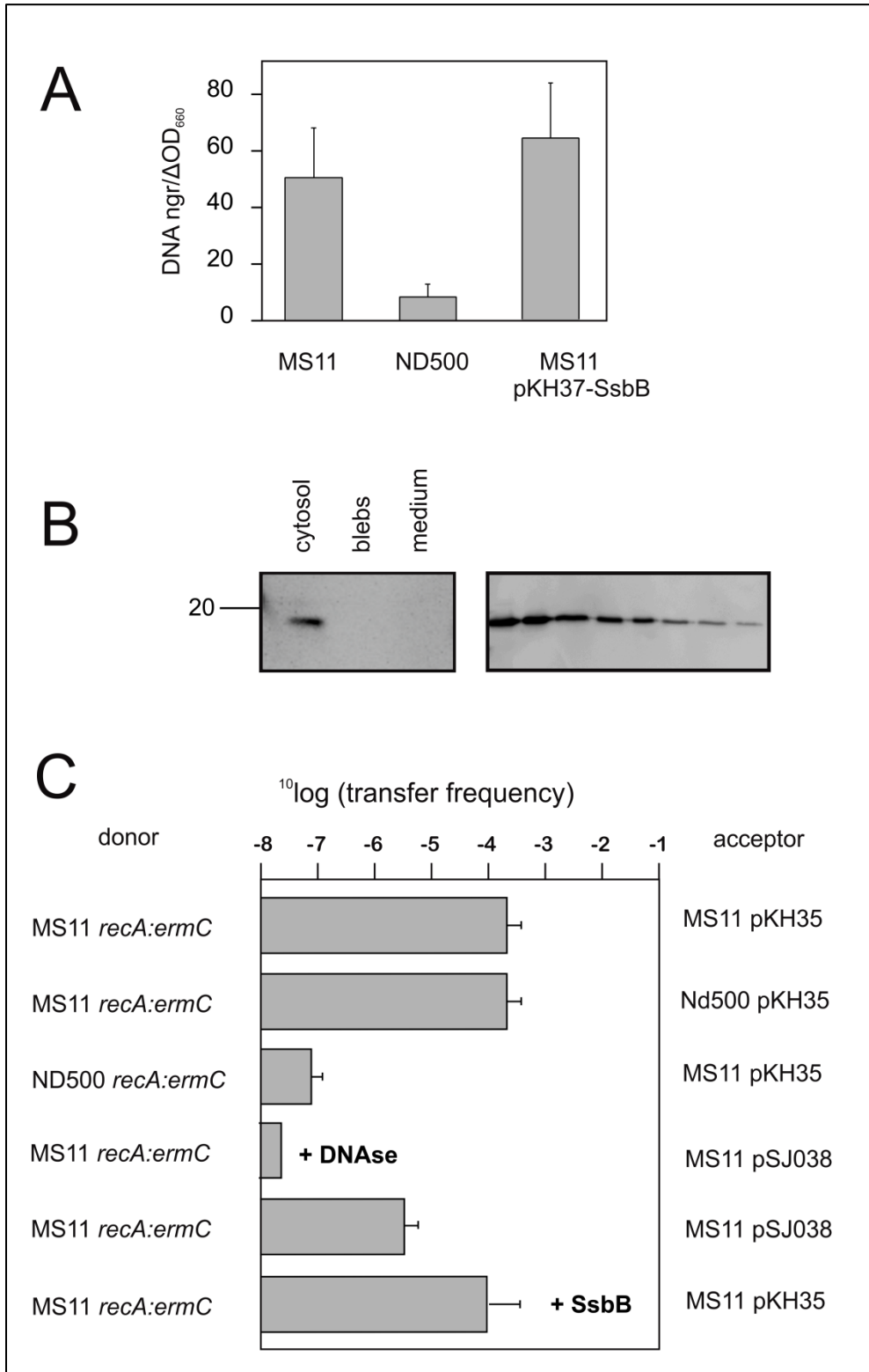


Figure 5-2: *In vivo* functional analysis of SsbB in *Neisseria gonorrhoeae*.

A) DNA secretion assay with fluorimetric detection of the secreted DNA in the culture supernatant. MS11 is the wild type strain which contains the GGI and ND500 is the MS11 strain in which the GGI was deleted. This strain does not secrete DNA into the medium. Strain MS11 transformed with plasmid pKH37-SsbB expresses SsbB from an inducible *lac* promoter. Results depicted are the average of at least 3 independent experiments. (B-left panel) Western blot using anti-Strep II antibody to detect the secretion of SsbB in the medium. Different fractions of the *Neisseria gonorrhoeae* strain SJ023-MS overexpressing N-terminal OneSTrEP-tagged SsbB from an inducible *lac* promoter were isolated and run on a 15% SDS-PAGE gel. The different lanes are representative of the cytosolic, blebs and the medium fractions, isolated from 240  $\mu$ l, 20 ml and 2 ml of a logarithmically growing culture of  $OD_{600} \sim 0.5$ . (B-right panel) Western blotting with purified OneSTrEP-tagged SsbB showed that the detection limit is 50 fmol (corresponding to 1 ng or 10  $\mu$ l of 5 nM solution) (C) Co-culture DNA transfer assay to determine the effect of SsbB on the DNA uptake efficiency. Donor and recipient strains were mixed and grown together at 37°C for 5 hrs and plated on selective media. The donor strains contain the erythromycin marker in the *recA* gene and the recipients contain the pKH37 or pSJ038 plasmids that contain the chloramphenicol marker and are integrated into the chromosome between the *aspC* and *lctP* genes. Vector pSJ038 is derived from pKH37 and expresses SsbB from an inducible *lac* promoter. The transfer of the erythromycin was measured as transfer frequency (CFU of transconjugants per CFU of donor). The values are the average from three independent experiments. It is indicated when purified SsbB (3.5  $\mu$ M) and DNase I were added to the medium.

## 7 References

1. Gerbase AC, Rowley JT, Mertens TE (1998) Global epidemiology of sexually transmitted diseases. *Lancet* 351 Suppl 3: 2-4.
2. Seifert HS (1992) Molecular mechanisms of antigenic variation in *Neisseria gonorrhoeae*. *Mol Cell Biol Hum Dis Ser* 1: 1-22.
3. Kerle KK, Mascola JR, Miller TA (1992) Disseminated gonococcal infection. *Am Fam Physician* 45: 209-214.
4. Carney FE, Jr., Taylor-Robinson D (1973) Growth and effect of *Neisseria gonorrhoeae* in organ cultures. *Br J Vener Dis* 49: 435-440.
5. Johnson AP, Clark JB, Osborn MF, Taylor-Robinson D (1980) A comparison of the association of *Neisseria gonorrhoeae* with human and guinea-pig genital mucosa maintained in organ culture. *Br J Exp Pathol* 61: 521-527.
6. McGee ZA, Johnson AP, Taylor-Robinson D (1976) Human fallopian tubes in organ culture: preparation, maintenance, and quantitation of damage by pathogenic microorganisms. *Infect Immun* 13: 608-618.
7. Stephens DS (1989) Gonococcal and meningococcal pathogenesis as defined by human cell, cell culture, and organ culture assays. *Clin Microbiol Rev* 2 Suppl: S104-111.
8. McGee ZA, Stephens DS, Hoffman LH, Schlech WF, 3rd, Horn RG (1983) Mechanisms of mucosal invasion by pathogenic *Neisseria*. *Rev Infect Dis* 5 Suppl 4: S708-714.
9. Virji M, Everson JS (1981) Comparative virulence of opacity variants of *Neisseria gonorrhoeae* strain P9. *Infect Immun* 31: 965-970.
10. Virji M, Everson JS, Lambden PR (1982) Effect of anti-pilus antisera on virulence of variants of *Neisseria gonorrhoeae* for cultured epithelial cells. *J Gen Microbiol* 128: 1095-1100.
11. Virji M, Heckels JE (1984) The role of common and type-specific pilus antigenic domains in adhesion and virulence of gonococci for human epithelial cells. *J Gen Microbiol* 130: 1089-1095.
12. Higashi DL, Zhang GH, Biais N, Myers LR, Weyand NJ, et al. (2009) Influence of type IV pilus retraction on the architecture of the *Neisseria gonorrhoeae*-infected cell cortex. *Microbiology* 155: 4084-4092.
13. Merz AJ, Enns CA, So M (1999) Type IV pili of pathogenic *Neisseriae* elicit cortical plaque formation in epithelial cells. *Mol Microbiol* 32: 1316-1332.
14. Bos MP, Grunert F, Belland RJ (1997) Differential recognition of members of the carcinoembryonic antigen family by Opa variants of *Neisseria gonorrhoeae*. *Infect Immun* 65: 2353-2361.
15. Edwards JL, Apicella MA (2004) The molecular mechanisms used by *Neisseria gonorrhoeae* to initiate infection differ between men and women. *Clin Microbiol Rev* 17: 965-981, table of contents.
16. McGee ZA, Gorby GL, Wyrick PB, Hodinka R, Hoffman LH (1988) Parasite-directed endocytosis. *Rev Infect Dis* 10 Suppl 2: S311-316.
17. Lynch EC, Blake MS, Gotschlich EC, Mauro A (1984) Studies of Porins: Spontaneously Transferred from Whole Cells and Reconstituted from Purified Proteins of *Neisseria gonorrhoeae* and *Neisseria meningitidis*. *Biophys J* 45: 104-107.
18. Smith H, Parsons NJ, Cole JA (1995) Sialylation of neisserial lipopolysaccharide: a major influence on pathogenicity. *Microb Pathog* 19: 365-377.
19. van Putten JP (1993) Phase variation of lipopolysaccharide directs interconversion of invasive and immuno-resistant phenotypes of *Neisseria gonorrhoeae*. *EMBO J* 12: 4043-4051.
20. Morse SA (1996) *Neisseria*, *Moraxella*, *Kingella* and *Eikenella*. In: Baron S, editor. *Medical Microbiology*. 4th ed. Galveston (TX).
21. Pohlner J, Halter R, Meyer TF (1987) *Neisseria gonorrhoeae* IgA protease. Secretion and implications for pathogenesis. *Antonie Van Leeuwenhoek* 53: 479-484.

## References

---

22. Swanson J, Kraus SJ, Gotschlich EC (1971) Studies on gonococcus infection. I. Pili and zones of adhesion: their relation to gonococcal growth patterns. *J Exp Med* 134: 886-906.
23. Spence JM, Wright L, Clark VL (2008) Laboratory maintenance of *Neisseria gonorrhoeae*. *Curr Protoc Microbiol* Chapter 4: Unit 4A 1.
24. Annear DI, Wild B (1982) Growth of *Neisseria gonorrhoeae* in brain heart infusion. *J Clin Pathol* 35: 119.
25. Elmros T, Burman LG, Bloom GD (1976) Autolysis of *Neisseria gonorrhoeae*. *J Bacteriol* 126: 969-976.
26. Wade JJ, Graver MA (2007) A fully defined, clear and protein-free liquid medium permitting dense growth of *Neisseria gonorrhoeae* from very low inocula. *FEMS Microbiol Lett* 273: 35-37.
27. Short HB, Clark VL, Kellogg DS, Jr., Young FE (1982) Anaerobic survival of clinical isolates and laboratory strains of *Neisseria gonorrhoea*: use in transfer and storage. *J Clin Microbiol* 15: 915-919.
28. Biswas GD, Sox T, Blackman E, Sparling PF (1977) Factors affecting genetic transformation of *Neisseria gonorrhoeae*. *J Bacteriol* 129: 983-992.
29. Goodman SD, Scoocca JJ (1988) Identification and arrangement of the DNA sequence recognized in specific transformation of *Neisseria gonorrhoeae*. *Proc Natl Acad Sci U S A* 85: 6982-6986.
30. Davidsen T, Rodland EA, Lagesen K, Seeberg E, Rognes T, et al. (2004) Biased distribution of DNA uptake sequences towards genome maintenance genes. *Nucleic Acids Res* 32: 1050-1058.
31. Cannon JG, Sparling PF (1984) The genetics of the gonococcus. *Annu Rev Microbiol* 38: 111-133.
32. Smith JM, Smith NH, O'Rourke M, Spratt BG (1993) How clonal are bacteria? *Proc Natl Acad Sci U S A* 90: 4384-4388.
33. Hamilton HL, Dominguez NM, Schwartz KJ, Hackett KT, Dillard JP (2005) *Neisseria gonorrhoeae* secretes chromosomal DNA via a novel type IV secretion system. *Mol Microbiol* 55: 1704-1721.
34. Hebelers BH, Young FE (1975) Autolysis of *Neisseria gonorrhoeae*. *J Bacteriol* 122: 385-392.
35. Chapman SJ, Perkins HR (1983) Peptidoglycan-degrading enzymes in ether-treated cells of *Neisseria gonorrhoeae*. *J Gen Microbiol* 129: 877-883.
36. Gubish ER, Jr., Chen KC, Buchanan TM (1982) Detection of a gonococcal endo-beta-N-acetyl-D-glucosaminidase and its peptidoglycan cleavage site. *J Bacteriol* 151: 172-176.
37. Dillard JP, Seifert HS (1997) A peptidoglycan hydrolase similar to bacteriophage endolysins acts as an autolysin in *Neisseria gonorrhoeae*. *Mol Microbiol* 25: 893-901.
38. Dillard JP, Seifert HS (2001) A variable genetic island specific for *Neisseria gonorrhoeae* is involved in providing DNA for natural transformation and is found more often in disseminated infection isolates. *Mol Microbiol* 41: 263-277.
39. Snyder LA, Jarvis SA, Saunders NJ (2005) Complete and variant forms of the 'gonococcal genetic island' in *Neisseria meningitidis*. *Microbiology* 151: 4005-4013.
40. Ramsey ME, Woodhams KL, Dillard JP (2011) The Gonococcal Genetic Island and Type IV Secretion in the Pathogenic *Neisseria*. *Front Microbiol* 2: 61.
41. Dominguez NM, Hackett KT, Dillard JP (2011) XerCD-mediated site-specific recombination leads to loss of the 57-kilobase gonococcal genetic island. *J Bacteriol* 193: 377-388.
42. Carnoy C, Roten CA (2009) The dif/Xer recombination systems in proteobacteria. *PLoS One* 4: e6531.
43. Fronzes R, Christie PJ, Waksman G (2009) The structural biology of type IV secretion systems. *Nat Rev Microbiol* 7: 703-714.
44. Christie PJ, Vogel JP (2000) Bacterial type IV secretion: conjugation systems adapted to deliver effector molecules to host cells. *Trends Microbiol* 8: 354-360.
45. Seubert A, Hiestand R, de la Cruz F, Dehio C (2003) A bacterial conjugation machinery recruited for pathogenesis. *Mol Microbiol* 49: 1253-1266.
46. Llosa M, Roy C, Dehio C (2009) Bacterial type IV secretion systems in human disease. *Mol Microbiol* 73: 141-151.



47. Juhas M, Crook DW, Hood DW (2008) Type IV secretion systems: tools of bacterial horizontal gene transfer and virulence. *Cell Microbiol* 10: 2377-2386.
48. Schroder G, Lanka E (2005) The mating pair formation system of conjugative plasmids-A versatile secretion machinery for transfer of proteins and DNA. *Plasmid* 54: 1-25.
49. Grohmann E, Muth G, Espinosa M (2003) Conjugative plasmid transfer in gram-positive bacteria. *Microbiol Mol Biol Rev* 67: 277-301, table of contents.
50. Lawley TD, Klimke WA, Gubbins MJ, Frost LS (2003) F factor conjugation is a true type IV secretion system. *FEMS Microbiol Lett* 224: 1-15.
51. Smeets LC, Kusters JG (2002) Natural transformation in *Helicobacter pylori*: DNA transport in an unexpected way. *Trends Microbiol* 10: 159-162; discussion 162.
52. Hamilton HL, Dillard JP (2006) Natural transformation of *Neisseria gonorrhoeae*: from DNA donation to homologous recombination. *Mol Microbiol* 59: 376-385.
53. Fronzes R, Schafer E, Wang L, Saibil HR, Orlova EV, et al. (2009) Structure of a type IV secretion system core complex. *Science* 323: 266-268.
54. Christie PJ, Atmakuri K, Krishnamoorthy V, Jakubowski S, Cascales E (2005) Biogenesis, architecture, and function of bacterial type IV secretion systems. *Annu Rev Microbiol* 59: 451-485.
55. Krause S, Barcena M, Pansegrau W, Lurz R, Carazo JM, et al. (2000) Sequence-related protein export NTPases encoded by the conjugative transfer region of RP4 and by the *cag* pathogenicity island of *Helicobacter pylori* share similar hexameric ring structures. *Proc Natl Acad Sci U S A* 97: 3067-3072.
56. Arechaga I, Pena A, Zunzunegui S, del Carmen Fernandez-Alonso M, Rivas G, et al. (2008) ATPase activity and oligomeric state of TrwK, the VirB4 homologue of the plasmid R388 type IV secretion system. *J Bacteriol* 190: 5472-5479.
57. Jain S, Zweig M, Peeters E, Siewering K, Hackett KT, et al. (2012) Characterization of the single stranded DNA binding protein SsbB encoded in the Gonococcal Genetic Island. *PLoS One* 7: e35285.
58. Francia MV, Varsaki A, Garcillan-Barcia MP, Latorre A, Drainas C, et al. (2004) A classification scheme for mobilization regions of bacterial plasmids. *FEMS Microbiol Rev* 28: 79-100.
59. Garcillan-Barcia MP, Francia MV, de la Cruz F (2009) The diversity of conjugative relaxases and its application in plasmid classification. *FEMS Microbiol Rev* 33: 657-687.
60. Guglielmini J, Quintais L, Garcillan-Barcia MP, de la Cruz F, Rocha EP (2011) The repertoire of ICE in prokaryotes underscores the unity, diversity, and ubiquity of conjugation. *PLoS Genet* 7: e1002222.
61. Guglielmini J, de la Cruz F, Rocha EP (2013) Evolution of Conjugation and Type IV Secretion Systems. *Mol Biol Evol* 30: 315-331.
62. Grandoso G, Avila P, Cayon A, Hernando MA, Llosa M, et al. (2000) Two active-site tyrosyl residues of protein TrwC act sequentially at the origin of transfer during plasmid R388 conjugation. *J Mol Biol* 295: 1163-1172.
63. Smillie C, Garcillan-Barcia MP, Francia MV, Rocha EP, de la Cruz F (2010) Mobility of plasmids. *Microbiol Mol Biol Rev* 74: 434-452.
64. Alvarez-Martinez CE, Christie PJ (2009) Biological diversity of prokaryotic type IV secretion systems. *Microbiol Mol Biol Rev* 73: 775-808.
65. Ragonese H, Haisch D, Villareal E, Choi JH, Matson SW (2007) The F plasmid-encoded TraM protein stimulates relaxosome-mediated cleavage at oriT through an interaction with TraI. *Mol Microbiol* 63: 1173-1184.
66. Bowie JU, Sauer RT (1990) TraY proteins of F and related episomes are members of the Arc and Mnt repressor family. *J Mol Biol* 211: 5-6.

## References

---

67. Moncalian G, de la Cruz F (2004) DNA binding properties of protein TrwA, a possible structural variant of the Arc repressor superfamily. *Biochim Biophys Acta* 1701: 15-23.
68. Varsaki A, Moncalian G, Garcillan-Barcia Mdel P, Drainas C, de la Cruz F (2009) Analysis of ColE1 MbeC unveils an extended ribbon-helix-helix family of nicking accessory proteins. *J Bacteriol* 191: 1446-1455.
69. Pansegrau W, Schroder W, Lanka E (1993) Relaxase (Tral) of IncP alpha plasmid RP4 catalyzes a site-specific cleaving-joining reaction of single-stranded DNA. *Proc Natl Acad Sci U S A* 90: 2925-2929.
70. Pansegrau W, Ziegelin G, Lanka E (1990) Covalent association of the tral gene product of plasmid RP4 with the 5'-terminal nucleotide at the relaxation nick site. *J Biol Chem* 265: 10637-10644.
71. Atmakuri K, Cascales E, Christie PJ (2004) Energetic components VirD4, VirB11 and VirB4 mediate early DNA transfer reactions required for bacterial type IV secretion. *Mol Microbiol* 54: 1199-1211.
72. Llosa M, Gomis-Ruth FX, Coll M, de la Cruz Fd F (2002) Bacterial conjugation: a two-step mechanism for DNA transport. *Mol Microbiol* 45: 1-8.
73. Jain S, Kahnt J, van der Does C (2011) Processing and maturation of the pilin of the type IV secretion system encoded within the gonococcal genetic island. *J Biol Chem* 286: 43601-43610.
74. Salgado-Pabon W, Jain S, Turner N, van der Does C, Dillard JP (2007) A novel relaxase homologue is involved in chromosomal DNA processing for type IV secretion in *Neisseria gonorrhoeae*. *Mol Microbiol* 66: 930-947.
75. Hacker J, Kaper JB (2000) Pathogenicity islands and the evolution of microbes. *Annu Rev Microbiol* 54: 641-679.
76. Fischer W (2011) Assembly and molecular mode of action of the *Helicobacter pylori* Cag type IV secretion apparatus. *FEBS J* 278: 1203-1212.
77. Wu Z, Xu L, Tu Y, Chen R, Yu Y, et al. (2011) The relationship between the symptoms of female gonococcal infections and serum progesterone level and the genotypes of *Neisseria gonorrhoeae* multi-antigen sequence type (NG-MAST) in Wuhan, China. *Eur J Clin Microbiol Infect Dis* 30: 113-116.
78. Zola TA, Strange HR, Dominguez NM, Dillard JP, Cornelissen CN (2010) Type IV secretion machinery promotes ton-independent intracellular survival of *Neisseria gonorrhoeae* within cervical epithelial cells. *Infect Immun* 78: 2429-2437.
79. Hagen TA, Cornelissen CN (2006) *Neisseria gonorrhoeae* requires expression of TonB and the putative transporter TdfF to replicate within cervical epithelial cells. *Mol Microbiol* 62: 1144-1157.
80. Woodhams KL, Benet ZL, Blonsky SE, Hackett KT, Dillard JP (2012) Prevalence and detailed mapping of the gonococcal genetic island in *Neisseria meningitidis*. *J Bacteriol* 194: 2275-2285.
81. Yakovchuk P, Protozanova E, Frank-Kamenetskii MD (2006) Base-stacking and base-pairing contributions into thermal stability of the DNA double helix. *Nucleic Acids Res* 34: 564-574.
82. Frederico LA, Kunkel TA, Shaw BR (1993) Cytosine deamination in mismatched base pairs. *Biochemistry* 32: 6523-6530.
83. Grange W, Duckely M, Husale S, Jacob S, Engel A, et al. (2008) VirE2: a unique ssDNA-compacting molecular machine. *PLoS Biol* 6: e44.
84. Wold MS (1997) Replication protein A: a heterotrimeric, single-stranded DNA-binding protein required for eukaryotic DNA metabolism. *Annu Rev Biochem* 66: 61-92.
85. Lohman TM, Ferrari ME (1994) *Escherichia coli* single-stranded DNA-binding protein: multiple DNA-binding modes and cooperativities. *Annu Rev Biochem* 63: 527-570.

86. Cha TA, Alberts BM (1989) The bacteriophage T4 DNA replication fork. Only DNA helicase is required for leading strand DNA synthesis by the DNA polymerase holoenzyme. *J Biol Chem* 264: 12220-12225.
87. Kim YT, Richardson CC (1993) Bacteriophage T7 gene 2.5 protein: an essential protein for DNA replication. *Proc Natl Acad Sci U S A* 90: 10173-10177.
88. Pestryakov PE, Lavrik OI (2008) Mechanisms of single-stranded DNA-binding protein functioning in cellular DNA metabolism. *Biochemistry (Mosc)* 73: 1388-1404.
89. Murzin AG (1993) OB(oligonucleotide/oligosaccharide binding)-fold: common structural and functional solution for non-homologous sequences. *EMBO J* 12: 861-867.
90. Theobald DL, Mitton-Fry RM, Wuttke DS (2003) Nucleic acid recognition by OB-fold proteins. *Annu Rev Biophys Biomol Struct* 32: 115-133.
91. Philipova D, Mullen JR, Maniar HS, Lu J, Gu C, et al. (1996) A hierarchy of SSB protomers in replication protein A. *Genes Dev* 10: 2222-2233.
92. Suck D (1997) Common fold, common function, common origin? *Nat Struct Biol* 4: 161-165.
93. Bycroft M, Hubbard TJ, Proctor M, Freund SM, Murzin AG (1997) The solution structure of the S1 RNA binding domain: a member of an ancient nucleic acid-binding fold. *Cell* 88: 235-242.
94. Bochkarev A, Bochkareva E (2004) From RPA to BRCA2: lessons from single-stranded DNA binding by the OB-fold. *Curr Opin Struct Biol* 14: 36-42.
95. Raghunathan S, Kozlov AG, Lohman TM, Waksman G (2000) Structure of the DNA binding domain of *E. coli* SSB bound to ssDNA. *Nat Struct Biol* 7: 648-652.
96. Merrill BM, Williams KR, Chase JW, Konigsberg WH (1984) Photochemical cross-linking of the *Escherichia coli* single-stranded DNA-binding protein to oligodeoxynucleotides. Identification of phenylalanine 60 as the site of cross-linking. *J Biol Chem* 259: 10850-10856.
97. Savvides SN, Raghunathan S, Futterer K, Kozlov AG, Lohman TM, et al. (2004) The C-terminal domain of full-length *E. coli* SSB is disordered even when bound to DNA. *Protein Sci* 13: 1942-1947.
98. Robbins JB, Murphy MC, White BA, Mackie RI, Ha T, et al. (2004) Functional analysis of multiple single-stranded DNA-binding proteins from *Methanosarcina acetivorans* and their effects on DNA synthesis by DNA polymerase B1. *J Biol Chem* 279: 6315-6326.
99. Dabrowski S, Olszewski M, Piatek R, Brillowska-Dabrowska A, Konopa G, et al. (2002) Identification and characterization of single-stranded-DNA-binding proteins from *Thermus thermophilus* and *Thermus aquaticus* - new arrangement of binding domains. *Microbiology* 148: 3307-3315.
100. Shokri L, Rouzina I, Williams MC (2009) Interaction of bacteriophage T4 and T7 single-stranded DNA-binding proteins with DNA. *Phys Biol* 6: 025002.
101. Fairman MP, Stillman B (1988) Cellular factors required for multiple stages of SV40 DNA replication in vitro. *EMBO J* 7: 1211-1218.
102. Wold MS, Kelly T (1988) Purification and characterization of replication protein A, a cellular protein required for in vitro replication of simian virus 40 DNA. *Proc Natl Acad Sci U S A* 85: 2523-2527.
103. Brill SJ, Bastin-Shanower S (1998) Identification and characterization of the fourth single-stranded-DNA binding domain of replication protein A. *Mol Cell Biol* 18: 7225-7234.
104. Chedin F, Seitz EM, Kowalczykowski SC (1998) Novel homologs of replication protein A in archaea: implications for the evolution of ssDNA-binding proteins. *Trends Biochem Sci* 23: 273-277.
105. Kerr ID, Wadsworth RI, Blankenfeldt W, Staines AG, White MF, et al. (2001) Overexpression, purification, crystallization and data collection of a single-stranded DNA-binding protein from *Sulfolobus solfataricus*. *Acta Crystallogr D Biol Crystallogr* 57: 1290-1292.
106. Kelly TJ, Simancek P, Brush GS (1998) Identification and characterization of a single-stranded DNA-binding protein from the archaeon *Methanococcus jannaschii*. *Proc Natl Acad Sci U S A* 95: 14634-14639.

## References

---

107. Kerr ID, Wadsworth RI, Cubeddu L, Blankenfeldt W, Naismith JH, et al. (2003) Insights into ssDNA recognition by the OB fold from a structural and thermodynamic study of *Sulfolobus* SSB protein. *EMBO J* 22: 2561-2570.
108. Wadsworth RI, White MF (2001) Identification and properties of the crenarchaeal single-stranded DNA binding protein from *Sulfolobus solfataricus*. *Nucleic Acids Res* 29: 914-920.
109. Chrysogelos S, Griffith J (1982) *Escherichia coli* single-strand binding protein organizes single-stranded DNA in nucleosome-like units. *Proc Natl Acad Sci U S A* 79: 5803-5807.
110. Lohman TM, Overman LB, Datta S (1986) Salt-dependent changes in the DNA binding co-operativity of *Escherichia coli* single strand binding protein. *J Mol Biol* 187: 603-615.
111. Griffith JD, Harris LD, Register J, 3rd (1984) Visualization of SSB-ssDNA complexes active in the assembly of stable RecA-DNA filaments. *Cold Spring Harb Symp Quant Biol* 49: 553-559.
112. Ferretti JJ, Dyer DW, Roe BA (1997) Data available. *Nature* 386: 320.
113. Bujalowski W, Lohman TM (1986) *Escherichia coli* single-strand binding protein forms multiple, distinct complexes with single-stranded DNA. *Biochemistry* 25: 7799-7802.
114. Lohman TM, Overman LB (1985) Two binding modes in *Escherichia coli* single strand binding protein-single stranded DNA complexes. Modulation by NaCl concentration. *J Biol Chem* 260: 3594-3603.
115. Wei TF, Bujalowski W, Lohman TM (1992) Cooperative binding of polyamines induces the *Escherichia coli* single-strand binding protein-DNA binding mode transitions. *Biochemistry* 31: 6166-6174.
116. Lindner C, Nijland R, van Hartskamp M, Bron S, Hamoen LW, et al. (2004) Differential expression of two paralogous genes of *Bacillus subtilis* encoding single-stranded DNA binding protein. *J Bacteriol* 186: 1097-1105.
117. Redfield RJ, Cameron AD, Qian Q, Hinds J, Ali TR, et al. (2005) A novel CRP-dependent regulon controls expression of competence genes in *Haemophilus influenzae*. *J Mol Biol* 347: 735-747.
118. Grove DE, Bryant FR (2006) Effect of Mg<sup>2+</sup> on the DNA binding modes of the *Streptococcus pneumoniae* SsbA and SsbB proteins. *J Biol Chem* 281: 2087-2094.
119. Grove DE, Willcox S, Griffith JD, Bryant FR (2005) Differential single-stranded DNA binding properties of the paralogous SsbA and SsbB proteins from *Streptococcus pneumoniae*. *J Biol Chem* 280: 11067-11073.
120. Benam AV, Lang E, Alfsnes K, Fleckenstein B, Rowe AD, et al. (2011) Structure-function relationships of the competence lipoprotein ComL and SSB in meningococcal transformation. *Microbiology* 157: 1329-1342.
121. Golub EI, Low KB (1985) Conjugative plasmids of enteric bacteria from many different incompatibility groups have similar genes for single-stranded DNA-binding proteins. *J Bacteriol* 162: 235-241.
122. Howland CJ, Rees CE, Barth PT, Wilkins BM (1989) The *ssb* gene of plasmid Collb-P9. *J Bacteriol* 171: 2466-2473.
123. Golub EI, Low KB (1986) Derepression of single-stranded DNA-binding protein genes on plasmids derepressed for conjugation, and complementation of an *E. coli* *ssb*- mutation by these genes. *Mol Gen Genet* 204: 410-416.
124. Fernandez-Lopez R, Garcillan-Barcia MP, Revilla C, Lazaro M, Vielva L, et al. (2006) Dynamics of the IncW genetic backbone imply general trends in conjugative plasmid evolution. *FEMS Microbiol Rev* 30: 942-966.
125. Costerton JW, Stewart PS, Greenberg EP (1999) Bacterial biofilms: a common cause of persistent infections. *Science* 284: 1318-1322.
126. Davies D (2003) Understanding biofilm resistance to antibacterial agents. *Nat Rev Drug Discov* 2: 114-122.

## References

---

127. Donlan RM (2000) Role of biofilms in antimicrobial resistance. *ASAIO J* 46: S47-52.
128. Richards JJ, Melander C (2009) Controlling bacterial biofilms. *Chembiochem* 10: 2287-2294.
129. Flemming HC, Wingender J (2010) The biofilm matrix. *Nat Rev Microbiol* 8: 623-633.
130. Whitchurch CB, Tolker-Nielsen T, Ragas PC, Mattick JS (2002) Extracellular DNA required for bacterial biofilm formation. *Science* 295: 1487.
131. Moscoso M, Garcia E, Lopez R (2006) Biofilm formation by *Streptococcus pneumoniae*: role of choline, extracellular DNA, and capsular polysaccharide in microbial accretion. *J Bacteriol* 188: 7785-7795.
132. Thomas VC, Thurlow LR, Boyle D, Hancock LE (2008) Regulation of autolysis-dependent extracellular DNA release by *Enterococcus faecalis* extracellular proteases influences biofilm development. *J Bacteriol* 190: 5690-5698.
133. Rice KC, Mann EE, Endres JL, Weiss EC, Cassat JE, et al. (2007) The *cidA* murein hydrolase regulator contributes to DNA release and biofilm development in *Staphylococcus aureus*. *Proc Natl Acad Sci U S A* 104: 8113-8118.
134. Qin Z, Ou Y, Yang L, Zhu Y, Tolker-Nielsen T, et al. (2007) Role of autolysin-mediated DNA release in biofilm formation of *Staphylococcus epidermidis*. *Microbiology* 153: 2083-2092.
135. Izano EA, Shah SM, Kaplan JB (2009) Intercellular adhesion and biocide resistance in nontypeable *Haemophilus influenzae* biofilms. *Microb Pathog* 46: 207-213.
136. Lappann M, Claus H, van Alen T, Harmsen M, Elias J, et al. (2010) A dual role of extracellular DNA during biofilm formation of *Neisseria meningitidis*. *Mol Microbiol* 75: 1355-1371.
137. Steichen CT, Cho C, Shao JQ, Apicella MA (2011) The *Neisseria gonorrhoeae* biofilm matrix contains DNA, and an endogenous nuclease controls its incorporation. *Infect Immun* 79: 1504-1511.
138. Allesen-Holm M, Barken KB, Yang L, Klausen M, Webb JS, et al. (2006) A characterization of DNA release in *Pseudomonas aeruginosa* cultures and biofilms. *Mol Microbiol* 59: 1114-1128.
139. Hall-Stoodley L, Nistico L, Sambanthamoorthy K, Dice B, Nguyen D, et al. (2008) Characterization of biofilm matrix, degradation by DNase treatment and evidence of capsule downregulation in *Streptococcus pneumoniae* clinical isolates. *BMC Microbiol* 8: 173.
140. Izano EA, Amarante MA, Kher WB, Kaplan JB (2008) Differential roles of poly-N-acetylglucosamine surface polysaccharide and extracellular DNA in *Staphylococcus aureus* and *Staphylococcus epidermidis* biofilms. *Appl Environ Microbiol* 74: 470-476.
141. Vilain S, Pretorius JM, Theron J, Brozel VS (2009) DNA as an adhesin: *Bacillus cereus* requires extracellular DNA to form biofilms. *Appl Environ Microbiol* 75: 2861-2868.
142. Conover MS, Mishra M, Deora R (2011) Extracellular DNA is essential for maintaining *Bordetella* biofilm integrity on abiotic surfaces and in the upper respiratory tract of mice. *PLoS One* 6: e16861.
143. Finkel SE, Kolter R (2001) DNA as a nutrient: novel role for bacterial competence gene homologs. *J Bacteriol* 183: 6288-6293.
144. Mulcahy H, Charron-Mazenod L, Lewenza S (2010) *Pseudomonas aeruginosa* produces an extracellular deoxyribonuclease that is required for utilization of DNA as a nutrient source. *Environ Microbiol* 12: 1621-1629.
145. Li YH, Lau PC, Lee JH, Ellen RP, Cvitkovitch DG (2001) Natural genetic transformation of *Streptococcus mutans* growing in biofilms. *J Bacteriol* 183: 897-908.
146. Wang BY, Chi B, Kuramitsu HK (2002) Genetic exchange between *Treponema denticola* and *Streptococcus gordonii* in biofilms. *Oral Microbiol Immunol* 17: 108-112.
147. Hendrickx L, Hausner M, Wuertz S (2003) Natural genetic transformation in monoculture *Acinetobacter* sp. strain BD413 biofilms. *Appl Environ Microbiol* 69: 1721-1727.

## References

---

148. Heilmann C, Hussain M, Peters G, Gotz F (1997) Evidence for autolysin-mediated primary attachment of *Staphylococcus epidermidis* to a polystyrene surface. *Mol Microbiol* 24: 1013-1024.
149. Steichen CT, Shao JQ, Ketterer MR, Apicella MA (2008) Gonococcal cervicitis: a role for biofilm in pathogenesis. *J Infect Dis* 198: 1856-1861.
150. Greiner LL, Edwards JL, Shao J, Rabinak C, Entz D, et al. (2005) Biofilm Formation by *Neisseria gonorrhoeae*. *Infect Immun* 73: 1964-1970.
151. Falsetta ML, Bair TB, Ku SC, Vanden Hoven RN, Steichen CT, et al. (2009) Transcriptional profiling identifies the metabolic phenotype of gonococcal biofilms. *Infect Immun* 77: 3522-3532.
152. Falsetta ML, McEwan AG, Jennings MP, Apicella MA (2010) Anaerobic metabolism occurs in the substratum of gonococcal biofilms and may be sustained in part by nitric oxide. *Infect Immun* 78: 2320-2328.
153. Lim KH, Jones CE, vanden Hoven RN, Edwards JL, Falsetta ML, et al. (2008) Metal binding specificity of the MntABC permease of *Neisseria gonorrhoeae* and its influence on bacterial growth and interaction with cervical epithelial cells. *Infect Immun* 76: 3569-3576.
154. Potter AJ, Kidd SP, Edwards JL, Falsetta ML, Apicella MA, et al. (2009) Esterase D is essential for protection of *Neisseria gonorrhoeae* against nitrosative stress and for bacterial growth during interaction with cervical epithelial cells. *J Infect Dis* 200: 273-278.
155. Potter AJ, Kidd SP, Edwards JL, Falsetta ML, Apicella MA, et al. (2009) Thioredoxin reductase is essential for protection of *Neisseria gonorrhoeae* against killing by nitric oxide and for bacterial growth during interaction with cervical epithelial cells. *J Infect Dis* 199: 227-235.
156. Seib KL, Wu HJ, Srikhanta YN, Edwards JL, Falsetta ML, et al. (2007) Characterization of the OxyR regulon of *Neisseria gonorrhoeae*. *Mol Microbiol* 63: 54-68.
157. Sparling PF (1966) Genetic transformation of *Neisseria gonorrhoeae* to streptomycin resistance. *J Bacteriol* 92: 1364-1371.
158. Stohl EA, Gruenig MC, Cox MM, Seifert HS (2011) Purification and characterization of the RecA protein from *Neisseria gonorrhoeae*. *PLoS One* 6: e17101.
159. Larbig KD, Christmann A, Johann A, Klockgether J, Hartsch T, et al. (2002) Gene islands integrated into tRNA(Gly) genes confer genome diversity on a *Pseudomonas aeruginosa* clone. *J Bacteriol* 184: 6665-6680.
160. van der Meer JR, Ravatn R, Sentchilo V (2001) The *clc* element of *Pseudomonas* sp. strain B13 and other mobile degradative elements employing phage-like integrases. *Arch Microbiol* 175: 79-85.
161. Szczepankowska AK, Prestel E, Mariadassou M, Bardowski JK, Bidnenko E (2011) Phylogenetic and complementation analysis of a single-stranded DNA binding protein family from lactococcal phages indicates a non-bacterial origin. *PLoS One* 6: e26942.
162. Porter RD, Black S (1991) The single-stranded-DNA-binding protein encoded by the *Escherichia coli* F factor can complement a deletion of the chromosomal *ssb* gene. *J Bacteriol* 173: 2720-2723.
163. de Vries J, Wackernagel W (1994) Cloning and sequencing of the *Proteus mirabilis* gene for a single-stranded DNA-binding protein (SSB) and complementation of *Escherichia coli* *ssb* point and deletion mutations. *Microbiology* 140 ( Pt 4): 889-895.
164. Jan HC, Lee YL, Huang CY (2011) Characterization of a single-stranded DNA-binding protein from *Pseudomonas aeruginosa* PAO1. *Protein J* 30: 20-26.
165. Huang YH, Lee YL, Huang CY (2011) Characterization of a single-stranded DNA binding protein from *Salmonella enterica* serovar Typhimurium LT2. *Protein J* 30: 102-108.
166. Schwarz G, Watanabe F (1983) Thermodynamics and kinetics of co-operative protein-nucleic acid binding. I. General aspects of analysis of data. *J Mol Biol* 163: 467-484.
167. Hamon L, Pastre D, Dupaigne P, Le Breton C, Le Cam E, et al. (2007) High-resolution AFM imaging of single-stranded DNA-binding (SSB) protein--DNA complexes. *Nucleic Acids Res* 35: e58.

## References

---

168. Hobbs MD, Sakai A, Cox MM (2007) SSB protein limits RecOR binding onto single-stranded DNA. *J Biol Chem* 282: 11058-11067.
169. Sikder D, Unniraman S, Bhaduri T, Nagaraja V (2001) Functional cooperation between topoisomerase I and single strand DNA-binding protein. *J Mol Biol* 306: 669-679.
170. Gaillard M, Vallaeyts T, Vorholter FJ, Minoia M, Werlen C, et al. (2006) The *clc* element of *Pseudomonas* sp. strain B13, a genomic island with various catabolic properties. *J Bacteriol* 188: 1999-2013.
171. Acharya N, Varshney U (2002) Biochemical properties of single-stranded DNA-binding protein from *Mycobacterium smegmatis*, a fast-growing mycobacterium and its physical and functional interaction with uracil DNA glycosylases. *J Mol Biol* 318: 1251-1264.
172. Purnapatre K, Varshney U (1999) Cloning, over-expression and biochemical characterization of the single-stranded DNA binding protein from *Mycobacterium tuberculosis*. *Eur J Biochem* 264: 591-598.
173. Bujalowski W, Lohman TM (1989) Negative co-operativity in *Escherichia coli* single strand binding protein-oligonucleotide interactions. I. Evidence and a quantitative model. *J Mol Biol* 207: 249-268.
174. Citovsky V, Zupan J, Warnick D, Zambryski P (1992) Nuclear localization of *Agrobacterium* VirE2 protein in plant cells. *Science* 256: 1802-1805.
175. Sundberg C, Meek L, Carroll K, Das A, Ream W (1996) VirE1 protein mediates export of the single-stranded DNA-binding protein VirE2 from *Agrobacterium tumefaciens* into plant cells. *J Bacteriol* 178: 1207-1212.
176. Umezu K, Chi NW, Kolodner RD (1993) Biochemical interaction of the *Escherichia coli* RecF, RecO, and RecR proteins with RecA protein and single-stranded DNA binding protein. *Proc Natl Acad Sci U S A* 90: 3875-3879.
177. Hedgethorne K, Webb MR (2012) Fluorescent SSB as a reagentless biosensor for single-stranded DNA. *Methods Mol Biol* 922: 219-233.
178. Olszewski M, Mickiewicz M, Kur J (2008) Two highly thermostable paralogous single-stranded DNA-binding proteins from *Thermoanaerobacter tengcongensis*. *Arch Microbiol* 190: 79-87.
179. McAfee JG, Edmondson SP, Zegar I, Shriver JW (1996) Equilibrium DNA binding of Sac7d protein from the hyperthermophile *Sulfolobus acidocaldarius*: fluorescence and circular dichroism studies. *Biochemistry* 35: 4034-4045.
180. Dillingham MS, Tibbles KL, Hunter JL, Bell JC, Kowalczykowski SC, et al. (2008) Fluorescent single-stranded DNA binding protein as a probe for sensitive, real-time assays of helicase activity. *Biophys J* 95: 3330-3339.
181. Koerdt A, Godeke J, Berger J, Thormann KM, Albers SV (2010) Crenarchaeal biofilm formation under extreme conditions. *PLoS One* 5: e14104.
182. O'Toole GA, Kolter R (1998) Flagellar and twitching motility are necessary for *Pseudomonas aeruginosa* biofilm development. *Mol Microbiol* 30: 295-304.
183. Seifert HS, Ajioka R, So M (1988) Alternative model for *Neisseria gonorrhoeae* pilin variation. *Vaccine* 6: 107-109.
184. Das T, Sharma PK, Busscher HJ, van der Mei HC, Krom BP (2010) Role of extracellular DNA in initial bacterial adhesion and surface aggregation. *Appl Environ Microbiol* 76: 3405-3408.
185. Olszewski M, Grot A, Wojciechowski M, Nowak M, Mickiewicz M, et al. (2010) Characterization of exceptionally thermostable single-stranded DNA-binding proteins from *Thermotoga maritima* and *Thermotoga neapolitana*. *BMC Microbiol* 10: 260.
186. Mulcahy H, Charron-Mazenod L, Lewenza S (2008) Extracellular DNA chelates cations and induces antibiotic resistance in *Pseudomonas aeruginosa* biofilms. *PLoS Pathog* 4: e1000213.

## References

---

187. Fuxman Bass JI, Russo DM, Gabelloni ML, Geffner JR, Giordano M, et al. (2010) Extracellular DNA: a major proinflammatory component of *Pseudomonas aeruginosa* biofilms. *J Immunol* 184: 6386-6395.
188. Harmsen M, Lappann M, Knochel S, Molin S (2010) Role of extracellular DNA during biofilm formation by *Listeria monocytogenes*. *Appl Environ Microbiol* 76: 2271-2279.
189. Steinberger RE, Holden PA (2005) Extracellular DNA in single- and multiple-species unsaturated biofilms. *Appl Environ Microbiol* 71: 5404-5410.
190. Bockelmann U, Janke A, Kuhn R, Neu TR, Wecke J, et al. (2006) Bacterial extracellular DNA forming a defined network-like structure. *FEMS Microbiol Lett* 262: 31-38.
191. Jurcisek JA, Bakaletz LO (2007) Biofilms formed by nontypeable *Haemophilus influenzae* in vivo contain both double-stranded DNA and type IV pilin protein. *J Bacteriol* 189: 3868-3875.
192. Kellogg DS, Jr., Peacock WL, Jr., Deacon WE, Brown L, Pirkle DI (1963) *Neisseria Gonorrhoeae*. I. Virulence Genetically Linked to Clonal Variation. *J Bacteriol* 85: 1274-1279.
193. Brock TD, Brock KM, Belly RT, Weiss RL (1972) *Sulfolobus*: a new genus of sulfur-oxidizing bacteria living at low pH and high temperature. *Arch Mikrobiol* 84: 54-68.
194. Miroux B, Walker JE (1996) Over-production of proteins in *Escherichia coli*: mutant hosts that allow synthesis of some membrane proteins and globular proteins at high levels. *J Mol Biol* 260: 289-298.
195. Jain S, Moscicka KB, Bos MP, Pachulec E, Stuart MC, et al. Structural characterization of outer membrane components of the type IV pili system in pathogenic *Neisseria*. *PLoS One* 6: e16624.
196. Pachulec E, van der Does C (2010) Conjugative plasmids of *Neisseria gonorrhoeae*. *PLoS One* 5: e9962.
197. Schelert J, Dixit V, Hoang V, Simbahan J, Drozda M, et al. (2004) Occurrence and characterization of mercury resistance in the hyperthermophilic archaeon *Sulfolobus solfataricus* by use of gene disruption. *J Bacteriol* 186: 427-437.
198. Hamilton HL, Schwartz KJ, Dillard JP (2001) Insertion-duplication mutagenesis of *neisseria*: use in characterization of DNA transfer genes in the gonococcal genetic island. *J Bacteriol* 183: 4718-4726.
199. Kohler PL, Hamilton HL, Cloud-Hansen K, Dillard JP (2007) *AtIA* functions as a peptidoglycan lytic transglycosylase in the *Neisseria gonorrhoeae* type IV secretion system. *J Bacteriol* 189: 5421-5428.
200. Kado CI, Liu ST (1981) Rapid procedure for detection and isolation of large and small plasmids. *J Bacteriol* 145: 1365-1373.
201. Morse SA, Bartenstein L (1974) Factors affecting autolysis of *Neisseria gonorrhoeae*. *Proc Soc Exp Biol Med* 145: 1418-1421.
202. Despalins A, Marsit S, Oberto J (2011) Absynte: a web tool to analyze the evolution of orthologous archaeal and bacterial gene clusters. *Bioinformatics* 27: 2905-2906.
203. Lappann M, Haagensen JA, Claus H, Vogel U, Molin S (2006) Meningococcal biofilm formation: structure, development and phenotypes in a standardized continuous flow system. *Mol Microbiol* 62: 1292-1309.
204. Gelvin SB (2010) Finding a way to the nucleus. *Curr Opin Microbiol* 13: 53-58.
205. Post DM, Zhang D, Eastvold JS, Teghanemt A, Gibson BW, et al. (2005) Biochemical and functional characterization of membrane blebs purified from *Neisseria meningitidis* serogroup B. *J Biol Chem* 280: 38383-38394.



### Acknowledgments

I wish to thank, first and foremost, my supervisor Dr. Chris van der Does. Chris, thank you for giving me a possibility to work on this challenging project. Thank you for your supervision, trust and support in all situations. This thesis would not have possible without your innovative ideas, your excellent guidance and encouragement during the last 4 years. It was a great pleasure to work with you, Chris. One simply could not wish for a better or friendlier supervisor!

I am deeply indebted to my thesis and defense committee members, Prof. Dr. Sjøgaard-Andersen, Prof. Dr. Thanbichler, Prof. Dr. Renkawitz-Pohl, Prof. Maier, Prof. Dr. Bremer, Prof. Dr. Feldbrügge and Dr. Thormann for their time for the valuable suggestions and discussions that brought me to finish this thesis.

My sincere thanks go to our collabotarors. It gives me great pleasure in acknowledging the support and help of Prof. Dr. Molin and Dr. Sternberg, who supervised and supported me during my stay in Copenhagen. It was a best period of my PhD! I share the credit of my work with Dr. Eveline Peeters who made wonderful AFM pictures and introduced me into the world of AFM.

I would like to thank all colleagues from Department of Ecophysiology for crucial comments on my thesis, helpful discussions and for providing friendly working environment.

I am especially indebted to the people from S2-lab, Jürgen, Said, Sabine and Susann, who gave so much assistance and enjoyable time during my PhD period. I am most grateful to Sabine Schork who joined me in Denmark during my second stay and performed all the dangerous Neisseria-work.

I am grateful to International Max Planck Research School for Environmental, Cellular and Molecular Microbiology and Boehringer Ingelheim Foundation for providing financial support during my research in Marburg and Copenhagen.

This thesis would have remained a dream without a huge support of my wonderful Mum. My dear Mum, thank you so much that you have taken care of the little Nataly for so many days and nights, giving me a chance to finish the thesis. My dear Dad, thank you that you always believe in me!

Last, but by no means least, I thank my best friend, my husband, my soulmate Goscha. You have given me unequivocal support throughout, as always, for which my mere expression of thanks likewise does not suffice!

I would like to thank my little daughter Nataly who makes me happy every day!

It would not have been possible to write this doctoral thesis without the help and support of so many kind people around me. I want to thank all the others which are not mentioned on this page, but still contributed in some way to my scientific and personal life.

## Lebenslauf

### Persönliche Daten

Name Maria Zweig (geb. Valevich)  
Geburtsdatum 16.08.1984  
Familienstand verheiratet  
Kinder Tochter



### Ausbildung

02.2011 – 02.2013 Fernstudium an der Deutschen Akademie für Management, Berlin  
10.2008 – 02.2013 Promotionsstudium am Max-Planck Institut für terrestrische Mikrobiologie, Marburg  
10.2003 – 07.2008 Biologiestudium an der Philipps-Universität Marburg  
Hauptfächer: Zellbiologie, Genetik, Mikrobiologie, Entwicklungsbiologie  
Diplomarbeit: Functional analysis of the genes of the cluster 2A from *Sporisorium reilianum*.  
Leitung: Prof. Dr. Jan Schirawski  
07.2003 Abitur an der Augustiner Schule Friedberg (Hessen)  
09.1998- 09.2000 Besuch des Gymnasiums 183, Moskau

### Stipendien

2008 Stipendium der internationalen Max-Planck Research School (IMPRS)  
2011 Stipendium für Auslandsaufenthalt der Boehringer Ingelheim Foundation  
2011 Stipendium der ESCMID für Konferenz „Eurobiofilms 2011“ in Kopenhagen

### Hobbies

Eventmanagement, Squash, Kochen für Freunde und Familie

## Erklärung

Hiermit versichere ich, dass ich die vorliegende Dissertation mit dem Titel

### **“Role and visualization of the single-stranded and double-stranded DNA in the biofilm of *Neisseria gonorrhoeae*”**

selbstständig verfasst, keine anderen als die im Text angegebenen Hilfsmittel verwendet und sämtliche Stellen, die im Wortlaut oder dem Sinn nach anderen Werken entnommen sind, mit Quellenangaben kenntlich gemacht habe.

Die Dissertation wurde in der jetzigen oder einer ähnlichen Form noch bei keiner anderen Hochschule eingereicht und hat noch keinen sonstigen Prüfungszwecken gedient.

Bad Nauheim, den 07.04.2013

Maria Zweig

### **Einverständniserklärung**

Ich erkläre mich damit einverstanden, dass die vorliegende Dissertation mit dem Titel

**“Role and visualization of the single-stranded and double-stranded DNA in the biofilm of *Neisseria gonorrhoeae*”**

in Bibliotheken allgemein zugänglich gemacht wird. Dazu gehört, dass sie

- von der Bibliothek der Einrichtung, in der ich meine Arbeit angefertigt habe, zur Benutzung in ihren Räumen bereitgehalten wird
- in konventionellen und maschinenlesbaren Katalogen, Verzeichnissen und Datenbanken verzeichnet wird
- der Universitätsbibliothek für die lokale Nutzung und für Fernleihzwecke zur Verfügung steht und
- im Rahmen der urheberrechtlichen Bestimmungen für Kopierzwecke genutzt werden kann.

Bad Nauheim, den 07.04.2013

Maria Zweig (Verfasserin)

Dr. Chris van der Does (Betreuer)